UNIVERSIDADE FEDERAL DO RIO GRANDE DO SUL
FACULDADE DE ODONTOLOGIA
PROGRAMA DE PÓS-GRADUAÇÃO EM ODONTOLOGIA
NIVEL DOUTORADO
ÁREA DE CONCENTRAÇÃO – PATOLOGIA BUCAL

FELIPE NÖR

INIBIÇÃO TERAPÊUTICA DA INTERAÇÃO MDM2-P53: UMA ALTERNATIVA PARA O TRATAMENTO DO CARCINOMA ADENOIDE CÍSTICO

Porto Alegre
2016

FELIPE NÖR

INIBIÇÃO TERAPÊUTICA DA INTERAÇÃO MDM2-P53: UMA ALTERNATIVA PARA O TRATAMENTO DO CARCINOMA ADENOIDE CÍSTICO

Tese apresentada ao programa de Pós-graduação em Odontologia da Universidade Federal do Rio Grande do Sul, como requisito final para obtenção do titulo de Doutor em Odontologia, área de concentração Patologia Bucal.

Orientação:
Prof. Dr. Manoel Sant'Ana Filho
Prof. Dr. Jacques Eduardo Nör

Linha de pesquisa: Câncer Bucal.

Porto Alegre
2016

CIP - Catalogação na Publicação

Nor, Felipe
Inibição terapêutica da interação MDM2-p53: uma alternativa para o tratamento do carcinoma adenoide cístico. / Felipe Nor. -- 2016.
85 f.

Orientador: Manoel Sant'Ana Filho.
Coorientador: Jacques Eduardo Nor.

Tese (Doutorado) -- Universidade Federal do Rio Grande do Sul, Faculdade de Odontologia, Programa de Pós-Graduação em Odontologia, Porto Alegre, BR-RS, 2016.

1. carcinoma adenoide cístico. 2. quimioterapia. 3. recorrência. 4. MDM2. 5. p53. I. Sant'Ana Filho, Manoel , orient. II. Nor, Jacques Eduardo, coorient. III. Título.

Elaborada pelo Sistema de Geração Automática de Ficha Catalográfica da UFRGS com os dados fornecidos pelo(a) autor(a).

DEDICATÓRIA

Aos meus pais, **Ricardo** e **Miriam**, minha irmã **Carolina** e minha dinda **Nair**, por entenderem e apoiarem as minhas escolhas e sempre se fazerem muito presentes pelos caminhos que estas me levaram. Acima de tudo, por me ensinarem os valores da honestidade, humildade e responsabilidade, alicerces nos quais procuro basear a minha conduta de vida.

À **Nathália**, por todo amor, carinho e compreensão nesta fase final de doutorado, e por me mostrar que a vida pode ser tão boa quanto *petit gateau* com *haagen dazs* de morango.

À vocês, dedico este trabalho.

AGRADECIMENTOS

Seria muita pretensão minha tentar agradecer, neste espaço restrito, a todos aqueles que participaram e contribuíram, de alguma forma, na realização deste trabalho. Àqueles que, por este motivo, não encontrarem seu nome escrito aqui, deixo a certeza da gratidão eterna guardada em minha mente e meu coração. **Obrigado!**

Ao professor Dr. **Manoel Sant'Ana Filho**, por ter aceito a proposta de orientar esta tese de doutorado. Pelas lições valorosas em patologia e por ter dado seu apoio incondicional para a realização do estágio sanduiche no exterior;

Ao professor Dr. **Jacques Eduardo Nör**, orientador no exterior, exemplo de profissional, tio e grande amigo, por todos os ensinamento em pesquisa, em odontologia e para a vida. À tia **Silvia** e primo **Lucas,** por todo o carinho e atenção que sempre tiveram comigo, e por fazerem da sua casa o meu lar em Ann Arbor;

À professora Dra. **Anna Christina Medeiros Fossati**, minha primeira orientadora e "mãe cientifica", por ter guiado os meus primeiros passos no então desconhecido campo da ciência e da pesquisa;

À professora Dra. **Manoela Domingues Martins**, co-orientadora informal desta tese e grande incentivadora para a realização deste doutorado. Ao professor Dr. **Marco Antonio Trevizani Martins**, amigo e grande exemplo de estomatologista, pelos bons momentos compartilhados em Ann Arbor;

Ao colega, amigo e primo **Duarte Silvestre Matzenbacher,** pelo exemplo de ética e dedicação, e por ser um grande incentivador da odontologia**.** À **Rose, Gabriel** e **Amanda**, pelo carinho e confiança, e por fazerem de Igrejinha a minha segunda casa;

Aos colegas, professores e funcionários da clinica **Dental** e da **Faculdade Tecnológica (FATEC) Dental CEEO,** instituições de excelência na prática e no ensino da odontologia, representados pelo coordenador cientifico, professor Dr.

João Batista Burzlaff, e pelo coordenador do curso de especialização em implantodontia, professor Dr. **Carlos Fernando Rozas Cardoso**, pela oportunidade de constante aprendizado e promoção da saúde bucal em um ambiente leve e familiar;

Ao professor, amigo e companheiro de basquete Dr. **Pantelis Varvaki Rados**, pelo exemplo de caráter e compromisso, e pelo apoio institucional na realização de estágio no exterior durante o período da graduação em odontologia, o qual determinou, por fim, a intenção de realizar o estágio sanduiche do doutorado no exterior;

Ao Prof. Dr. **Fernando Borba de Araujo**, amigo colorado, por ter despertado em mim a ideia de realizar este doutorado e não ter medido esforços para que essa ideia se tornasse realidade.

Ao Prof. Dr. **Fernando Neves Hugo** e ao Prof. Dr. **Cassiano Kuchenbecker Rösing**, pela disponibilidade em viabilizar o adiantamento de créditos e, por fim, tornar possível o afastamento para realização do primeiro estágio na Universidade de Michigan;

Aos professores da **Faculdade de Odontologia da UFRGS**, da qual muito me orgulho de ter sido aluno de graduação e pós-graduação, em especial àqueles da área de **Patologia**, minha gratidão pelos ensinamentos transmitidos e incentivo a seguir a carreira docente;

Aos colegas e amigos da **pós-graduação,** especialmente da **patologia bucal**, pelo companheirismo e troca de conhecimento durante o doutorado;

Aos colegas e amigos do **Laboratório de Pesquisa em Angiogênese da Universidade de Michigan**, em especial ao **Zhang** e à **Kristy**, pelo constante suporte e disponibilidade no dia-a-dia da pesquisa no laboratório, e pela troca de experiências culturais;

Aos colegas, professores, funcionários e amigos da **Faculdade de Odontologia da Universidade de Michigan**, por me mostrarem uma nova face do ensino e pesquisa em Odontologia.

Ao **Conselho Nacional de Desenvolvimento Cientifico e Tecnológico (CNPq)**, através do programa **Ciência sem Fronteiras**, pelo investimento financeiro que proporcionou a realização do estágio sanduíche no exterior;

À **banca** desta defesa de tese, pelo pronto aceite e pelo tempo dedicado à avaliação e aperfeiçoamento deste documento.

Acima de tudo, à **Deus**, por ter me proporcionado saúde, paciência e persistência. E por ter iluminado a minha mente e meus caminhos.

Obrigado!

“A vida é um grande ensaio de orquestra.”

Felipe Nör

SUMÁRIO

RESUMO

Introdução: O carcinoma adenoide cístico (CAC) é uma das neoplasias de glândula salivar mais comuns para o qual não se encontra quimioterapia eficaz. Um conceito emergente na terapia do câncer é atingir proteínas especificas do tumor. MDM2 (*murine double minute 2*) é um importante inibidor do supressor tumoral p53, e sua expressão é aumentada em CAC. O objetivo do Artigo 1 foi avaliar o efeito de um novo inibidor da interação MDM2-p53 (MI-773) no CAC *in vitro* e *in vivo*. O Artigo 2 teve como objetivo entender o papel da combinação de MI-773 com cisplatina, além de avaliar a recorrência de CAC frente a regime neoadjuvante de MI-773. **Materiais e Métodos**: 3 modelos de xenoenxerto derivado de paciente (XEDP, UM-PDX-HACC-5; ACCx6; ACCx9) e 5 culturas primarias de CAC (UM-HACC-1, -2A, -2B, -5, -6) foram usados para experimentos *in vitro* e *in vivo*. Ensaio de Sulforrodamina B (SRB) foi realizado para avaliar o efeito dos agentes experimentais na viabilidade celular, além de determinar valores de IC_{50}. Western blots revelaram a expressão de p53, fosfo-p53, MDM2, p21, PUMA, BAX, Bcl-2 e Bcl-x_L. Lâminas histológicas (UM-PDX-HACC-5) foram avaliadas por imunohistoquímica e imunofluorescência para determinar a localização de p53. Técnica de TUNEL *in situ* revelou o número de células de UM-PDX-HACC-5 no processo de apoptose. Citometria de fluxo foi realizada para determinar o efeito da terapia na proporção de células-tronco tumorais ($ALDH^{high}CD44^{high}$) e para avaliar o ciclo celular. Para os estudos *in vivo*, animais transplantados com tumores (UM-PDX-HACC5, ACCx6, ou ACCx9) receberam protocolo terapêutico (MI-773 – gavagem; cisplatina – injeção intraperitoneal; ou veículo controle) conforme indicado. ANOVA, seguido de testes post-hoc (Tukey), Mann-Whitney U-test ou Student's t-test foram usados para determinar as diferenças no crescimento tumoral, peso, volume, apoptose, viabilidade celular, expressão de TUNEL e p53. Significância estatística: $p<0.05$. **Resultados: MI-773 causa regressão do tumor em todos os modelos pré-clínicos de CAC.** Doses diárias de 100mg/kg de MI-773 reduziram significativamente o volume tumoral quando comparado com doses intermediárias (10 ou 50 mg/kg MI-773) ou veículo controle, em todos os modelos de CAC. Alternativamente, camundongos transplantados com tumores UM-PDX-HACC-5 receberam doses semanais de MI-773 (200 mg/kg) e/ou cisplatina (5 mg/kg) por 30

dias, a fim de se avaliar o efeito da combinação das drogas. MI-773, como agente único, causou regressão tumoral, sendo mais efetivo do que a cisplatina. Cisplatina, por outro lado, mostrou limitado efeito terapêutico, estabilizando o crescimento tumoral. Notavelmente, a combinação MI-773 + cisplatina foi mais efetiva do que os agentes isoladamente, e não foi verificada retomada do tumor no período pós-operatório. Importantemente, os protocolos experimentais não comprometeram a saúde geral dos animais. Coletivamente, estes resultados *in vivo* demonstram que MI-773 atua como mediador na regressão tumoral de CAC e sensibiliza os tumores à cisplatina. **A inibição terapêutica da interação MDM2-p53 ativa p53 e induz apoptose.** MI-773 potentemente induz expressão de p53, seu alvo p21 e proteínas relacionadas à apoptose, como PUMA, BAX, Bcl-2 e Bcl-x_L *in vitro* e *in vivo*. Análise do ciclo celular mostrou que a inibição terapêutica da interação MDM2-p53 por MI-773 causa parada no ciclo celular no primeiro ponto de checagem (G_1). Marcação por TUNEL revelou número significativamente maior de células em apoptose quando tumores de UM-PDX-HACC-5 foram tratados com MI-773 em comparação com controle ($p<0.05$) Utilizando o mesmo modelo de xenoenxerto, a técnica de imunohistoquímica mostrou que MI-773 não somente aumentou a porcentagem de células p53-positivas ($p<0.001$), como causou uma translocação parcial de p53 ao citoplasma. **MI-773 reduz a fração de células-tronco tumorais (CTT) e previne recorrência do CAC.** Tratamento com MI-773 como agente único ou combinado com cisplatina reduziu a fração de CTT ($p<0.05$). Notavelmente, nenhum animal tratado com regime neoadjuvante de MI-773 apresentou recorrência tumoral mesmo após 300 dias de acompanhamento. Em contraste, em 62,5% dos animais do grupo controle houve recorrência ($p=0.0097$). **Conclusões:** Em resumo, os estudos demonstram que a inibição terapêutica da interação MDM2-p53 com MI-773 é uma estratégia antitumoral eficaz, é capaz de sensibilizar tumores à cisplatina e previne recorrência neste modelo pré-clínico de CAC. Coletivamente, os dados sugerem que pacientes com carcinoma adenoide cístico podem ser beneficiados através de terapias-alvo contra MDM2.

Palavras-chave: carcinoma adenoide cístico; quimioterapia; MDM2; p53; recorrência.

ABSTRACT

Introduction: Adenoid cystic carcinoma (ACC) is one of the most common salivary gland malignancies for which no effective chemotherapy is available. An emerging concept in cancer therapy is to target specific tumor-related proteins. Murine double minute 2 (MDM2) is an important inhibitor of the tumor suppressor p53 and has been found overexpressed in ACC. Paper #1 aimed to evaluate the effect of a novel small molecule inhibitor of the MDM2-p53 interaction (MI-773) on ACC *in vitro* and *in vivo*. Paper #2 aimed to understand the role of combining MI-773 with cisplatin, and to evaluated ACC recurrence using a neoadjuvant regimen of MI-773. **Material and Methods:** 3 patient-derived xenograft (PDX) models (UM-PDX-HACC-5; ACCx6; ACCx9) and 5 low passage primary human ACC cells pools (UM-HACC-1, -2A, -2B, -5, -6) were used for *in vivo* and *in vitro* experiments. Sulforhodamine B (SRB) assay was performed to evaluate the effect of experimental agents on ACC cell viability and to determine IC_{50} values. Western blots revealed the expression of p53, phospho-p53, MDM2, p21, PUMA, BAX, Bcl-2 and Bcl-x_L. Histological sections from UM-PDX-HACC-5 tumors were stained using immunohistochemistry and immunofluorescence techniques to determine p53 status. *In situ* TUNEL staining revealed the number of UM-PDX-HACC-5 cells undergoing apoptosis. Flow cytometry was carried out to determine the effect of therapy on the proportion of cancer stem cells ($ALDH^{high}CD44^{high}$) and for cell cycle analysis. For *in vivo* studies, mice harboring UM-PDX-HACC5, ACCx6, or ACCx9 tumors were treated following specific therapeutic protocol (MI-773 – gavage; cisplatin – intraperitoneal injection; or vehicle control), as opportunely indicated. One-way ANOVA, followed by post-hoc tests (Tukey), Mann-Whitney U-test or Student's t-test were used to determine significant differences in tumor growth, weight, volume, apoptosis levels, cell viability, TUNEL and p53 expression. Significance was determined at $p<0.05$. **Results: MI-773 caused tumor regression in all ACC PDX models.** Daily doses of 100 mg/kg MI-773 significantly reduced tumor volume when compared to intermediate doses (10 or 50 mg/kg MI-773) or vehicle-treated controls in all ACC xenograft models. Alternatively, mice harboring UM-PDX-HACC-5 tumors received either weekly doses of MI-773 (200 mg/kg) and/or cisplatin (5 mg/kg) for 30 days, in order to evaluate the effect of this drug combination. MI-773 as single agent caused tumor regression,

being more effective than single agent cisplatin. Cisplatin showed limited therapeutic response stabilizing tumor growth. Notably, combination of MI-773 with cisplatin was more effective than single agent therapies and no tumor rebound was observed during the follow up period. Importantly, experimental protocols did not compromise the overall health status of mice. Collectively, these *in vivo* results demonstrate that MI-773 mediates ACC tumor regression, and sensitizes ACC xenograft tumors to cisplatin. **Therapeutic inhibition of the MDM2-p53 interaction activates p53 and induces apoptosis.** MI-773 potently induced the expression of p53, its downstream target p21 and apoptosis-related proteins PUMA, BAX, Bcl-2 and Bcl-x_L *in vitro* and *in vivo*. Cell cycle analysis showed that therapeutic inhibition of the MDM2-p53 interaction by MI-773 causes cell cycle arrest at the first checkpoint (G_1). *In situ* TUNEL revealed a significant higher number of cells undergoing apoptosis in UM-PDX-HACC-5 tumors treated with MI-773 compared to vehicle control ($p<0.05$). Using the same xenograft model, immunohistochemistry assay showed that MI-773 not only increased the percentage of p53-positive cells ($p<0.001$), but also caused a partial translocation of p53 to the cytoplasm. **MI-773 reduces the fraction of cancer stem cells (CSC) and prevents recurrence in ACC.** Treatment with MI-773 as single agent or combined with cisplatin significantly reduced the fraction of CSC ($p<0.05$). Notably, not a single animal treated with neoadjuvant MI-773 presented recurrence even after 300 days of follow-up. In contrast, 62,5% of mice that received vehicle control experienced tumor reappearance within this time period ($p=0.0097$). **Conclusions:** In summary, these studies demonstrate that therapeutic inhibition of the MDM2-p53 interaction with MI-773 is an effective anti-tumor strategy that mediates tumor regression, sensitizes tumors to cisplatin and prevents recurrence in this pre-clinical model of ACC. Collectively, these data suggest that patients with adenoid cystic carcinoma might benefit from MDM2-targeted therapies.

Key words: adenoid cystic carcinoma; chemotherapy; MDM2; p53; recurrence.

LISTA DE ABREVIATURAS, SIGLAS E SÍMBOLOS

% = porcentagem

AAC = área abaixo da curva

B = bleomicina

C = ciclofosfamida

CAC = carcinoma adenoide cístico

CAP = cisplatina + ciclofosfamida + doxorrubicina

Cb = carboplatina

Cis = cisplatina

D = doxorrubicina

E = epirubicina

EGFR = *epidermal growth factor receptor*

EUA = Estados Unidos da América

F = fluorouracila

G = gencitabina

H/E = hematoxilina/eosina

HCPA = Hospital de Clínicas de Porto Alegre

IV = intra venoso

M = mitoxantrona

MDM2 = *murine double minute 2*

N = número amostral

NCCN = *national comprehensive cancer center*

NI = não informado

NMGS = neoplasias malignas de glândula salivar

Pr = pirarubicina

SRB = Sulforrodamina B

STR = short tandem repeat

T = paclitaxel

V = vinorelbina

Vn = vincristina

VO = via oral

XEDP = xenoenxerto derivado de paciente

1. APRESENTAÇÃO

Esta tese é apresentada em quatro sessões principais:

- **Revisão da literatura:** nesta sessão será apresentada uma breve introdução geral sobre o carcinoma adenoide cístico, suas características morfológicas, histopatológicas e moleculares. A seguir, é feita uma revisão sobre as opções terapêuticas para o tratamento desta neoplasia, com enfoque nos ensaios clínicos que avaliaram o efeito da quimioterapia. O próximo tópico busca revisar o conceito de xenoenxertado derivado de paciente (XEDP) e seu uso como modelo experimental pré-clínico. A revisão segue com uma apresentação sucinta, uma vez que os artigos científicos já revisam este assunto, da interação MDM2-p53 na fisiologia e no desenvolvimento de tumores, sua relação com o carcinoma adenoide cístico e as opções terapêuticas advindas do bloqueio desta interação com drogas de alvo especifico (MI-773).
- **Artigo 1:** Artigo publicado no periódico *Clinical Cancer Research* (Qualis A, fator de impacto 8.73) que descreve os primeiros resultados sobre o efeito da inibição terapêutica da interação MDM2-p53 com MI-773 no carcinoma adenoide cístico *in vitro* e *in vivo*. A ativação da apoptose, aliado com a robusta regressão tumoral em modelos pré-clínicos, demonstram o potencial de MI-773 como alternativa para o tratamento desta neoplasia.
- **Artigo 2:** Artigo publicado no periódico *Clinical Cancer Research* (Qualis A, fator de impacto 8.73) que apresenta resultados semelhantes ao artigo 1 de regressão tumoral e ativação de apoptose com o uso de MI-773 em modelo pré-clínico de CAC. Além disso, demonstra que MI-773 foi capaz de sensibilizar os tumores xenoenxertados à cisplatina e, talvez mais importante, preveniu a recorrência do tumor.
- **Considerações finais:** esta sessão apresenta reflexões complementares ao tema exposto nos dois artigos científicos, as sua implicações, limitações, e perspectivas para futuras investigações.

2. REVISÃO DA LITERATURA

Introdução ao Carcinoma Adenoide Cístico

As neoplasias malignas das glândulas salivares (NMGS) são patologias incomuns, representando cerca de 3-5% dos cânceres de cabeça e pescoço. Sua incidência mundial anual é de 0.4–2.6 casos novos a cada 100,000 habitantes (CAWSON, ODELL, 2003; BARNES, *et al.*, 2005). De modo geral, a baixa prevalência das NMGS faz com que o acesso a exemplares para estudo e pesquisa seja muito limitado. O pouco conhecimento acerca dessas lesões e de seu prognóstico a longo prazo, aliado à diversidade de apresentações clinicas e padrões histopatológicos, tornam o diagnóstico e manejo dos pacientes portadores de NMGS um verdadeiro desafio para cirurgiões-dentistas e profissionais da saúde (SEETHALA, 2009).

Dentre as NMGS mais comuns, destaca-se o carcinoma adenoide cístico (CAC). Em um levantamento dos casos de NMGS diagnosticados e tratados no Hospital de Clínicas de Porto Alegre (HCPA), no período de 1995 a 2010 (n:109), verificamos que o CAC foi a neoplasia mais frequente (58,3%). Além disso, os pacientes diagnosticados com esta condição apresentaram o pior prognóstico clínico, com uma média de sobrevida de 6,2 anos (VASCONCELOS, *et al.*, 2016).

Tipicamente, o carcinoma adenoide cístico tem origem nas glândulas salivares, acometendo principalmente a glândula parótida, podendo ocorrer também na glândula submandibular e glândulas salivares menores. Muito raramente, esta neoplasia surge em outras localizações, como a traquéia, pulmão, mama, pele, esôfago, colo do útero e mucosa genital. Afeta pacientes de todas as idades, porém é predominante em adultos, com um pico de incidência entre a quinta e a sexta décadas de vida. Não existe predileção por gênero, exceto no caso em que ocorre envolvimento da glândula submandibular, quando mulheres são mais acometidas (LOYOLA, *et al.*, 1995; BARNES, *et al.*, 2005).

Histologicamente, caracteriza-se por apresentar dois tipos celulares principais: células ductais e células mioepiteliais modificadas. Existem três padrões histológicos

definidos: tubular, cribriforme e sólido (ou basalóide). No padrão tubular, ductos e túbulos bem formados com luz central são revestidos por uma camada epitelial, internamente, e outra mioepitelial, na porção externa. O padrão cribriforme, o mais frequente, é caracterizado por apresentar ninhos de células com espaços microcísticos cilindromatosos, preenchidos por material mucóide hialino ou basófilo. O padrão sólido (ou basalóide) é formado por folhetos e células basalóides uniformes, sem existir formação tubular ou microcística. O estroma tumoral é, geralmente, hialinizado e pode manifestar característica mixóide. Este subtipo sólido está associado com um pior prognóstico clínico dos pacientes (BARNES, *et al.*, 2005).

Em nível molecular, alguns autores têm demonstrado que a grande maioria dos casos de CAC (80%-90%) apresentam a fusão do oncogene *MYB* com o fator de transcrição *NFIB*, caracterizado pela translocação t(6;9)(q22-23;p23-24). *MYB* desempenha um papel importante como oncogene no controle da proliferação celular, apoptose e diferenciação. Curiosamente, a fusão de *MYB-NFIB* não foi encontrada em nenhum outro carcinoma de glândula salivar além do CAC, demonstrando a grande especificidade deste achado e sua possível contribuição como biomarcador no diagnóstico desta lesão (SIMPSON, *et al.*, 2014; BRILL, *et al.*, 2011; DI PALMA, *et al.*, 2014). Além de potencialmente útil no diagnóstico, a fusão *MYB-NFIB* já foi associada com um pior prognóstico clínico dos pacientes (STENMAN, 2013; MITANI, *et al.*, 2010).

Outros possíveis biomarcadores moleculares de CAC já foram descritos, como c-kit e o receptor do fator de crescimento epidermal (do inglês EGFR) (ADELSTEIN, *et al.*, 2012). Kit é um receptor transmembrana codificado pelo gene c-kit. Este gene está associado com a regulação da migração, diferenciação e proliferação celular. Assim como a fusão de *MYB-NFIB*, em torno de 90% dos casos de CAC apresentam expressão aumentada de c-kit (HOTTE, *et al.*, 2005; BELL, *et al.*, 2010). EGFR, por sua vez, tem sido associado com aumento da proliferação e motilidade celular, diminuição de apoptose, promoção de angiogênese e sobrevivência de células do câncer (LAURIE *et al.*, 2011). A incidência de expressão desta proteína é menor, sendo evidenciada em torno de 40% dos casos de CAC. Sua relevância como biomarcador ainda é incerta. (BELL, *et al.*, 2010; AGULNIK, *et al.*, 2007)

Clinicamente, o tumor apresenta-se como uma massa sólida, de cor castanho-claro, bem circunscrito, porém não encapsulado. Seu comportamento biológico é único entre os tumores de glândula salivar. Exibe progressão lenta, porém com alto poder de invasão e destruição dos tecidos adjacentes. Sua capacidade de invasão perineural já foi bem documentada, o que explica a sintomatologia dolorosa referida por alguns pacientes. Esse comportamento invasivo pode levar a disseminação do tumor ao cérebro, além de promover a disseminação de células cancerosas para além das margens possíveis de serem ressecadas cirurgicamente, facilitando a recidiva do tumor (SIMPSON, *et al.*, 2014; COCA-PELAZ, *et al.*, 2015; KOWALSKI, PAULINO, 2002).

Opções terapêuticas

O tratamento padrão para o CAC é a excisão cirúrgica seguida por radioterapia (DODD, SLEVIN, 2006; MILANO, *et al.*, 2007; MENDENHALL, *et al.*, 2004; ADELSTEIN, *et al.*, 2012). Porém, o índice de sobrevida dos pacientes em um período de 10 anos não ultrapassa 50%. Isso se deve ao alto índice de recidiva local e metástase à distância, que acomete principalmente o pulmão, tecido ósseo, fígado e, com menor frequência, a cadeia de linfonodos (DILLON, *et al.*, 2016; LAURIE, *et al.*, 2011; SIMPSON, *et al.*, 2014). Em casos de metástase, a estimativa média de vida cai para 3 anos, e somente 10% destes pacientes sobrevivem por um período maior do que uma década (VAN DER WAL, *et al.*, 2002; TERHAARD, *et al.*, 2004). A quimioterapia vem sendo empregada em casos avançados, seja por impossibilidade na realização da excisão cirúrgica, seja por recidiva do tumor. Entretanto, os medicamentos quimioterápicos disponíveis não tem demonstrado eficácia clínica satisfatória no tratamento dos pacientes com CAC (LAURIE, *et al.*, 2011; CHAE, *et al.*, 2015).

Em função da raridade desta lesão, poucos são os estudos investigando a eficácia da quimioterapia no CAC. Aqui, serão apresentados resultados de ensaios clínicos de fase 2 (ensaios piloto, com número restrito de participantes, buscando demonstrar a atividade terapêutica e toxicidade das drogas) e fase 3 (ensaios com número amostral grande, geralmente multicêntricos, buscando avaliar a eficácia e inocuidade do tratamento) que avaliaram o efeito da quimioterapia em pacientes com

estágio avançado da doença, ou seja, aqueles que apresentavam recorrência local e/ou metástase. A maioria dos estudos apresenta os resultados na forma de resposta objetiva. Assim, a efetividade da terapia é classificada como resposta parcial, resposta completa ou estabilização da doença.

A cisplatina é uma das drogas mais usadas em quimioterapia dos tumores malignos de cabeça e pescoço (PAPASPYROU, *et al.*, 2011; LAURIE, LICITRA, 2006; SURAKANTI, AGULNIK, 2008; VATTEMI, *et al.*, 2008; RIZK, *et al.*, 2007). Entretanto, sua eficácia no tratamento de casos avançados de CAC é discutível, em função da grande inconsistência dos dados disponíveis na literatura. Enquanto alguns trabalhos (HILL, *et al.*, 1997; DE HAAN, *et al.*, 1992) não encontraram nenhuma resposta objetiva com o uso desta droga, outros mostraram uma taxa de resposta que varia de 18% a 25%, essencialmente quando a cisplatina está associada com a ciclofosfamida e doxorrubicina (CAP) (LICITRA, *et al.*, 1996). É importante ressaltar que a variação nos resultados pode ser devido ao tamanho amostral muito limitado. Além disso, a maioria dos ensaios clínicos foram conduzidos em um único centro de tratamento, limitando a população alvo em estudo (DILLON, *et al.*, 2016).

Além da cisplatina (SCHRAMM, SRODES, MYERS, 1981; LICITRA, *et al.*, 1991), outros agentes quimioterápicos têm sido estudados isoladamente em ensaios clínicos randomizados, como é o caso da mitoxantrona (MATTOX, VON HOFF, BALCERZAK, 1990; VERWEIJ, *et al.*, 1996), epirubicina (VERMORKEN, *et al.*, 1993), vinorelbina (AIROLDI, *et al.*, 2001), paclitaxel (GILBERT, *et al.*, 2006) e gentamicina (VAN HERPEN, *et al.*, 2008). De modo geral, a taxa de resposta objetiva completa da monoterapia no CAC é baixa. Apenas 18 pacientes (de um total de 141, quando somados 8 ensaios clínicos de fase 2 ou 3) foram beneficiados de alguma maneira pela intervenção sistêmica. Na maioria dos estudos, nenhuma resposta objetiva foi alcançada. A estabilização da doença foi o resultado mais frequente, ocorrendo em 64 dos 111 pacientes tratados. Entretanto, este dado só apresenta validade quando os pacientes selecionados para o estudo tem comprovada progressão de doença antes do início da intervenção e, talvez mais importante, tem-se o controle sobre o tratamento prévio realizado. Caso contrário, fica comprometida a análise de eficácia dos fármacos, uma vez que a lesão pode ter estabilizado por terapia prévia ou outro fator desconhecido, e não em função da

intervenção em estudo (LAURIE, *et al.*, 2001). A Tabela 1 sumariza os principais resultados dos ensaios clínicos utilizando monoterapia no carcinoma adenoide cístico.

Estudo	***Droga/regimento***	***n***	***Resposta objetiva (duração)***	***Estabilização da doença (duração)***	***Sobrevida média (meses)***
Schramm et al	Cisplatina 80-100 mg/m^2 (a cada 4-6 semanas)	10	7 de 10 (NI)	NI	NI
Mattox et al	Mitoxantrona 12 mg/m^2 (a cada 3 semanas)	18	1 de 18 (19 meses)	12 de 18 (5-18 meses)	19
Verweij et al	Mitoxantrona 14 mg/m^2 (a cada 3 semanas)	32	4 de 32 (3-13 meses)	22 de 32 (2.5-30 meses)	1813
Vermorken et al	Epirubicina 30 mg/m^2 (semanalmente); sem resposta, 90 mg/m^2 (a cada 3 semanas)	20	2 de 20 (7.5 e 20 meses)	NI	14
Van Herpen et al	Gencitabina 1250 mg/m^2 (dias 1 e 8 a cada 3 semanas)	21	0 de 21	11 de 21 (NI)	NI
Licitra et al	Cisplatina 100 mg/m^2 (a cada 3 semanas)	13	2 de 13 (5 e 8 meses)	6 de 13 (NI)	20
Gilbert et al	Paclitaxel 200 mg/m^2 (3 horas, a cada 3 semanas)	14	0 de 14 (NI)	7 de 14 (NI)	25
Airoldi et al	Vinorelbina 30 mg/m^2 (semanal)	13	2 de 13 (NI)	6 de 13 (NI)	NI

n=numero de pacientes. NI=Não informado.

Tabela 1. Estudos de monoterapia no carcinoma adenoide cístico (adaptado de LAURIE, *et al.*, 2011).

Uma vez que a monoterapia não tem se mostrado eficaz no tratamento do CAC, buscou-se avaliar a associação de drogas e regimes de tratamento. Dos 17 ensaios clínicos (n total: 143 pacientes) avaliados na revisão de Laurie et al. (2011), a combinação mais utilizada foi de cisplatina com doxorrubicina (droga da família

das antraciclinas). Em 4 ensaios clínicos, ciclofosfamida foi adicionada a essa combinação. Embora protocolos terapêuticos distintos tenham sido utilizados, a combinação destes três agentes levou a uma resposta terapêutica em 9 dos 36 pacientes tratados (DREYFUSS, *et al.*, 1987; BELANI, EISENBERGER, GRAY, 1988; CREAGAN, *et al.*, 1988; LICITRA, *et al.*, 1996). Taxas de reposta semelhantes (25%) também foram alcançadas com a associação de diferentes drogas da família das platinas (ex. cisplatina e carboplatina) associadas com drogas da família das antraciclinas (ex. doxorrubicina, epirubicina, mitoxantrona) (ROSS, *et al.*, 2009; TSUKUDA, *et al.*, 1993; AIROLDI, *et al.*, 1989; AIROLDI, *et al.*, 2000; AIROLDI, *et al.*, 2001; GEDLICKA, *et al.*, 2002; LAURIE, *et al.*, 2010). Entretanto, uma grande limitação de muitos dos ensaios listados é a falta de dados acerca do tempo de duração das respostas encontradas, o que limita a análise sobre a eficácia destas terapias a longo prazo. No carcinoma adenoide cístico, este dado é de especial importância, pois o tumor costuma apresentar recidiva tardia (após 10 anos do seu diagnóstico) (LLOYD, *et al.*, 2011). A Tabela 2 apresenta um resumo destes estudos e seus principais resultados.

Estudo	***Droga/regimento***	***n***	***Resposta objetiva (duração)***	***Estabilização da doença (duração)***	***Sobrevida média (meses)***
Hill et al	Cis: 100 mg/m^2 dia 1 F: 1 g/m^2 diário x4 (ambos a cada 4 semanas)	11	0 de 11	9 de 11 (NI)	12
De Haan et al	Cis: 20 mg/m^2 dias 1-5 D: 50 mg/m^2 dia 1 B: 30 mg/m^2 dias 1-5 (todos a cada 3 semanas)	9	3 de 9 (6, 21, 77 meses)	5 de 9 (3-24 meses)	67
Triozzi et al	C: 1000 mg/m^2 dia 1 Vn: 1 mg dias 1, 4 F: 750 mg/m^2 diário x4 (todos a cada 4 semanas)	8	2 de 8 (NI)	4 de 8 (NI)	NI
Ross	Cis: 60 mg/m^2	8	1 de 8	5 de 8	27

et al	E: 50 mg/m^2 F: 200 mg/m^2 diário (todos a cada 3 semanas)		(34 meses)	(4-16 meses)	
Posner et al	C: 450 mg/m^2 D: 45 mg/m^2 (ambos dia 1 a cada 3 semanas)	5	2 de 5 (2, 8 meses)	NI	8
Dreyfuss et al	C: 500 mg/m^2 D: 50 mg/m^2 Cis: 50 mg/m^2 (ambos dia 1 a cada 4 semanas)	9	3 de 9 (NI)	NI	NI
Belani et al	C: 400 mg/m^2 D: 40 mg/m^2 Cis: 60 mg/m^2 (todos dia 1 a cada 3-5 semanas)	4	1 de 4 (16 meses)	NI	NI
Tsukuda et al	C: 400 mg/m^2 Pr: 40 mg/m^2 Cis: 60 mg/m^2 (todos dia 1 a cada 4 semanas)	6	2 de 6 (NI)	NI	NI
Creagan et al	CAP: diversos	11	2 de 11 (NI)	NI	NI
Licitra et al	C: 500 mg/m^2 D: 50 mg/m^2 Cis: 50 mg/m^2 (todos dia 1 a cada 3 semanas)	12	3 de 12 (resposta parcial 5, 9, 13 meses)	5 de 12 (NI)	34
Dimery et al	C: 500 mg/m^2 dia 1 D: 50 mg/m^2 dia 1 Cis: 40 mg/m^2 dias 2, 3 F: 500 mg/m^2 dias 1, 2 (todos dia 1 a cada 3 semanas)	7	3 de 7 (24, 52, 72 semanas)	4 de 7 (NI)	30

Airoldi et al	Cis: 60 mg/m^2 E: 50 mg/m^2 F: 600 mg/m^2 (todos dia 1 a cada 3 semanas)	4	2 de 4 (9 e 13 meses)	0 de 4	10
Venook et al	Cis: 50 mg/m^2 D: 30 mg/m^2 F: 500 mg/m^2 (todos dia 1, 8 a cada 4 semanas)	9	2 de 9 (resposta parcial)	2 de 9 (NI)	16
Airoldi et al	Cis: 80 mg/m^2 dia 1 V: 25 mg/m^2 dias 1, 8 (ambos a cada 3 semanas)	9	4 de 9 (NI)	NI	NI
Airoldi et al	Cb: AAC 5.5 T: 175 mg/m^2 (3 horas) (ambos dia 1 a cada 3 semanas)	10	2 de 10 (5 e 12 meses)	NI	NI
Gedlicka et al	Cis: 30 mg/m^2 dias 1, 3 M: 12 mg/m^2 dia 1 (ambos a cada 3 semanas)	11	1 de 11 (50 meses)	8 de 11 (9-18 meses)	48
Laurie et al	G: 1000 mg/m^2 dias 1, 8 Cis: 70 mg/m^2 dia 2 ou Cb: AAC 5 dia 1 (todos a cada 3 semanas)	10	2 de 10 (NI)	NI	NI

n=numero de pacientes. NI=Não informado. Cis=cisplatina. F=fluorouracila. D=doxorrubicina. B=bleomicina. C=ciclofosfamida. Vn: vincristina. E=epurubicina. Cb=carboplatina. AAC=área abaixo da curva. Pr=pirarubicina. V=vinorelbina. T=paclitaxel. M=mitoxantrona. G=gencitabina.

Tabela 2. Estudos de politerapia no carcinoma adenoide cístico (adaptado de LAURIE, *et al.*, 2011).

Recentemente, novas drogas de alvo específico têm sido testadas como alternativa ao tratamento do CAC. Como mencionado anteriormente, em torno de 90% destes tumores apresentam expressão aumentada do proto oncogene c-kit (HOLST, *et al.*, 1999; JENG, LIN, HSU, 2000). Este dado justifica a hipótese de que a inibição terapêutica desta proteína pode ser benéfica no tratamento do CAC. De fato, 7 ensaios clínicos de fase 2 ou 3 avaliaram a ação de imatinibe (inibidor especifico de c-kit) (LAURIE, *et al.*, 2011; HOTTE, *et al.*, 2005; LIN, *et al.*, 2005; PFEFFER, *et al.*, 2007; OCHEL, *et al.*, 2005). Entretanto, apenas um estudo apresentou resposta objetiva em 2 dois 21 pacientes tratados. A estabilização da doença foi o evento mais frequente, ocorrendo em 34 dos 71 participantes. Quando imatinibe foi associado com cisplatina, houve melhora na resposta objetiva dos pacientes, sugerindo um efeito benéfico desta associação (GHOSAL, *et al.*, 2011) De modo geral, os estudo não avaliaram o estado de progressão da doença previamente à intervenção. A tabela 3 sumariza os resultados dos ensaios clínicos utilizando imatinibe.

Estudo	***Droga/regimento***	***n***	***Resposta objetiva (duração)***	***Estabilização da doença (duração)***	***Sobrevida média (meses)***
Hotte et al	400 mg VO 2x/dia	15	0 de 15	9 de 15	7
Slevin et al	800 mg/dia por 2 meses; pacientes com doença estabilizada recebiam cisplatina 80 mg/m^2 a cada 3 semana + imatinibe 400 mg diário	17	0 de 17	15 de 17	NI
Pfeiffer et al	400 mg/dia escalada para 800 mg em 4 pacientes	10	0 de 10	2 de 10	NI
Lin et al	400 mg VO 2x/dia	4	0 de 4	1 de 4	6
Ochel et al	400 mg VO diário	4	0 de 4	1 de 4	NI
Guigay	400 mg VO	21	2 de 21	6 de 21	NI

et al	2x/dia	(14 e 15 meses)
n=numero de pacientes. NI=Não informado. VO=via oral		

Tabela 3. Estudos utilizando imatinibe no carcinoma adenoide cístico (adaptado de LAURIE, *et al.*, 2011).

EGFR é outro marcador que, assim como c-kit, apresenta expressão aumentada no CAC (JAIN, *et al.*, 2016). Terapia com agentes de ação específica contra EGFR, como Gefitinibe (GLISSON, *et al.*, 2005) e Cetuximabe (LICITRA, *et al.*, 2006) já foram testados no CAC, porém nenhuma resposta objetiva foi encontrada. Estabilização da lesão ocorreu na maioria dos casos, entretanto nem todos os pacientes estavam experenciando progressão da lesão no momento de entrada no estudo. A tabela 4 mostra um resumo dos principais resultados evidenciados com o uso de fármacos com ação específica.

Estudo	***Droga/regimento***	***n***	***Resposta objetiva (duração)***	***Estabilização da doença (duração)***	***Sobrevida média (meses)***
Glisson et al	Gefitinibe 250 mg VO (diário)	19	0 de 19	13 de 19 (média de 13 semanas)	NI
Locati et al	Cetuximabe 400 mg/m^2 inicial 250 mg/m^2 IV (semanalmente)	23	0 de 23	20 de 23 (média de 6 meses)	NI
Agulnik et al	Lapatinibe 1500 mg VO (diário)	19	0 de 19	15 de 19	NI
Argiris et al	Bortezomibe 1.3 mg/m^2 dias 1, 4, 8, 11 a cada 3 semanas; em progressão da doença, doxorubicina 20 mg/m^2 adicionada dias 1, 8	25	0 de 25	17 de 25	NI
n=numero de pacientes. NI=Não informado. VO=via oral. IV=intra venoso.					

Lapatinibe=inibidor dual de EGRF e HER2. Bortezomibe=inibidor do proteassoma 26S.

Tabela 4. Estudos utilizando agentes de alvo específico no carcinoma adenoide cístico (adaptado de LAURIE, *et al.*, 2011).

De forma geral, os ensaios clínicos apresentados mostraram:

- Numero amostral baixo. A maioria dos estudos, especialmente os que investigaram associação das terapias, o número de 15 participantes não foi ultrapassado;

- Regimes e esquemas de administração dos fármacos não foram padronizados. Quando um fármaco ou associação era testada em mais de um ensaio, seu esquema de administração não seguia uma padronização, dificultando a comparação dos resultados.

- Estabilização da doença foi a resposta mais frequente. A resposta objetiva parcial ou completa foi rara. O desfecho “estabilização da doença” muitas vezes ficou comprometido pela falta de controle acerca da progressão da lesão prévia ao inicio da intervenção.

- Para terapia isolada, baseado somente em dados prospectivos, mitoxantrona e vinorelbina parecem ser opções razoáveis, assim como epirubicina.

- Para terapia combinada, a evidência existente suporta o uso de cisplatina associada com antraciclinas, como doxorrubicina.

- Os dados não favoráveis com o uso de agentes de alvo específico, como imatinibe (c-kit) e cetuximabe (EGFR), não suportam seu emprego na rotina clínica.

Após a análise dos ensaios clínicos, fica evidente a falta de uma opção quimioterápica viável e eficaz para o tratamento dos pacientes com carcinoma adenoide cístico em estado avançado. O retrato desta carência se mostra no último guia do *National Comprehensive Cancer Center* (NCCN), órgão com sede nos EUA. Nele, não existe nenhuma indicação de droga quimioterápica ou protocolo de tratamento medicamentoso específico para pacientes com carcinoma adenoide cístico (https://www.nccn.org/professionals/physician_gls/pdf/head-and-neck.pdf). Dessa forma, é grande a necessidade do desenvolvimento de novas terapias que

beneficiem estes pacientes. Além da necessidade de ensaios clínicos de qualidade avaliando as drogas existentes, é preciso viabilizar a translação de agentes terapêuticos testados em laboratório até a prática clínica.

Modelo de xenoenxerto derivado de paciente

Tradicionalmente, o teste de novos agentes terapêuticos é feito em cultura de células imortalizadas de câncer *in vitro*. Neste modelo, a ação da droga acontece por contato direto com as células dispostas em um ambiente "artificial", muito diferente do microambiente tumoral em que estas se encontrariam em humanos. Por isso, frequentemente se verifica a incompatibilidade dos resultados desses compostos *in vitro* em comparação com seus efeitos em ensaios clínicos com humanos. (PEARSON, *et al.*, 2016; JOHNSON, *et al.*, 2001). Mesmo assim, este modelo tradicional encontra importância na obtenção de dados iniciais sobre toxicidade e ativação de vias de sinalização, por exemplo.

Nesse contexto, os modelos de xenoenxerto derivado de paciente (XEDP, do inglês patient-derived xenograft models, PDX) têm se apresentado como uma alternativa mais eficaz na pesquisa translacional de novos agentes terapêuticos para o combate ao câncer (IZUMCHENKO, *et al.*, 2016). Esta metodologia, que se baseia no direto transplante de fragmento tumoral de paciente em camundongo imunocomprometido, apresenta, entre outras vantagens: (i) capacidade de preservar as características histopatológicas e moleculares do tumor original em um modelo pré-clínico; (ii) possibilita a continuidade e expansão do modelo através de passagens do tumor xenoenxertado em outros animais, sem comprometer as características citadas anteriormente. Cria-se, dessa forma, a possibilidade de se "multiplicar" o tumor de um determinado paciente em inúmeros exemplares para testes terapêuticos *in vivo*. (IZUMCHENKO, *et al.*, 2016, HIDALGO, *et al.*, 2014). Esta característica é de especial valia no estudo de tumores raros, como é caso do CAC.

O modelo XEDP já foi descrito e estabelecido em inúmeros tipos de cânceres (FICHTNER, *et al.*, 2008; DEROSE, *et al.*, 2011; ZHANG, *et al.*, 2013), incluindo o carcinoma espinocelular de cabeça e pescoço (PENG, *et al.*, 2013). Foi verificada a

correlação entre a resposta terapêutica do tumor humano original, em ensaios clínicos, com a resposta verificada em tumores xenoenxertados derivados do mesmo paciente (HIDALGO, *et al.*, 2014). Além disso, estes tumores apresentam estabilidade no perfil de expressão gênica e na resposta a agentes terapêuticos nas diferentes passagens *in vivo* (RUBIO-VIQUEIRA, *et al.*, 2006; KEYSAR, *et al.*, 2013).

O primeiro modelo XEDP de carcinoma adenoide cístico foi desenvolvido por Moskaluk et al. (2011). Naquela ocasião, 17 dos 23 tumores de pacientes implantados efetivamente tiveram sucesso em camundongos. Notavelmente, o aspecto histológico do tumor original humano foi mantido em 100% dos tumores xenoenxertados. De um modo geral, a análise por imunohistoquímica mostrou similaridade na marcação por versican e p63 em ambos os tumores. Além disso, os tumores XEDP também possuíam a translocação t(6;9) de fusão dos genes *MYB-NFIB*, comentada anteriormente nesta revisão. Este trabalho apresentou a primeira evidência mostrando o sucesso no estabelecimento do modelo XEDP de carcinoma adenoide cístico que recapitula as características morfológicas e moleculares do tumor proveniente de paciente sugerindo, assim, o seu potencial como modelo pré-clínico no estudo de protocolos terapêuticos (MOSKALUK, *et al.*, 2011).

Posteriormente, outros grupos de pesquisa foram desenvolvendo os seus próprios modelos XEDP a partir de amostras de tumores provenientes de pacientes (https://www.accrf.org/research/resources-for-researchers/databases/). No ano de 2014, tive a oportunidade de realizar o meu estágio sanduíche de doutorado no laboratório coordenado pelo Prof. Jacques E. Nör, na Faculdade de Odontologia da Universidade de Michigan/EUA. Naquela ocasião, uma das linhas de pesquisa em andamento era a avaliação de agentes terapêuticos em modelos pré-clínicos (XEDP) de carcinoma mucoepidermóide e carcinoma adenoide cístico, provenientes de biópsias realizadas no Hospital da referida universidade.

Em 2015, Acasigua et al publicaram o primeiro relato utilizando o modelo XEDP de CAC estabelecido no laboratório, chamado de UM-PDX-HACC-5 (abreviação para University of Michigan – patient-derived xenograft – human adenoid cystic carcinoma – patient #5) (ACASIGUA, *et al.*, 2015). O objetivo do trabalho foi avaliar a resposta dos tumores UM-PDX-HACC-5 frente à terapia com uma pequena molécula inibidora de Bcl-2 (BM-1197), desenvolvida no laboratório do Prof.

Shaomeng Wang (Centro de Câncer da Universidade de Michigan) (BAI, *et al.*, 2014). A semelhança deste tumor xenoenxertado com o seu doador humano foi confirmada através de comparação morfológica (H/E) e genotipagem de DNA (Short Tandem Repeat (STR) profiling) (WARNER, *et al.*, 2016). Além do inibidor de Bcl-2, Dr. Wang disponibilizou outros agentes terapêuticos para testes nos modelos XEDP de NMGS, entre eles a droga (pequena molécula) inibidora de MDM2 (murine double minute 2), chamada de MI-773. Essa droga, patenteada pela empresa farmacêutica Sanofi (SAR405838), foi desenhada sinteticamente para se ligar a MDM2 e impedir a sua ação inibitória em p53. Dessa forma, p53 é reativado e pode exercer suas funções conhecidas de agente supressor tumoral (WANG, *et al.*, 2014). A interação MDM2-p53, por sua importância nesta tese, será abordada no tópico a seguir.

A Interação MDM2-p53

p53 é, provavelmente, uma das proteínas mais estudadas na literatura. Sua ativação por uma variedade de estressores celulares pode levar à parada do ciclo celular, indução de apoptose e até morte de células que potencialmente poderiam perpetuar alguma mutação oncogênica. Por isso, sua atuação como supressor tumoral é bem estabelecida. Para tal fim, p53 age como fator de transcrição, causando a ativação de proteínas relacionadas com o controle do ciclo celular e indução de apoptose, como p21 e BAX. Os níveis de expressão de p53 também estão sujeitos a regulação através da ação de diversas proteínas (HIF1α, WTq, p300, TAF1131, SV40). Dentre os principais inibidores de p53, destaca-se a proteína MDM2 (ALARCON-VARGAS, RONAI, 2002; DAUJAT, NEEL, PIETTE, 2001).

MDM2 é uma proteína de 491 aminoácidos que interage, através de sua porção N-terminal, com a α-hélice presente no domínio de transativação de p53. O domínio C-terminal de MDM2, por sua vez, possui ação de ubiquitina-ligase E3 em p53. Assim, MDM2 é capaz de neutralizar a ação de p53 não somente pelo fechamento do domínio de ativação transcricional, mas também promovendo a degradação de p53 através de sua ubiquitinização e posterior ação de proteossomas (OLINER, *et al.*, 1993; KUBBUTAT, JONES, VOUSDEN, 1997; HAUPT, *et al.*, 1997).

Dessa forma, a interação MDM2-p53 forma um “feedback” autoregulatório negativo. Isso ocorre pois MDM2 é alvo transcricional de p53. Ao mesmo tempo, MDM2 se liga e inibe a expressão de p53, provocando sua degradação. Em outras palavras, quanto maior a expressão de p53, maior será também a síntese do seu inibidor, MDM2 (WU, *et al.*, 1993). Essa interação é importante para a manutenção da homeostase nos seres vivos, mantendo baixos os níveis de p53. O aumento da expressão dessa proteína pode levar a uma indesejada parada no ciclo celular e indução de apoptose em células do organismo (DAUJAT, NEEL, PIETTE, 2001). De fato, o silenciamento total de MDM2 e o descontrole sobre a expressão de p53 provou ser letal em ratos (JONES, *et al.*, 1995; MONTES DE OCA LUNA, WAGNER, LOZANO, 1995).

Por outro lado, a expressão aumentada de MDM2 pode levar a uma inibição exacerbada de p53 e de suas funções como supressor tumoral, favorecendo os eventos relacionados com a carcinogênese e progressão do câncer (MICHAEL, OREN, 2002). Diversos tumores já apresentaram expressão aumentada de MDM2, que foi associada com um pior prognóstico clínico dos pacientes (CORDON-CARDO, *et al.*, 1994; MOMAND, *et al.*, 1998; JONES, *et al.*, 1998). Especificamente no caso do CAC, o acúmulo de MDM2 vem sendo relacionado com sua tumorigênese e agressividade. A baixa expressão de MDM2 foi observada em subtipos menos agressivos (padrão cribriforme), enquanto que uma alta expressão foi encontrada em subtipos tumorais que apresentam pior prognóstico clínico (padrão sólido) (DE LIMA MDE, *et al.*, 2009; MANTESSO, *et al.*, 2004). Estes dados sugerem que agentes terapêuticos com alvo específico em MDM2 podem apresentar efeito antitumoral em neoplasias com expressão conhecida desta proteína.

Como introduzido anteriormente, MI-773 faz parte família das pequenas moléculas inibidoras de MDM2 (SHANGARY, WANG, 2008; WANG, *et al.*, 2014). A sua estrutura molecular foi desenhada para ocupar os sítios de ligação de MDM2 com p53 com alta especificidade (K_i=0.88 nmol/L). Dessa forma, a droga previne a interação entre MDM2 e p53, levando a reativação de p53 selvagem. O mecanismo de ação de MI-773 foi testado *in vitro* e *in vivo* em modelos de leucemia, osteossarcoma, câncer de próstata e de colo. MI-773 efetivamente ativou p53 selvagem e alguns de seus alvos transcricionais, como p21 e PUMA, induzindo a parada do ciclo celular e indução de apoptose *in vitro*. Além disso, tratamento com

MI-773 em modelos de tumores xenoenxertados causou regressão tumoral duradoura e, em alguns casos, redução completa do tumor (WANG, *et al.*, 2014). Estes dados suportaram a translação de MI-773 para 2 ensaios clínicos (fase 1) visando o tratamento de pacientes portadores de tumores malignos sólidos em estágio avançado (ZHAO, *et al.*, 2015). Um destes estudos continua ativo, porém sem o recrutamento de novos participantes. O outro já foi finalizado, mas seus resultados finais ainda não foram divulgados (https://clinicaltrials.gov).

Em resumo, esta breve introdução buscou salientar o panorama adverso no tratamento de pacientes com carcinoma adenoide cístico em estágio avançado, pela inexistência de uma droga quimioterápica eficaz. Por ser uma doença rara, a metodologia baseada no uso de tumores xenoenxertados derivados de paciente parece ser uma solução potencial para o estudo de novas terapias no tratamento desta neoplasia, uma vez que o tumor de um único paciente pode ser expandido em modelo experimental animal. Os resultados promissores evidenciados com o uso do agente inibidor de MDM2 (MI-773) em diferentes neoplasias, aliado ao fato de que, na maioria das vezes, MDM2 tem sua expressão aumentada no CAC, nos fizeram levantar a hipótese que permeia esta tese: a inibição terapêutica da interação MDM2-p53 com MI-773 é uma alternativa para o tratamento do CAC.

Esta hipótese foi testada e os resultados foram organizados em dois artigos científicos, publicados na revista *Clinical Cancer Research*. Resumidamente, o primeiro artigo buscou avaliar o efeito antitumoral de MI-773 em modelos pré-clínicos de CAC (WARNER, *et al.*, 2016). O segundo artigo, além de confirmar os resultados do primeiro trabalho, buscou avaliar o efeito da combinação terapêutica de MI-773 com cisplatina. Além disso, através de um desenho experimental que mimetiza um ensaio clínico, buscou avaliar o efeito da excisão cirúrgica do tumor combinada com regime neoadjuvante de MI-773 no processo de recorrência do CAC (NÖR, *et al.*, 2016).

3. OBJETIVOS

Objetivo geral

Avaliar a eficácia da inibição terapêutica da interação MDM2-p53 no tratamento do carcinoma adenoide cístico.

Objetivos específicos

- Verificar o efeito terapêutico do inibidor da interação MDM2-p53 (MI-773) no carcinoma adenoide cístico *in vitro* e *in vivo*.

- Verificar o efeito de MI-773 quando associado com cisplatina e na recorrência do carcinoma adenoide cístico.

4. ARTIGOS CIENTÍFICOS

Artigo 1 – WARNER, K. A. et al. Targeting MDM2 for Treatment of Adenoid Cystic Carcinoma. **Clin Cancer Res.**, v. 22, no. 14, p. 3550-3559, Jul. 2016.

Cancer Therapy: Preclinical

Clinical Cancer Research

Targeting MDM2 for Treatment of Adenoid Cystic Carcinoma

Kristy A. Warner[1], Felipe Nör[1,2], Gerson A. Acasigua[1,2], Manoela D. Martins[2,3], Zhaocheng Zhang[1], Scott A. McLean[4,5], Matthew E. Spector[4,5], Douglas B. Chepeha[6], Joseph Helman[5,7], Michael J. Wick[8], Christopher A. Moskaluk[9], Rogerio M. Castilho[3], Alexander T. Pearson[1,5,10], Shaomeng Wang[5,10,11,12], and Jacques E. Nör[1,4,5,13]

Abstract

Purpose: There are no effective treatment options for patients with advanced adenoid cystic carcinoma (ACC). Here, we evaluated the effect of a new small molecule inhibitor of the MDM2–p53 interaction (MI-773) in preclinical models of ACC.

Experimental Design: To evaluate the anti-tumor effect of MI-773, we administered it to mice harboring three different patient-derived xenograft (PDX) models of ACC expressing functional p53. The effect of MI-773 on MDM2, p53, phospho-p53, and p21 was examined by Western blots in 5 low passage primary human ACC cell lines and in MI-773-treated PDX tumors.

Results: Single-agent MI-773 caused tumor regression in the 3 PDX models of ACC studied here. For example, we observed a tumor growth inhibition index of 127% in UM-PDX-HACC-5 tumors that was associated with an increase in the fraction of apoptotic cells ($P = 0.015$). The number of p53-positive cells was increased in MI-773-treated PDX tumors ($P < 0.001$), with a correspondent shift in p53 localization from the nucleus to the cytoplasm. Western blots demonstrated that MI-773 potently induced expression of p53 and its downstream targets p21, MDM2, and induced phosphorylation of p53 (serine 392) in low passage primary human ACC cells. Notably, MI-773 induced a dose-dependent increase in the fraction of apoptotic ACC cells and in the fraction of cells in the G_1 phase of cell cycle ($P < 0.05$).

Conclusions: Collectively, these data demonstrate that therapeutic inhibition of the MDM2–p53 interaction with MI-773 activates downstream effectors of apoptosis and causes robust tumor regression in preclinical models of ACC. *Clin Cancer Res; 22(14); 3550–9. ©2016 AACR.*

Introduction

Adenoid cystic carcinoma (ACC) is one of the two most common malignant salivary gland tumors (1). ACC presents with three different histologic growth patterns. Tubular is the least aggressive, followed by cribriform, and most aggressive is the solid growth pattern (1). Perineural invasion and metastatic spread to distant sites (bones, lungs) are frequently seen in these patients and contribute to poor long-term prognosis (1–4). Although the primary site can be controlled in approximately 30% of ACC patients, they tend to develop distant metastasis and succumb to their disease (5). The standard treatment for these patients is surgery followed by radiation (5, 6). Systemic chemotherapy treatment has been attempted (e.g., cisplatin, paclitaxel, doxorubicin); however, these therapies have low responsive rates (5, 6). An effective systemic therapeutic intervention is required to improve outcomes for patients with ACC.

The function of the tumor suppressor p53 can be inactivated by gene deletion or mutation (7); however, many tumors exhibit wild-type and fully active p53. When p53 is not mutated, its ability to regulate cellular growth, initiate apoptosis, and repair DNA is prevented by the direct interaction with murine double minute (MDM)-2 (8). The proto-oncogene MDM2 was first identified in a spontaneously transformed mouse cell line, and functions as a key negative regulator of p53 that "marks" it for polyubiquitination and degradation through the 26S proteasomal pathway (8, 9). Several studies have reported the expression and function of p53 and MDM2 in malignant salivary gland tumors (10–14). Indeed, it has been suggested that MDM2 participates in ACC tumorigenesis (10, 13, 14), providing a scientific rationale for therapeutic targeting of the MDM2–p53 interaction in these tumors.

[1]Department of Cariology, Restorative Sciences, Endodontics, University of Michigan School of Dentistry, Ann Arbor, Michigan. [2]Department of Oral Pathology, Universidade Federal do Rio Grande do Sul, Porto Alegre, RS, Brazil. [3]Department of Periodontics and Oral Medicine, University of Michigan School of Dentistry, Ann Arbor, Michigan. [4]Department of Otolaryngology, University of Michigan School of Medicine, Ann Arbor, Michigan. [5]University of Michigan Comprehensive Cancer Center, Ann Arbor, Michigan. [6]Department of Otolaryngology, University of Toronto, Ontario, Canada. [7]Department of Oral and Maxillofacial Surgery, University of Michigan School of Dentistry, Ann Arbor, Michigan. [8]South Texas Accelerated Research Therapeutics, San Antonio, Texas. [9]Department of Pathology, University of Virginia, Charlottesville, Virginia. [10]Department of Internal Medicine, University of Michigan School of Medicine, Ann Arbor, Michigan. [11]Department of Pharmacology, University of Michigan School of Medicine, Ann Arbor, Michigan. [12]Department of Medicinal Chemistry, University of Michigan College of Pharmacy, Ann Arbor, Michigan. [13]Department of Biomedical Engineering, University of Michigan College of Engineering, Ann Arbor, Michigan.

Note: Supplementary data for this article are available at Clinical Cancer Research Online (http://clincancerres.aacrjournals.org/).

Corresponding Author: Jacques E. Nör, University of Michigan School of Dentistry, 1011 N. University Rm. 2353, Ann Arbor, MI 48109-1078. Phone: 734-936-0100; Fax: 734-936-1597; E-mail: jenor@umich.edu

doi: 10.1158/1078-0432.CCR-15-1698

Translational Relevance

There are no safe and effective therapies for advanced adenoid cystic carcinoma. Adenoid cystic carcinoma is typically treated with surgery and adjuvant radiation. However, even if the primary site is controlled, patients frequently succumb to distant disease. Despite multiple clinical trials, there is no effective chemotherapeutic for the recurrent/metastatic population. Here, we unveil the therapeutic efficacy of a new small molecule inhibitor of the MDM2–p53 interaction (MI-773) in preclinical models of adenoid cystic carcinoma. We show robust tumor regression in three patient-derived xenograft (PDX) tumor models of adenoid cystic carcinoma, and demonstrate that the mechanism of tumor regression is associated with MI-773–induced tumor cell apoptosis. Collectively, these data suggest that patients with adenoid cystic carcinoma might benefit from therapeutic inhibition of MDM2–p53 interaction.

We have recently reported the isolation and propagation of tumorigenic mucoepidermoid carcinoma cell lines (15). Using collagenase-hyaluronidase to digest human tumors, we were able to establish these tumorigenic cells *in vitro* using an optimal culture medium and *in vivo* in xenograft tumors. Similar approaches with human ACC tumors have failed to establish authentic, tumorigenic ACC cell lines. The Tetas laboratory reported contamination and misidentification of six established ACC cell lines (16). They were determined to be HeLa cells (ACC2, ACC3, ACCM), T24 bladder cancer cells (ACCS) or derived from mouse (ACCNS) or rat (GACC). The Queimado laboratory was able to establish ACC cell lines upon immortalization with HPV16 E6/E7 under a MMLV promoter (17), but these cells were nontumorigenic. Similarly, the El-Naggar laboratory developed an ACC cell line that was immortalized with human telomerase transcriptase (hTert) that is nontumorigenic when transplanted *in vivo* (18). We have attempted to generate tumorigenic ACC cell lines without success so far, and therefore the work presented here utilizes low passage primary ACC cells derived from surgical specimens for *in vitro* studies. Recently, the Moskaluk laboratory was able to develop and characterize xenograft model systems for the study of ACC *in vivo* (19) upon direct transplantation of human ACC tumor tissues into immunodeficient mice. We used a similar approach to establish a patient derived xenograft model (PDX) of ACC, that is UM-PDX-HACC-5. In addition to our in-house model, we also used the ACCx6 and ACCx9 models established by the Moskaluk laboratory (19) for the developmental therapeutic studies included here.

The Wang laboratory has recently developed a new class of small molecule inhibitors of the MDM2–p53 interaction. They have reported that MDM2 inhibitors induce tumor cell apoptosis and inhibit xenograft (e.g., osteosarcoma, prostate, and colon cancer) tumor growth (20–23). Indeed, MI-773 (SAR405838) has advanced into phase I clinical trials for cancer treatment (20). MI-773 binds to MDM2 with high affinity (K_i = 0.88 nmol/L) and blocks the p53–MDM2 interaction (20). Consequently, MI-773 inhibits MDM2-mediated p53 protein degradation resulting in p53 accumulation, activates downstream transcription of p53-targeted genes (e.g., MDM2, p21), and causes apoptotic cell death. However, it is unclear if MI-773 can overcome the typical resistance to therapy observed in ACCs. The purpose of this study was to evaluate the antitumor effect of single agent MI-773 in preclinical models of ACC.

Materials and Methods

Low passage primary human ACC cells

Patients with ACC were recruited and consented with the University of Michigan Head and Neck SPORE consent form that was reviewed and approved by our institutional review board (IRB). Human ACC tumors were minced and digested to generate primary cell cultures, as previously described (15). In contrast to mucoepidermoid carcinomas that were amenable to the spontaneous establishment of immortalized cell lines, the ACC cells used here could be expanded to <20 passages, and therefore are considered low passage primary ACC cells. These primary ACC cells were named the University of Michigan-Human ACC (UM-HACC) series (Supplementary Table S1), and were grown in a salivary gland culture medium (SGM) consisting of high glucose Dulbecco's Modified Eagle Medium (DMEM; Invitrogen) supplemented with 2 mmol/L L-glutamine (Invitrogen), 1% antibiotic (AAA; Sigma-Aldrich), 10% FBS, 20 ng/mL epidermal growth factor (Sigma-Aldrich), 400 ng/mL hydrocortisone, 5 μg/mL insulin, 50 ng/mL cystatin, and 1% amphotericin B (Sigma-Aldrich). UM-HACC-1 cells were derived from a tumor that presented with perineural invasion. UM-HACC-2A cells were derived from an aggressive primary tumor, which presented with a lymph node metastasis (UM-HACC-2B cells). UM-HACC-5 cells were derived from a patient that had perineural and bone invasion at the time of surgery. Cells derived from the UM-HACC-6 patient grew from a recurrent tumor that presented with perineural invasion approximately 15 years after initial diagnosis and treatment, reflecting the slow but aggressive course of ACC. In confirmatory studies, we used 2 additional PDX models of ACC: ACCx6 derived from a lung metastasis and ACCx9 derived from a primary tumor located in the parotid gland (Supplementary Table S1) that were generated and fully characterized in the Moskaluk laboratory (19).

Patient-derived xenograft ACC models

To establish a patient-derived xenograft (PDX) model of ACC, human tumor fragments from the UM-HACC-5 patient were transplanted subcutaneously into the dorsal region of male severe combined immunodeficient (SCID) mice (CB.17.SCID; Charles River). Two of six initial patient tumor fragments transplanted, grew, and were retransplanted *in vivo* into new male or female mice for up to 12 passages. When tumors reached an average of 250 mm^3, mice were randomized into groups and received either vehicle (polyethylene glycol-200 + α-tocopherol polyethylene glycol 1000 succinate; Sigma-Aldrich), or treatment with 10, 50, or 100 mg/kg MI-773 daily by oral gavage. The Institutional Animal Care and Use Committee of the University of Michigan reviewed and approved these procedures. The ACCx6 and ACCx9 models were treated with vehicle or 100 mg/kg MI-773 at South Texas Accelerated Research Therapeutics (START) using the same protocol as described above.

Patient, xenograft tumor, and primary ACC tumor cell authentication

To validate identification of UM-HACC-1, -2A, -2B, -5, and -6 cells, genomic DNA was extracted using the Wizard Genomic DNA Purification Kit (Promega). DNA genotyping by short

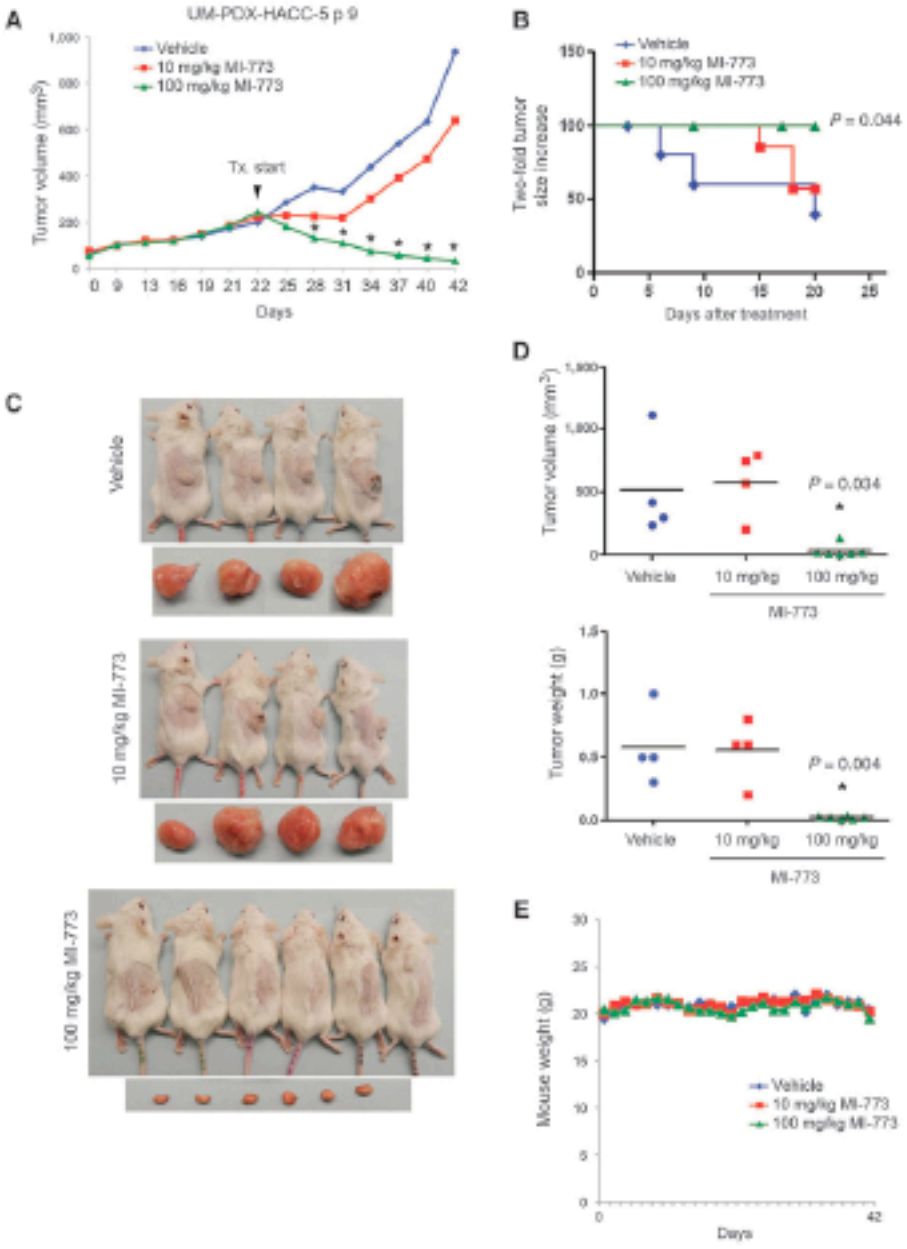
A
UM-PDX-HACC-5 p 9
Vehicle
10 mg/kg MI-773
100 mg/kg MI-773
Tumor volume (mm³)
Tx. start
0 9 13 16 19 21 22 25 28 31 34 37 40 42
Days
B
Vehicle
10 mg/kg MI-773
100 mg/kg MI-773
Two-fold tumor size increase
P = 0.044
Days after treatment
C
Vehicle
10 mg/kg MI-773
100 mg/kg MI-773
D
Tumor volume (mm³)
P = 0.004
Vehicle
10 mg/kg
100 mg/kg
MI-773
Tumor weight (g)
P = 0.004
E
Mouse weight (g)
Vehicle
10 mg/kg MI-773
100 mg/kg MI-773
Days

tandem repeat (STR) profiling was performed and analyzed independently by Genetica DNA laboratories (Burlington, NC) for each matching human tumor, xenograft tumor, and low passage cells. STR profiling confirmed the identity of the low passage primary ACC cells and UM-HACC-5 PDX model (Supplementary Table S2).

Gene sequencing, Western blot, immunohistochemistry, in situ TUNEL staining, and FISH

DNA was extracted from the UM-HACC-5 patient saliva and tumor tissue, UM-PDX-HACC-5 tumors (passages 9, 12), low passage primary human ACC cells UM-HACC-1 (p11), UM-HACC-5 (p8), UM-HACC-6 (p7), UM-HACC-2A (p6), and analyzed for p53 mutations at the University of Michigan DNA Sequencing Core. Sequences were analyzed using the BLAST tool from the National Center for Biotechnology Information (blast.ncbi.nlm.nih.gov). Amino acid sequences were generated using ExPASy online tool (Swiss Institute of Bioinformatics). RNA was extracted with TRizol and protein was extracted with NP-40 lysis buffer from UM-PDX-HACC-5 tumor tissue or UM-HACC cells plated at 2×10^5 cells per 60 mm^3 dishes and grown to 90% confluence in SGM. Lysates were analyzed by PAGE and membranes were blocked for 60 minutes in 5% milk in TBST. Membranes were probed with antibodies to MDM2, p53, EGFR, E-Cadherin, B-actin (Santa Cruz Biotechnology), phospho-p53 (S392), or p21 (Cell Signaling) in TBST, overnight at 4°C. For dose response studies, 2×10^5 cells were plated, attached overnight, treated in fresh medium with 0 to 10 μmol/L MI-773 for 24 hours. Immunohistochemistry was performed on vehicle and MI-773–treated tumors to detect p53, and cytokeratin-7 (Cell Signaling) using standard methods. TUNEL analysis was performed according to manufacturer's instruction using an *in situ* Cell Death Detection Kit (Roche). Morphometric image analysis was performed for cells undergoing apoptosis or expressing p53 using the software ImageJ (NIH, Bethesda, MD). Images of 10 fields of each slide (three slides per group) were captured at 400× magnification using a QImaging-ExiAqua monochrome digital camera attached to a Nikon Microscope (Nikon) and visualized with QCapturePro software. All positive and negative cells were counted in each field and the percentage of total number of positive cells was calculated. Fluorescence *in situ* hybridization (FISH) analysis was performed using a centromeric BAC probe labeled in fluorescein and a telomeric BAC probe labeled with 5-Rox (red), as described (19).

Cytotoxicity, flow cytometry, and p63 gene silencing

Sulforhodamine B (SRB) or the WST-1 (Roche) cytotoxicity assay were performed to determine the effect of MI-773 on ACC cell viability, as we described (24). Briefly, 1 to 3×10^3 UM-HACC cells were plated per well, and treated with 0 to 40 μmol/L MI-773 for 24 to 96 hours. To assess apoptosis, 2×10^5 cells were plated in 60 mm^3 dishes, attached overnight, and treated with 0 to 20 μmol/L MI-773 for 72 hours. Cells were lysed with a hypotonic buffer and stained with propidium iodide, as described (24). Primary low passage ACC cells (UM-HACC-5) were stably transduced with lentiviral vectors expressing shRNA-p53 or scrambled sequence control shRNA-C (University of Michigan Vector Core) and selected with 1.0 μg/mL puromycin (Sigma).

Statistical analyses

Censored survival estimates were determined using Kaplan–Meier curves and statistical significance was determined using log rank (Mantel–Cox) test. Tumor growth inhibition (TGI) was calculated using the formula: $1 - [(\text{Treated final} - \text{Treated initial})/(\text{Control final} - \text{Control initial})]$. Percent shrinkage was determined by $1 - (\text{Treated final} - \text{Treated initial}) \times 100$. One-way ANOVA, followed by *post hoc* tests (Tukey test), Mann–Whitney *U*-test, or Student *t*-test were used to determine significant differences in tumor growth, weight, volume, apoptosis levels, cell viability, TUNEL, and p53 expression in control and treated tumors. Significance was determined at $P < 0.05$.

Results

Establishment and characterization of a PDX model of ACC

To establish the UM-PDX-HACC-5 model, we transplanted human tumor fragments into SCID mice (Supplementary Fig. S1). Two oral pathologists (PN, MDM) evaluated the histopathology of these tumors and observed a tubular-cribriform pattern with areas of perineural invasion (Supplementary Fig. S1A), which is representative of the typical pathobiology of ACC. The first passage xenograft tumors showed similar histopathologic patterns to the human tumor. With increasing *in vivo* passages, the PDX tumors acquired a more solid subtype with frequent mitotic figures and cellular pleomorphism, which correlated with a sharp increase in tumor growth rates and tumor take (Supplementary Fig. S1A and S1B). Although first passage tumors reached 600 to 900 mm^3 within 70 to 84 days, higher passage tumors reached similar size in approximately 35 to 40 days (Supplementary Fig. S1B). Notably, tumor take was consistently high (93/113, 82.3%) for this model (Supplementary Fig. S1C).

To determine if UM-PDX-HACC-5 tumors had the MYB–NFIB translocation, fluorescent *in situ* hybridization (FISH) analysis was performed on passage 3 tumors. The break-apart photo shows at least two cells with two fused red/green signals indicating intact *MYB* loci. The fusion FISH photo shows a representative cell with distinct green and red signals indicating the 2 genes remain separate (Supplementary Fig. S1D). These results indicate that the UM-PDX-HACC-5 model is representative of the 30% to 40% of ACC that do not have the MYB–NFIB translocation. Notably, we observed that the expression of key targets of MI-773 (i.e., MDM2, p53, p63) is relatively stable over *in vivo* passaging (Supplementary Fig. S1E).

Figure 1.

MI-773 induces tumor regression in UM-PDX-HACC-5, a PDX model of ACC. A, graph depicting average tumor volume in mice that received 10, 100 mg/kg MI-773 or vehicle via daily oral gavage for 20 days. Treatment started when tumors were approximately 200 mm^3. *, $P < 0.05$. B, Kaplan-Meier analysis of time to failure, as defined by doubling tumor volume as compared to pretreatment volume ($n = 6$–8/group). C, photographs of the mice and tumors immediately after euthanasia. D, graphs depicting actual weight and volume of tumors retrieved from the mice at the termination of the experiment. E, graph depicting mouse weight for the duration of the experiment.

Table 1. Table showing tumor growth inhibition (TGI) index and percent tumor shrinkage in mice treated with vehicle, 10, 100 mg/kg MI-773, as compared to pretreatment volumes

Treatment	Dose (mg/kg)	Route/schedule	Pretreatment (mean ± SD)	Final (mean ± SD)	Mean difference	TGI	Shrinkage (%)
Vehicle	0	P.O.; daily	1612 ± 90.1	936.9 ± 936.0	+767.7	–	NA
MI-773	10	P.O.; daily	2592 ± 51.4	740.5 ± 350.2	+503.1	34	NA
MI-773	100	P.O.; daily	2423 ± 80.9	33.0 ± 4.9	−209.2	127	86

NOTE: TGI greater than 50 is typically considered significant.

MI-773 promotes ACC tumor regression

To evaluate the antitumor effect of MI-773, PDX tumors were transplanted into SCID mice, allowed to grow to an average of 250 mm^3, and then mice were treated with 0 to 100 mg/kg MI-773. MI-773 at 10 mg/kg modestly reduced the rate of tumor growth, whereas 100 mg/kg caused significant tumor regression (Fig. 1A). Control tumors reached an average of 1,000 mm^3 at 20 days of treatment, compared to an average volume of 600 mm^3 for the 10 mg/kg group and 30 mm^3 for the 100 mg/kg group. Kaplan–Meier analysis showed an increase in tumor failure, defined as two times increase in tumor volume as compared to pretreatment volume ($P = 0.044$), for vehicle-treated mice when compared to mice treated with 100 mg/kg MI-773 (Fig. 1B and C). These data were confirmed by the evaluation of tumor weight and volume at the end of the experiment (Fig. 1D). MI-773 was well tolerated by the mice, as shown by the lack of observable weight loss during the experimental period (Fig. 1E). To better understand the antitumor effect of MI-773 in preclinical models of ACC, the tumor growth inhibition (TGI) index was calculated for each treatment condition. Although 10 mg/kg MI-773 mediated a TGI of 34%, 100 mg/kg MI-773 had a TGI of 127%, with robust tumor shrinkage of 86% (Table 1). Two additional PDX models of ACC (ACCx6 and ACCx9; ref. 19) were used to verify the scope of the antitumor effect of MI-773. We observed that MI-773 mediated tumor regression in the ACCx6 model ($P = 0.044$) and in the ACCx9 model ($P = 0.012$), as compared to vehicle-treated controls (Fig. 2A and B). As expected, MI-773 was well tolerated in these mice, as demonstrated by maintenance of body weight in the treatment group (Fig. 2C and D).

To further verify the antitumor effect of MI-773, two independent experiments were performed using the UM-PDX-HACC-5 model. Again, 100 mg/kg MI-773 mediated potent tumor regression (Supplementary Figs. S2A, S2D, S2F and S3A, S3D, S3F). Treated tumors were visibly smaller, and mice did not lose weight upon treatment (Supplementary Figs. S2C, S2E and S3C, S3E). We noted that 10 or 50 mg/kg MI-773 were not sufficient to cause significant tumor regression, suggesting that a higher dose (e.g., 100 mg/kg) is necessary for measurable antitumor effect in mice (Fig. 1A and Supplementary Fig. S3A). Kaplan–Meier analyses confirmed that 100 mg/kg MI-773 prevents tumor failure, when compared to vehicle or lower dose MI-773 (Supplementary Figs. 2SB and 3SB). Taken together, these data demonstrate that single-agent MI-773 mediates ACC tumor regression without observable systemic cytotoxicity in mice.

MI-773 induces ACC apoptosis

To begin to evaluate possible mechanisms of MI-773–induced ACC tumor regression, we performed in situ TUNEL analysis (Fig. 3A) in tissues collected from mice treated in the experiment showed in Figure 1. The percentage of apoptotic cells in the MI-773–treated tumors was higher ($P = 0.015$) than in tumors from vehicle-treated mice (Fig. 3B). To further understand mechanisms of MI-773–induced ACC cell death, we performed viability assays on low passage UM-HACC-5 cells that showed low micromolar IC_{50} for MI-773 upon 48 or 96 hours of treatment (Fig. 3C). We also observed a dose-dependent induction of UM-HACC-5 apoptosis after 72 hours (Fig. 3D) that was accompanied by a gradual decrease in the fraction of cells in G_2–M phase of cell cycle (Fig. 3E). Additional cell viability assays performed in UM-HACC-5 and UM-HACC-6 cells in vitro showed similar trends of response to MI-773 treatment (Supplementary Fig. S4A and S4B). To verify the dependency of MI-773's effect on the function of p53, we partially silenced p53 expression in UM-HACC-5 cells with an shRNA-p53 construct. We observed that p53-silenced cells exhibit a higher IC_{50} than shRNA-C control cells (Supplementary Fig. S4C–S4E).

Histopathologic characteristics associated with MI-773–induced tumor regression

To improve the characterization of the tumors treated with MI-773, two oral pathologists (FN, MDM) performed histopathologic analysis of tissue specimens upon termination of treatment. In vehicle control tumors, intense cellular pleomorphism, cells with large and/or hyperchromatic nucleus, prominent nucleoli, and loosely packed chromatin, altered nuclear-cytoplasmic ratio, and frequent infiltration in muscle, nerve, and adipose tissue were observed (Supplementary Fig. S5A). The morphology of tumors treated with MI-773 was very different: round cells exhibited a vacuolated cytoplasm and many granules were surrounded by a hyaline connective tissue (Supplementary Fig. S5B). Treated tumors did not invade into adjacent muscle tissue, but infiltration of tumor cells into nerve and adipose tissues were present in some areas. To confirm that the unusual-shaped cells were indeed epithelial, immunohistochemical staining was performed and showed high cytokeratin-7 positivity in both vehicle and MI-773–treated tumors (Fig. 4A). Immunohistochemical staining also showed more p53-positive cells in MI-773–treated tumors than in vehicle control tumors ($P < 0.001$; Fig. 4A and B). Notably, although most of the vehicle-treated tumors exhibited p53 primarily localized in the nucleus, tumors treated with MI-773 showed primarily cytoplasmic localization of p53 (Fig. 4A and C). In addition, increased levels of p53 and phospho-p53 (S392) proteins were detected in tumors treated with MI-773, when compared to vehicle tumors (Fig. 4D).

MI-773 potently activates MDM2, p53, and p21 in low passage ACC cells

Low passage ACC cells were screened by Western blot for basal levels of p53, EGFR, and ECAD, using as controls two mucoepidermoid carcinoma cell lines (UM-HMC-3A, UM-HMC-3B) previously characterized in our laboratory

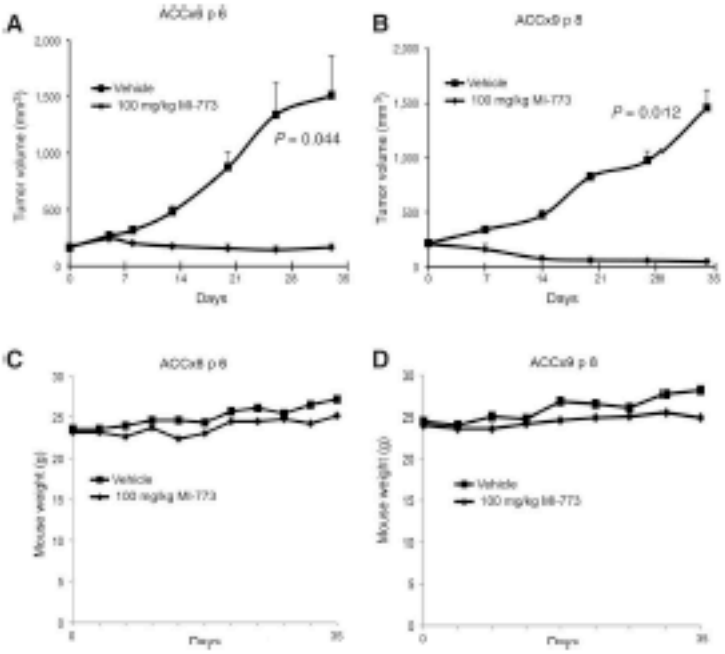

Figure 2.
MI-773 induces tumor regression in two additional PDX models of ACC. A, B, graphs depicting average tumor volume in mice harboring ACCx6 (A) or ACCx9 (B) that received 100 mg/kg MI-773 or vehicle via daily oral gavage. Treatment started when tumors were approximately 200 mm^3. C, D, graphs depicting mouse weight for the duration of the experiment.

(15). We observed that baseline p53 levels varied according to cell line, but they were relatively stable over different passages in most cell lines (Fig. 5A and B). EGFR and ECAD expression levels were lower in UM-HACC-2B cells than in the other UM-HACC cells (Fig. 5A), and highly expressed in UM-HMC-3A and UM-HMC-3B, as previously reported (15). We then evaluated the effect of MI-773 on the activation of key downstream effectors and observed a potent and dose-dependent activation of MDM2, p53, and p21 in all five low passage primary human ACC cell lines evaluated here (Fig. 5C). We also observed an overall pattern of induction of p53 phosphorylation at serine 392 promoted by increasing concentrations of MI-773 (Fig. 5D). These results suggested that the p53 axis is functional in the ACC models studied here. Nevertheless, we performed DNA sequencing that showed wild-type TP53 gene in all ACC models used here, except for a possible polymorphism at position 72 in the UM-HACC-5 cells that was not observed in the correspondent UM-PDX-HACC-5 model (Supplementary Fig. S6). Taken together, these data support a potent and specific pro-apoptotic effect of MI-773 mediated by the activation of the p53 signaling axis in several preclinical models of human ACC.

Discussion

A cure is typically not achievable for many patients with ACC due to the lack of effective and safe systemic antitumor agents for this malignancy. The lack of experimental models has hindered progress in the discovery of therapies for this cancer. Patients are left without alternatives beyond surgery (when possible) and radiation. Here we characterize a new PDX model of ACC, and used two previously established models of ACC (19), to test a novel potent and specific small molecule inhibitor of the MDM2–p53 interaction.

The UM-PDX-HACC-5 model was generated from an ACC located in a minor salivary gland from the hard palate that exhibited a primarily solid histopathologic subtype, which correlates with more aggressive disease in humans (1). PDX tumors at *in vivo* passages 2 and higher grew to 2,000 mm^3 within 30 days, exhibiting a vigorous growth pattern characteristic of highly aggressive tumors. We consider this model uniquely suited for developmental therapeutic studies because it is very aggressive, and therefore it provides a rigorous platform for the testing of new anticancer drugs. To better mimic epidemiological realities and clinical scenarios, we chose to perform our experiments in female mice reflecting the fact that ACC is more common in women (25). In addition, the work with the UM-PDX-HACC-5 model, we also tested MI-773 in ACCx6 PDX tumors derived from a lung metastasis (grade 2) and in the ACCx9 PDX model developed from a primary parotid tumor (grade 3). It is well-known that a specific gene translocation identified as t(6;9) results in the fusion of MYB proto-oncogene with the transcription factor NFIB and is rather frequent in ACCs (26–28). This translocation is detected in ACCx9 tumors, but was not present in ACCx6 (19) or UM-PDX-HACC-5 tumors. Therefore, the preclinical models used here represent a diverse panel of ACC tumors that is perhaps representative of the typical diversity of presentation of this disease.

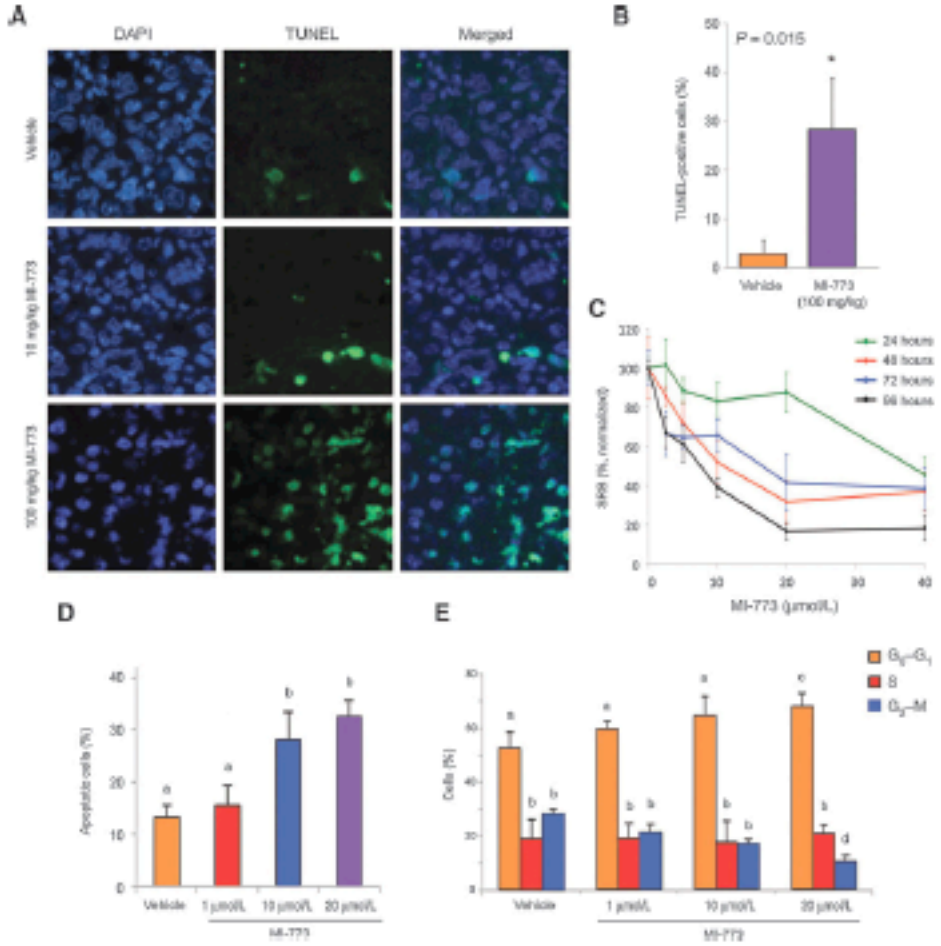

Figure 3.

MI-773 induces tumor cell apoptosis. A, photomicrographs of TUNEL-positive cells (green) and DAPI (blue) in tumors from mice that received vehicle, 10 or 100 mg/kg MI-773. B, graph depicting the percentage of TUNEL-positive cells from tumors represented in A. C, graph depicting toxicity of MI-773 in UM-HACC-5 cells *in vitro*, as determined by SRB assay. D, graph depicting the fraction of apoptotic cells after 72 hours of treatment with MI-773, as determined by the fraction of cells in sub-G_0–G_1 after propidium iodide staining. E, graph depicting the fraction of cells/cell cycle phase after 72 hours of treatment with MI-773, as determined by propidium iodide staining. Different lower case letters represent $P < 0.05$.

MI-773–mediated potent tumor regression in the three PDX models evaluated here, despite differences in tumor site, grade, or MYB-NFIB status. Indeed, we observed robust and unequivocal tumor regression caused by single-agent MI-773 in several independent experiments. Notably, the tumor regression observed here was not accompanied by objective signs of systemic toxicities, as shown by the maintenance of mouse weight throughout the experimental period.

The histopathologic changes reported here correlated with a significant increase in p53 expression and a shift in the localization of p53 from the nucleus to the cytoplasm in tumors treated with MI-773. It is well known that p53 has multiple roles depending on its cellular location and level of activation (29–31). When located in the nucleus, p53 functions primarily as a transcription factor to induce expression of several proteins related to cell signaling, angiogenesis, autophagy, and apoptosis. Cytoplasmic functions of p53 include transcription-independent mechanisms to induce apoptosis by interacting directly with pro-apoptotic proteins (29–31). The correlation of significant induction of apoptosis with the

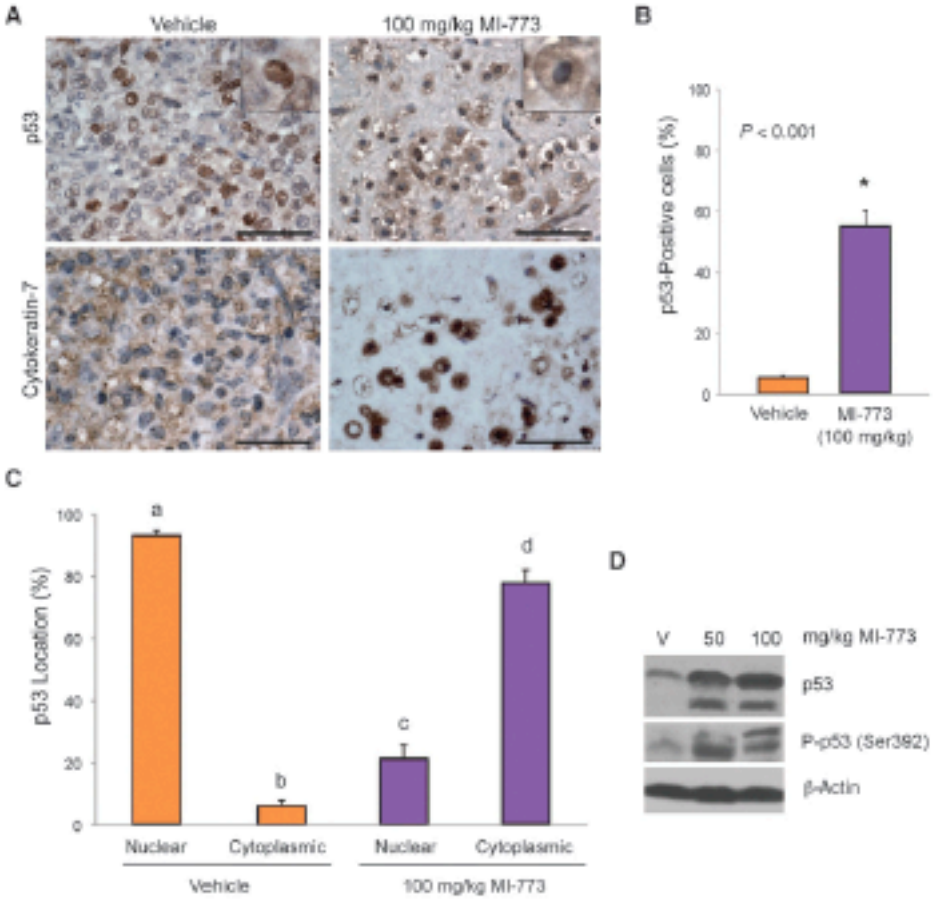

Figure 4.
MI-773 induces p53 expression in ACC tumors *in vivo*. A, photomicrographs of immunohistochemistry for p53 and cytokeratin 7 in vehicle or 100 mg/kg MI-773–treated tumors. Inserts depict representative cells at high magnification. Note the shift of p53 from the nucleus (vehicle group) to the cytoplasm (MI-773–treated group). B, graph depicting the percentage of p53-positive cells in ACC tumors represented in A. $P < 0.05$. C, graph depicting the localization of p53 (nucleus or cytoplasm) in tumors retrieved from mice that received vehicle or 100 mg/kg MI-773. Different lower case letters represent $P < 0.05$. Scale bars = 50 μm. D, Western blot showing p53 and phospho-p53 (Ser392) in whole tumor lysates prepared from mice that received vehicle, 50, or 100 mg/kg MI-773.

shuttling of p53 from the nucleus to the cytoplasm upon treatment with MI-773 suggests that this small molecule inhibitor is working through transcription-independent mechanisms to induce tumor cell death *in vivo*.

Results from our *in vivo* experiments, and particularly the Western blots performed with a panel of primary human low passage ACC cells demonstrated a potent, dose-dependent activation of p53 and its downstream transcriptional targets p21 and MDM2. We also observed potent induction of phosphorylation of p53 at the Serine 392 position by MI-773. This is considered a common site for p53 phosphorylation by various therapeutic agents, such as etoposide, UV, ionizing radiation, and Nutlin3, another inhibitor of the MDM2–p53 interaction (32, 33). Collectively, these data provide support to the specific effect of MI-773 on its expected targets, and suggest the function of wild-type p53 in these cells (20). Indeed, gene sequencing revealed that the TP53 gene was not mutated in any of the ACC models evaluated here. The only change that we observed was a polymorphism at amino acid 72 that was detected in our UM-HACC-5 low passage cells. This polymorphism (arginine

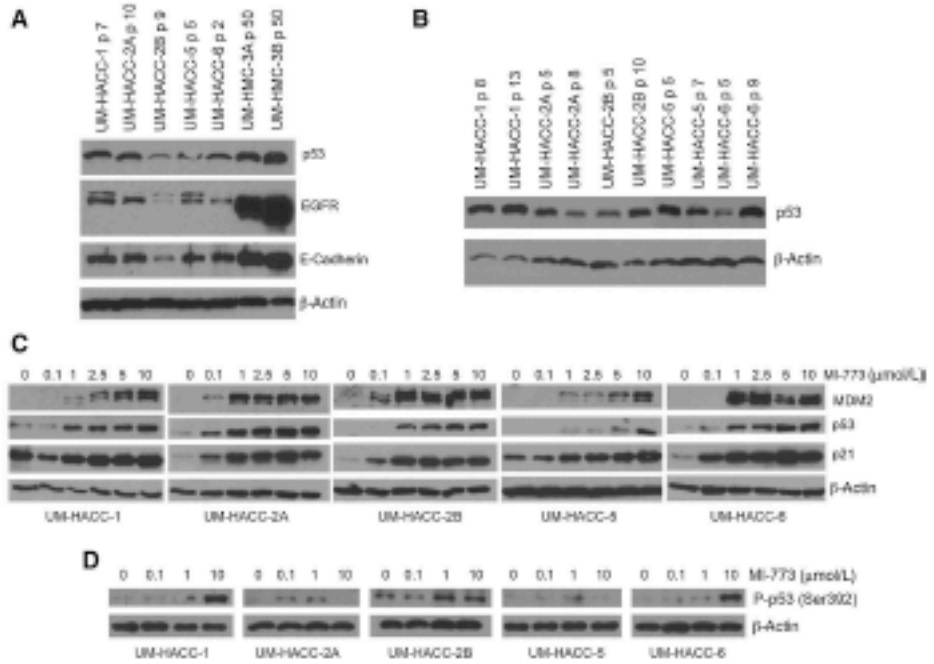

Figure 5.
Effect of MI-773 on its targets and downstream effectors in ACC tumor cells *in vitro*. A, Western blot for p53, EGFR, and E-Cadherin in a panel of low passage primary human cells (UM-HACC series). Mucoepidermoid carcinoma cells (UM-HMC-3A/-3B) served as controls for p53, EGFR, and E-Cadherin. B, Western blots showing levels of p53 over different passages in a panel of primary human ACC cells. C, D, Western blots for MDM2, p53, p21, and phospho-p53 (Ser392) expression upon treatment with increasing concentrations of MI-773 (24 hours) in a panel of low passage UM-HACC cells.

or proline) has been well documented as having no impact on p53 function (34, 35).

In summary, we present here strong preclinical evidence for the therapeutic potential of the new small molecule inhibitor of the MDM2–p53 interaction (MI-773) in ACC. The development of potent inhibitors of MDM2 is an area of intense research today, as demonstrated by the fact that seven small molecule inhibitors of MDM2 (including MI-773) are currently in clinical trials (33). Considering the potent tumor regression observed with single-agent MI-773 in models of aggressive ACC, it is tempting to say that MDM2 inhibition may offer the first effective therapy for these patients. This hypothesis, however, will have to be challenged in well-conducted randomized clinical trials.

Disclosure of Potential Conflicts of Interest

C.A. Moskaluk is a consultant/advisory board member for Novartis. S. Wang has ownership interest (including patents) in Ascenta Therapeutics, and reports receiving commercial research grants from Ascenta Therapeutics/Sanofi. No potential conflicts of interest were disclosed by the other authors.

Authors' Contributions

Conception and design: C.A. Acquaviva, J.E. Nör
Development of methodology: K.A. Warner, C.A. Acquaviva, Z. Zhang, M.J. Wick, J.E. Nör
Acquisition of data (provided animals, acquired and managed patients, provided facilities, etc.): K.A. Warner, F. Nör, C.A. Acquaviva, M.D. Martins, M.E. Spector, J. Hoffman, M.J. Wick, C.A. Moskaluk, R.M. Castilho, A.T. Pearson, J.E. Nör
Analysis and interpretation of data (e.g., statistical analysis, biostatistics, computational analysis): K.A. Warner, F. Nör, C.A. Acquaviva, M.D. Martins, C.A. Moskaluk, R.M. Castilho, A.T. Pearson, J.E. Nör
Writing, review, and/or revision of the manuscript: K.A. Warner, F. Nör, C.A. Acquaviva, S.A. McLean, M.E. Spector, D.B. Chepeha, A.T. Pearson, J.E. Nör
Administrative, technical, or material support (i.e., reporting or organizing data, constructing databases): K.A. Warner, M.E. Spector, D.B. Chepeha, J.E. Nör
Study supervision: J.E. Nör
Other (technical assistance and data analysis): Z. Zhang
Other (specimen collection): D.B. Chepeha
Other (providing the drug): S. Wang

Acknowledgments

The authors thank the patients who kindly provided the tumor specimens used to generate the ACC cells and PDX models that enabled this research project. The authors also thank the surgeons, nurses, and support staff that enabled the process of tumor specimen collection and processing for use in research. The authors also thank Jeffrey Kaufman and the Adenoid Cystic Carcinoma Research Foundation (AACRF)

for the strong support and encouragement received throughout this project.

Grant Support

This work was funded by a grant from the Adenoid Cystic Carcinoma Research Foundation (AACRF); University of Michigan Head Neck SPORE P50-CA-97248 from the NIH/NCI; and grants R01-DE21220, R01-DE21139 from the NIH/NIDCR (RN).

The costs of publication of this article were defrayed in part by the payment of page charges. This article must therefore be hereby marked advertisement in accordance with 18 U.S.C. Section 1734 solely to indicate this fact.

Received July 16, 2015; revised January 14, 2016; accepted February 8, 2016; published OnlineFirst March 2, 2016.

References

1. Seethala RR. An update on grading of salivary gland carcinomas. Head Neck Pathol 2009;3:69–77.
2. Simpson RH, Skálová A, Di Palma S, Leivo I. Recent advances in the diagnostic pathology of salivary carcinomas. Virchows Arch 2014;465: 371–84.
3. Kowalski PJ, Paulino AF. Perineural invasion in adenoid cystic carcinoma: In causation/promotion by brain-derived neurotrophic factor. Hum Pathol 2002;33:933–6.
4. Marchiò C, Weigelt B, Reis-Filho JS. Adenoid cystic carcinomas of the breast and salivary glands (or 'The strange case of Dr Jekyll and Mr. Hyde' of exocrine gland carcinomas). J Clin Pathol 2010;63:220–8.
5. Dodd RL, Slevin NJ. Salivary gland adenoid cystic carcinoma: a review of chemotherapy and molecular therapies. Oral Oncol 2006;42:759–69.
6. Milano A, Longo F, Basile M, Iaffaioli RV, Caponigro F. Recent advances in the treatment of salivary gland cancers: emphasis on molecular targeted therapy. Oral Oncol 2007;43:729–34.
7. Halazonetis TD, Gorgoulis VG, Bartek J. An oncogene-induced DNA damage model for cancer development. Science 2008;319:1352–5.
8. Hollstein M, Sidransky D, Vogelstein B, Harris CC. p53 mutations in human cancers. Science 1991;253:49–53.
9. Soussi T, Dehouche K, Béroud C. p53 website and analysis of p53 mutations in human cancer: forging a link between epidemiology and carcinogenesis. Hum Mutat 2000;15:105–13.
10. Soussi T, Wiman KG. Shaping genetic alterations in human cancer: the p53 mutation paradigm. Cell Death Differ 2007;14:251–9.
11. Vousden KH, Lane DP. p53 in health and disease. Nat Rev Mol Cell Biol 2007;8:275–83.
12. Vousden KH, Prives C. Blinded by the Light: The Growing Complexity of p53. Cell 2009;137:413–31.
13. Bond GL, Hu W, Levine A. MDM2 is a central node in the p53 pathway: 12 years and counting. Curr Cancer Drug Targets 2005;5:3–8.
14. Momand J, Zambetti GP, Olson DC, George D, Levine AJ. The mdm-2 oncogene product forms a complex with the p53 protein and inhibits p53-mediated transactivation. Cell 1992;69:1237–45.
15. Oliner JD, Pietenpol JA, Thiagalingam S, Gyuris J, Kinzler KW, Vogelstein B. Oncoprotein MDM2 conceals the activation domain of tumour suppressor p53. Nature 1993;362:857–60.
16. Kussie PH, Gorina S, Marechal V, Elenbaas B, Moreau J, Levine AJ, et al. Structure of the MDM2 oncoprotein bound to the p53 tumor suppressor transactivation domain. Science 1996;274:948–53.
17. Wade M, Wahl GM. Targeting tumor cells with small molecule antagonists of MDM2. Genes Cancer 2012;3:283–9.
18. Vassilev LT, Vu BT, Graves B, Carvajal D, Podlaski F, Filipovic Z, et al. In vivo activation of the p53 pathway by small-molecule antagonists of MDM2. Science 2004;303:844–8.
19. Shangary S, Qin D, McEachern D, Liu M, Miller RS, Qiu S, et al. Temporal activation of p53 by a specific MDM2 inhibitor is selectively toxic to tumors and leads to complete tumor growth inhibition. Proc Natl Acad Sci U S A 2008;105:3933–8.
20. Vu B, Wovkulich P, Pizzolato G, Lovey A, Ding Q, Jiang N, et al. Discovery of RG7112: A Small-Molecule Insensitive 1 Inhibitor Clinical Development. ACS Med Chem Lett 2013;4:466–70.
21. Ding Q, Zhang Z, Liu JJ, Jiang N, Zhang J, Ross TM, et al. Discovery of RG7388, a potent and selective p53-MDM2 inhibitor in clinical development. J Med Chem 2013;56:5979–83.
22. Wang S, Sun W, Zhao Y, McEachern D, Meaux I, Barrière C, et al. SAR405838: an optimized inhibitor of MDM2-p53 interaction that induces complete and durable tumor regression. Cancer Res 2014;74: 5855–65.
23. Yu S, Qin D, Shangary S, Chen J, Wang G, Ding K, et al. Potent and orally active small-molecule inhibitors of the MDM2-p53 interaction. J Med Chem 2009;52:7970–3.
24. Azmi AS, Aboukameel A, Banerjee S, Wang Z, Mohammad M, Wu J, et al. MDM2 inhibitor MI-319 in combination with cisplatin is an effective treatment for pancreatic cancer independent of p53 function. Eur J Cancer 2010;46:1122–31.
25. Zhao Y, Yu S, Sun W, Liu L, Lu J, McEachern D, et al. A potent small-molecule inhibitor of the MDM2-p53 interaction (MI-888) achieved complete and durable tumor regression in mice. J Med Chem 2013;56: 5553–61.
26. Zeldin RD, Jiao R, Dong Z, Warner K, Wang G, Nikolovska-Coleska Z, et al. Antiangiogenic effect of TW37, a small-molecule inhibitor of Bcl-2. Cancer Res 2006;66:6098–706.
27. Boukheris H, Curtis RE, Land CE, Dores GM. Incidence of carcinoma of the major salivary glands according to the WHO classification, 1992 to 2006: a population-based study in the United States. Cancer Epidemiol Biomarkers Prev 2009;18:2899–906.
28. Brill LB 2nd, Kanner WA, Fehr A, Andrén Y, Moskaluk CA, Löning T, et al. Analysis of MYB expression and MYB-NFIB gene fusions in adenoid cystic carcinoma and other salivary neoplasms. Mod Pathol 2011;24:1169–76.
29. West RB, Kong C, Clarke N, Gilks T, Lipsick JS, Cao H, et al. MYB expression and translocation in adenoid cystic carcinomas and other salivary gland tumors with clinicopathologic correlation. Am J Surg Pathol 2011;35:92–9.
30. Persson M, Andrén Y, Mark J, Horlings HM, Persson F, Stenman G. Recurrent fusion of MYB and NFIB transcription factor genes in carcinomas of the breast and head and neck. Proc Natl Acad Sci U S A. 2009;106: 18740–4.
31. Green DR, Kroemer G. Cytoplasmic functions of the tumour suppressor p53. Nature 2009;458:1127–30.
32. Vaseva AV, Moll UM. The mitochondrial p53 pathway. Biochim Biophys Acta 2009;1787:414–20.
33. Speidel D. Transcription-independent p53 apoptosis: an alternative route to death. Trends Cell Biol 2010;20:14–24.
34. Cox ML, Meek DW. Phosphorylation of serine 392 in p53 is a common and integral event during p53 induction by diverse stimuli. Cell Signal 2010; 22:564–71.
35. Zhao Y, Aguilar A, Bernard D, Wang S. Small-molecule inhibitors of the MDM2-p53 protein-protein interaction (MDM2 Inhibitors) in clinical trials for cancer treatment. J Med Chem 2015;58:1038–52.
36. Whibley C, Pharoah PD, Hollstein M. p53 polymorphisms: cancer implications. Nat Rev Cancer 2009;9:95–107.
37. Thomas M, Kalita A, Labrecque S, Pim D, Banks L, Matlashewski G. Two polymorphic variants of wild-type p53 differ biochemically and biologically. Mol Cell Biol 1999;19:1092–100.

Supplementary Table Legends

Supplementary Table S1. Table depicting patient demographics and tumor characteristics.

Supplementary Table S2. Table depicting short tandem repeat (STR) profiles of patient 5, UM-HACC-5 cells at passage 7, and patient-derived xenograft (PDX) tumors at passages 5, 9 and 12. STR profiles for UM-HACC-1 cells at passage 7 and 13. STR profiles for patient 2, UM-HACC-2A and UM-HACC-2B cells at passage 14. STR profiles for patient 6 and UM-HACC-6 cells at passage 6.

Supplementary Figure Legends

Supplementary Figure S1. Characterization of UM-PDX-HACC-5, a patient-derived xenograft (PDX) model of adenoid cystic carcinoma. A, photomicrographs depicting hematoxilin and eosin staining of the primary tumor (patient 5), and PDX adenoid cystic tumors (UM-PDX-HACC-5) at *in vivo* passages 1-12. B, graph depicting tumor volume over time for UM-PDX-HACC-5 tumors over 12 *in vivo* passages. C, table depicting percentage tumor take per *in vivo* passage of UM-PDX-HACC-5 tumors. D, Representative images of the FISH analysis. The break-apart image shows at least two cells with two fused red/green signals indicating intact MYB loci. The fusion FISH image shows a representative cell with distinct green and red signals indicating the 2 genes remain separate. E, Western blot showing expression levels of MDM2, p53 and p63 in UM-PDX-HACC-5 tumors at *in vivo* passages 2, 9 and 12.

Supplementary Figure S2. MI-773 induces ACC tumor regression. A, graph depicting average tumor volume of mice that received 100 mg/kg MI-773 or vehicle via daily oral gavage for 2 weeks. Treatment started when tumor were approximately 200 mm^3. *P<0.05. B, Kaplan-Meier analysis for time to failure, as defined by doubling tumor volume as compared to pre-treatment volume (n=4-5/group). C, photographs of mice and tumors immediately after euthanasia. D, graphs depicting actual weight and volume of tumors retrieved from the mice at the termination of the experiment. E, graph depicting mouse weight for the duration of the experiment. F, table

showing tumor growth inhibition (TGI) index and percent tumor shrinkage in mice treated with 100 mg/kg MI-773 or vehicle, as compared to pre-treatment volumes. TGI greater than 50 is typically considered significant.

Supplementary Figure S3. MI-773 induces ACC tumor regression. A, graph depicting average tumor volume of mice that received vehicle, 50, or 100 mg/kg MI-773 via daily oral gavage for 15 days. Treatment started when tumor were approximately 200 mm^3. *P<0.05. B, Kaplan-Meier analysis for time to failure, as defined by doubling tumor volume as compared to pre-treatment volume (n=6-8/group). C, photographs of mice and tumors immediately after euthanasia. D, graphs depicting actual weight and volume of tumors retrieved from the mice at the termination of the experiment. E, graph depicting mouse weight for the duration of the experiment. F, table showing tumor growth inhibition (TGI) index and percent tumor shrinkage in mice treated with vehicle 50, or 100 mg/kg MI-773, as compared to pretreatment volumes. TGI greater than 50 is typically considered significant.

Supplementary Figure S4. Effect of MI-773 is p53-dependent. A,B, graphs showing a dose response of MI-773 in UM-HACC-5 (passage 6) and UM-HACC-6 (passage 7) low passage cells (data not normalized). C,D graphs showing that p53-silenced UM-HACC-5 cells are more resistant to MI-773 than vector control cells. One graph depicts data not normalized (C), and the other depicts data normalized by vehicle control cells (D). E, Western blot verifying the expression levels of p53 in UM-HACC-5 cells stably transduced with shRNA-p53 or scramble sequence control (shRNA-C) lentiviral vector.

Supplementary Figure S5. Histopathology of UM-PDX-HACC-5 tumors treated with MI-773. A, hematoxylin and eosin staining of vehicle-treated tumor showing infiltration of tumor cells into muscle, nerve and adipose tissue. B, hematoxylin and eosin staining of 100 mg/kg MI-773 treated tumor showing a noticeable shift in cellular morphology, *i.e.* tumor cells with vacuolated cytoplasm surrounded by hyaline connective tissue (arrow), and infiltration into nerve and adipose tissue. Black arrows point to pleomorphic cells with hyperchromatic nuclei; Red arrows

point to cells in the MI-773 treatment group that are characterized by smaller nuclei with vacuolated cytoplasm; Asterisks indicate nerves; FT=fat tissue; MI=muscle invasion. Scale bars=50 µm.

Supplementary Figure S6. Aminoacid sequence of p53 in the ACC models used in this project. A, p53 reference sequence (GenBank:U94788.1). B-D, Aminoacid sequence for p53 in the ACC tumor retrieved from patient UM-HACC-5 (B); corresponding PDX tumors, *i.e.* UM-PDX-HACC-5, passage 12 (C); and low passage primary human UM-HACC-5 cells (D). E-G, Aminoacid sequence for p53 in UM-HACC-1 cells passage 11 (E), UM-HACC-2A cells passage 6 (F), and UM-HACC-6 cells passage 7 (G).

	Patient demographics	Site	TNM (at diagnosis)	Grade	Perineural invasion	Prior treatment
UM-HACC-1	37 years old, Caucasian male	Hard Palate	T4aN0M0	NA	Present	None
UM-HACC-2A	53 years old, Caucasian female	Minor salivary gland at base of tongue	T3N1M0	1	Absent	None
UM-HACC-2B		Lymph node (metastasis)				
UM-HACC-5	46 years old, Caucasian female	Hard Palate	T4aN0M0	1	Present	None
UM-HACC-6	58 years old, Caucasian male	Minor salivary gland and buccal space	T4aN0M0	NA	Present	Excision
ACCX8	33 years old, male	Lung metastasis	NA	2	NA	NA
ACCX9	77 years old, female	Parotid gland	NA	3	NA	NA

Suppl Table S1 - Warner et al

	D3S1358	D19S433	vWa	FGA	D8S1179	D21S11	D18S51	D5S818	D13S317	D7S820	TH01	TPOX	CSF1PO	AMEL	Penta D	Penta E	% Match
Patient-5	14, 17	11	16	23, 25	12, 14	30	17, 20	12	8, 12	10, 12	9.3	8, 11	10, 11	X	9, 12	9, 13	xxx
UM-HACC-5 p# 7	14, 17	11	16	23, 25	12, 14	30	17, 20	12	8, 12	10, 13	9.3	8, 11	10, 11	X	9, 12	9, 13	xxx
UM-PDX HACC-5 p# 8	14, 17	11	16	23, 25	12, 14	30	17, 20	12	8, 12	10, 13	9.3	8, 11	10, 11	X	9, 12	9, 13	xxx
UM-PDX HACC-5 p# 9	14, 17	11	16, 19	23, 25, 28	12, 14	30	17, 20	12	8, 12	10, 13	9.3	8, 11	10, 11	X	9, 12	9, 13	xxx
UM-PDX HACC-5 p# 12	14, 17	11	16, 19	23, 25	12, 14	30	17, 20	12, 15	8, 12	10, 12	9.3	8, 11	10, 11	X	9, 12	9, 13	xxx
UM-HNSCC-1 p# 7	14, 15	8, 10	14, 17	22, 25	12, 13	28, 30.2	13, 14	11, 12	8, 11	12	6, 9.3	8, 11	8, 12	X, Y	11, 12	5, 13	xxx
UM-HNSCC-1 p# 13	14, 15	8, 10	14, 17	22, 25	12, 13	28, 30.2	13, 14	11, 12	8, 11	12	6, 9.3	8, 11	8, 12	X, Y	11, 12	5, 13	xxx
Patient-2	15, 17	8, 15	14, 16	20, 21	13	30, 31.2	18	11, 12	11, 12	8, 11	6, 11	10, 11	12	X	8, 12	7, 12	xxx
UM-HNSCC-2A p# 14	15, 17	8, 15	14, 16	20, 21	13	30, 31.2	18	11, 12	11, 12	8, 11	6, 11	10, 11	12	X	8, 12	7, 12	xxx
UM-HNSCC-2B p# 14	15, 17	8, 15	14, 16	20, 21	13	30, 31.2	18	11, 12	11, 12	8, 11	6, 11	10, 11	12	X	8, 12	7, 12	xxx
Patient-6	15, 16	8, 9	16	ND	13, 13	32, 33.2	14, 19	11, 12	ND	11	9.3	8	11	ND	10, 12	13, 16	xxx
UM-HNSCC-6 p# 4	15, 16	8, 9	16	21, 25	13, 13	32, 33.2	14, 19	11, 12	11, 13	11	9.3	8	11	X, Y	10, 12	13, 16	xxx

Suppl Table S2 - Warner et al

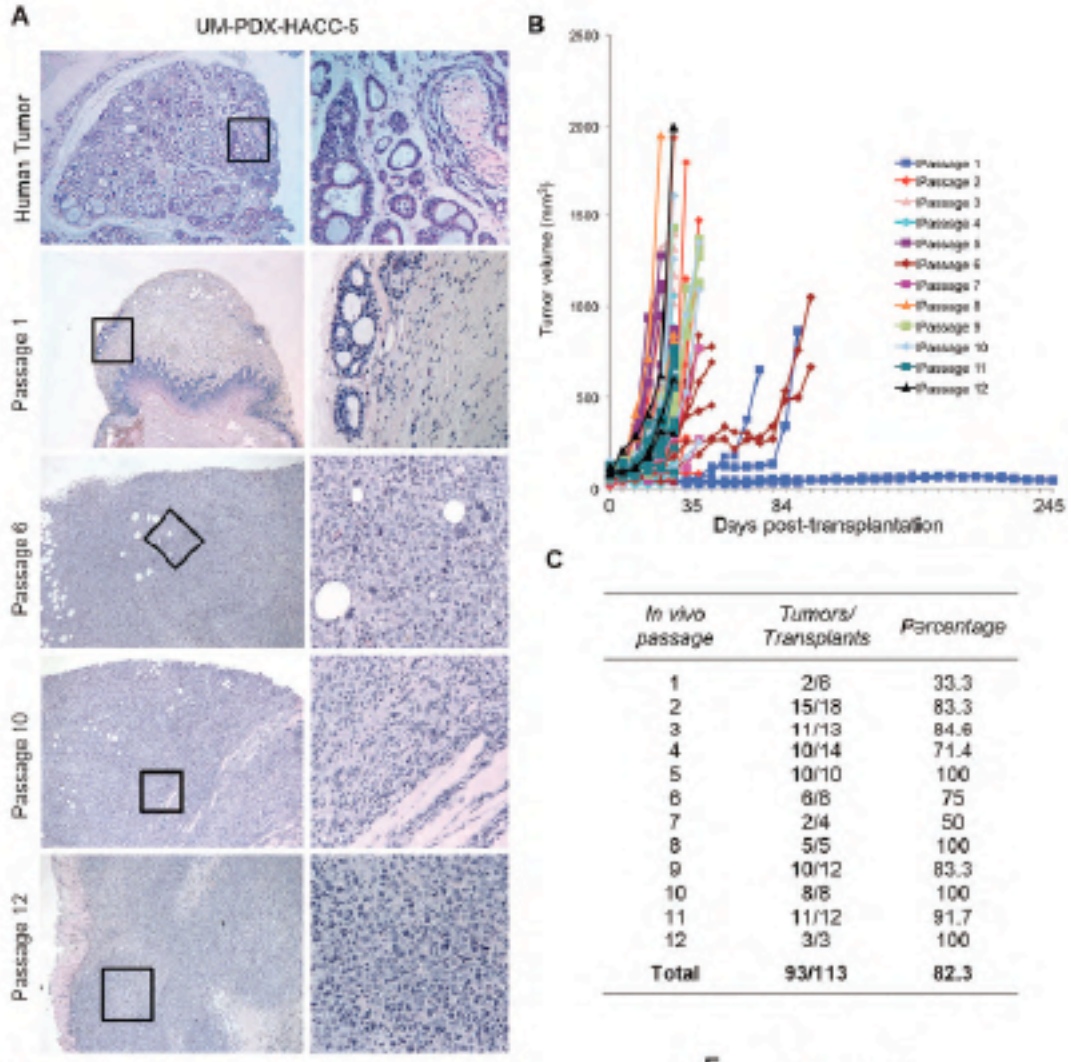

In vivo passage	*Tumors/ Transplants*	*Percentage*
1	2/6	33.3
2	15/18	83.3
3	11/13	84.6
4	10/14	71.4
5	10/10	100
6	6/8	75
7	2/4	50
8	5/5	100
9	10/12	83.3
10	8/8	100
11	11/12	91.7
12	3/3	100
Total	**93/113**	**82.3**

Suppl Figure S1 - Warner et al

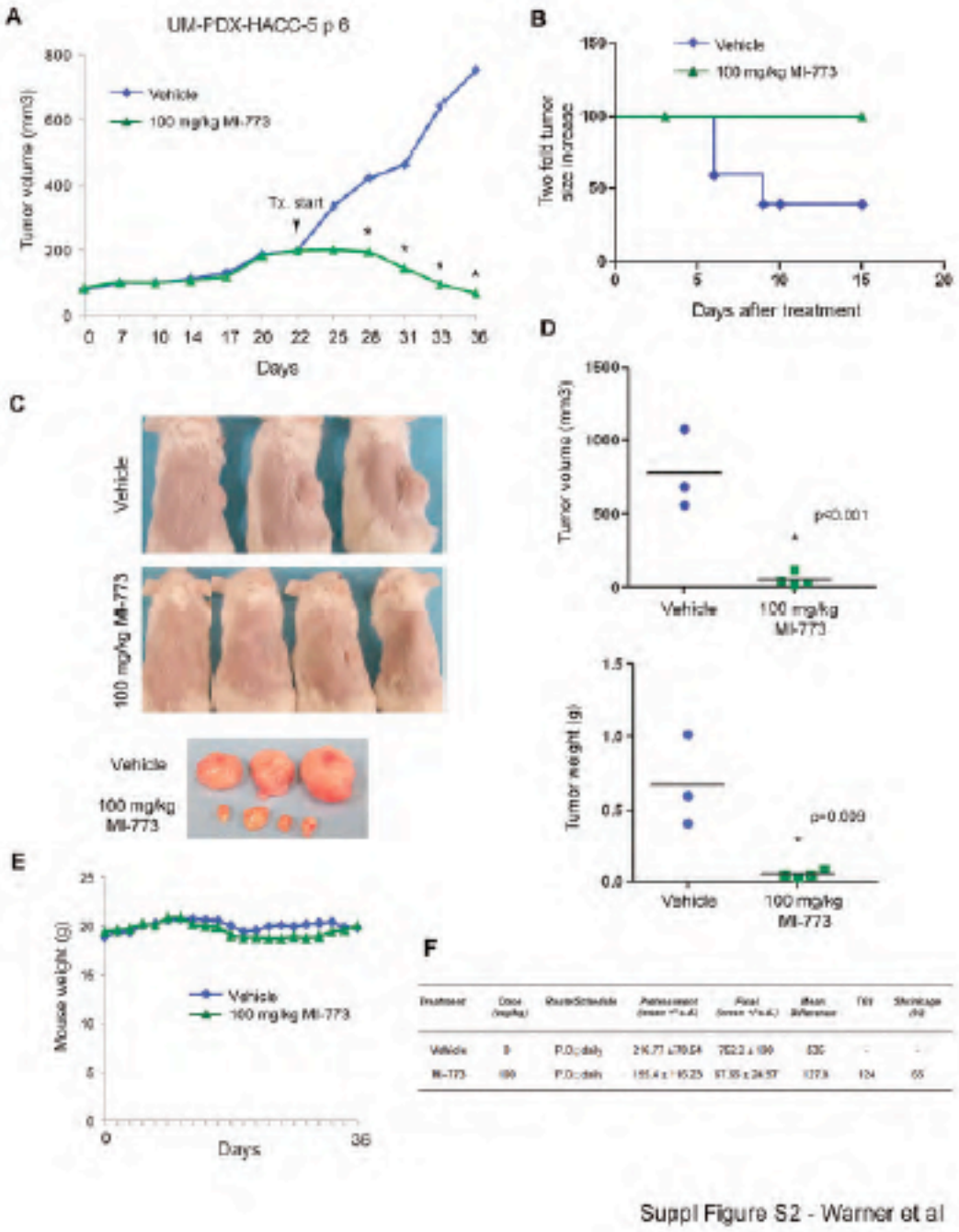

Suppl Figure S2 - Warner et al

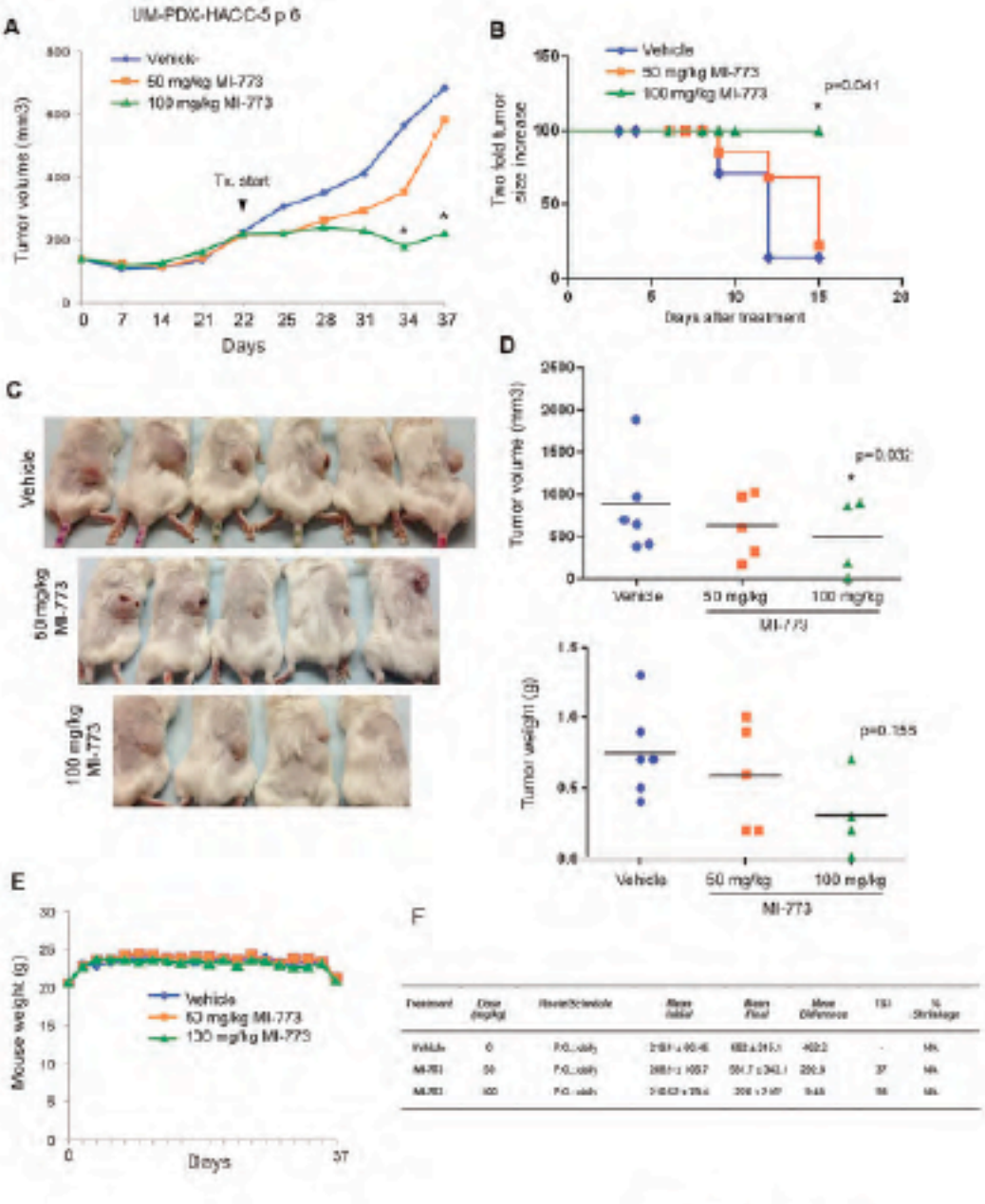

Suppl Figure S3 - Warner et al

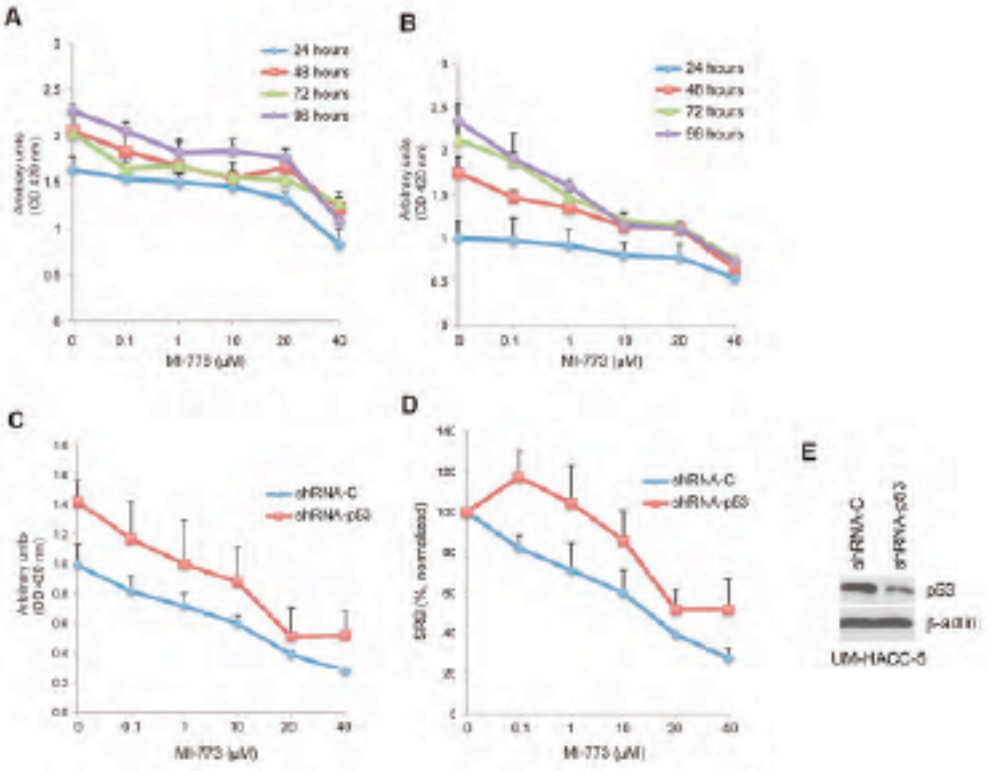

Suppl Figure S4 - Wamer et al

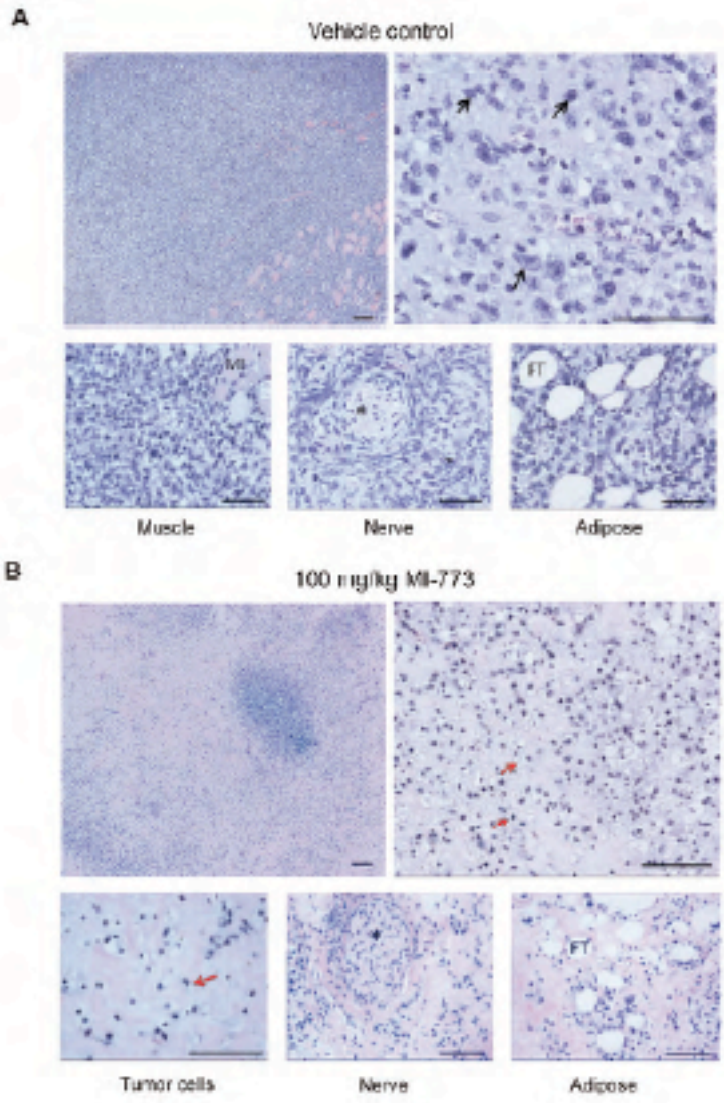

Suppl Figure S5 - Warner et al

Suppl Figure S6 - Warner et al

Artigo 2 - NÖR, F. et al. Therapeutic inhibition of the MDM2-p53 interaction prevents recurrence of adenoid cystic carcinomas. **Clin Cancer Res.**, in press. 2016.

Cancer Therapy: Preclinical

Clinical Cancer Research

Therapeutic Inhibition of the MDM2–p53 Interaction Prevents Recurrence of Adenoid Cystic Carcinomas

Felipe Nör[1,2], Kristy A. Warner[1], Zhaocheng Zhang[1], Gerson A. Acasigua[1,2], Alexander T. Pearson[1,3], Samuel A. Kerk[1], Joseph I. Helman[4,5], Manoel Sant'Ana Filho[2], Shaomeng Wang[3,5,6,7], and Jacques E. Nör[1,5,8,9]

Abstract

Purpose: Conventional chemotherapy has modest efficacy in advanced adenoid cystic carcinomas (ACC). Tumor recurrence is a major challenge in the management of ACC patients. Here, we evaluated the antitumor effect of a novel small-molecule inhibitor of the MDM2–p53 interaction (MI-773) combined with cisplatin in patient-derived xenograft (PDX) ACC tumors.

Experimental Design: Therapeutic strategies with MI-773 and/or cisplatin were evaluated in SCID mice harboring PDX ACC tumors (UM-PDX-HACC-5) and in low passage primary human ACC cells (UM-HACC-2A, -2B, -5, -6) *in vitro*. The effect of therapy on the fraction of cancer stem cells (CSC) was determined by flow cytometry for ALDH activity and CD44 expression.

Results: Combined therapy with MI-773 with cisplatin caused p53 activation, induction of apoptosis, and regression of ACC PDX tumors. Western blots revealed induction of MDM2, p53 and downstream p21 expression, and regulation of apoptosis-related proteins PUMA, BAX, Bcl-2, Bcl-x_L, and active caspase-9 upon MI-773 treatment. Both, single-agent MI-773 and MI-773 combined with cisplatin decreased the fraction of CSCs in PDX ACC tumors. Notably, neoadjuvant MI-773 and surgery eliminated tumor recurrences during a postsurgical follow-up of more than 300 days. In contrast, 62.5% of mice that received vehicle control presented with palpable tumor recurrences within this time period ($P = 0.0097$).

Conclusions: Collectively, these data demonstrate that therapeutic inhibition of MDM2–p53 interaction by MI-773 decreased the CSC fraction, sensitized ACC xenograft tumors to cisplatin, and eliminated tumor recurrence. These results suggest that patients with ACC might benefit from the therapeutic inhibition of the MDM2–p53 interaction. *Clin Cancer Res*; 1–15. ©2016 AACR.

Introduction

Salivary gland tumors are typically not responsive to conventional chemotherapy. Adenoid cystic carcinoma (ACC) is one of the most common malignancies arising from minor and major salivary glands (1). Despite the apparent "benign" behavior characterized by slow tumor growth, ACC is relentless. It is highly destructive to adjacent anatomic sites and exhibits a high frequency of perineural invasion events that leads to severe morbidity, particularly as this tumor grows toward the brain (2). The slow and indolent clinical course often leads to a late diagnosis, when tumor is already at advanced stages and systemic intervention is required to prevent distant metastasis and recurrence after surgical resection. Unfortunately, current standard chemotherapy (e.g., platinum-based drugs) has shown limited long-term efficacy in ACC patients (3–5). The prevalence of recurrence is high mainly due to late hematogenous dissemination of cancer cells primarily to lungs, bone, and liver (4). Novel mechanism-based therapies to overcome drug resistance are desperately needed to enhance the survival and quality of life for patients with ACC.

The mechanisms involved in the resistance of ACC to chemotherapy are poorly understood. The first-line chemotherapy for ACC often includes cisplatin, which is frequently combined with other classes of antineoplastic agents [e.g., 5-fluorouracil (5-FU); refs. 3, 6]. However, data from clinical trials with these drug combinations are not promising, with modest efficacy in ACC (7). The combination of cisplatin with doxorubicin and cyclophosphamide mediated only partial therapeutic responses (8). Another study tested the efficacy of combination cisplatin, 5-FU, and epirubicin in patients with advanced, symptomatic ACC (9). From 8 patients enrolled in this study, one showed partial response to therapy and 5 had stable disease. Besides the low sample size, one important limitation of this study is the total

[1]Department of Cariology, Restorative Sciences, and Endodontics, University of Michigan School of Dentistry, Ann Arbor, Michigan. [2]Department of Oral Pathology, Universidade Federal do Rio Grande do Sul, Porto Alegre, Rio Grande do Sul, Brazil. [3]Department of Internal Medicine, University of Michigan School of Medicine, Ann Arbor, Michigan. [4]Department of Oral and Maxillofacial Surgery, University of Michigan School of Dentistry, Ann Arbor, Michigan. [5]University of Michigan Comprehensive Cancer Center, Ann Arbor, Michigan, USA. [6]Department of Pharmacology, University of Michigan School of Medicine, Ann Arbor, Michigan. [7]Department of Medicinal Chemistry, University of Michigan College of Pharmacy, Ann Arbor, Michigan. [8]Department of Otolaryngology, University of Michigan School of Medicine, Ann Arbor, Michigan. [9]Department of Biomedical Engineering, University of Michigan College of Engineering, Ann Arbor, Michigan.

Note: Supplementary data for this article are available at Clinical Cancer Research Online (http://clincancerres.aacrjournals.org/).

Corresponding Author: Jacques E. Nör, University of Michigan, 1011 N. University Rm. 2353, Ann Arbor, MI 48109-1078. Phone: 734-936-9300; Fax: 734-936-9330; E-mail: jenor@umich.edu

doi: 10.1158/1078-0432.CCR-16-1233

Translational Relevance

Adenoid cystic carcinoma (ACC) is a relentless form of salivary gland cancer, typically treated with surgery and radiation, as these tumors are resistant to chemotherapy. In advanced disease, cisplatin is usually the first treatment option, but clinical response and long-term efficacy are modest at best. Here, we demonstrate that therapeutic inhibition of the MDM2–p53 interaction with a small molecule (MI-773) sensitizes adenoid cystic carcinomas to cisplatin in patient-derived xenograft (PDX) and low passage primary human ACC models. Combination of MI-773 and cisplatin mediates potent and durable tumor regression via p53 reactivation and tumor cell apoptosis. MI-773 reduces the fraction of cancer stem cells, which have been associated with resistance to therapy. Notably, neoadjuvant therapy with MI-773 and cisplatin eliminated recurrences of PDX ACC tumors for at least 300 days. Collectively, these data suggest that patients with ACC might benefit from combination therapy with a MDM2–p53 inhibitor and cisplatin.

period of evaluation (6.2.3 months), when it is known that around half of ACCs recur only after 10 years (10). Notably, most ACC tumors express the proto-oncogene c-KIT. However, dasatinib (a c-KIT inhibitor) was not effective in a phase II clinical trial with ACC patients (11). The scarcity of preclinical/clinical evidence and lack of response to conventional drugs in the daily clinical practice is reflected on the most recent guideline from the National Comprehensive Cancer Network (NCCN), in which no specific chemotherapeutic drug/regimen is indicated for the treatment of these patients. To improve the prediction of patient outcomes, NCCN has incorporated nomograms (i.e., statistical model using regression analysis) to guidelines as an alternative method for TNM staging system. Notably, this method was proven to be accurate in the prediction of survival and recurrence in ACC patients (12).

The tumor suppressor p53 is often inactivated in cancer (13). Important functions of wild-type p53 (e.g., cell-cycle control, DNA repair, induction of apoptosis) are regulated by its interaction with murine double minute 2 (MDM2; ref. 14). This protein interaction forms an autoregulatory negative feedback loop, that is, nuclear p53 induces the expression of MDM2, which in turn binds directly to p53, provoking its degradation through the 26S proteasomal pathway. This interaction is important to maintain low cellular levels of p53 in physiologic conditions (14, 15). However, overexpression of MDM2 leads to p53 inactivation, which contributes to tumorigenic processes (16). Of note, MDM2 expression levels have been associated with tumor progression and poor prognosis of ACC patients (17, 18).

Recently, Wang and colleagues have developed a small-molecule inhibitor of the MDM2–p53 interaction (MI-773, patented by Sanofi as SAR405838), pursuing the p53 activation as a new anticancer strategy (19). MI-773 has a high binding affinity to MDM2 (K_i = 0.88 nmol/L), preventing MDM2 interaction with p53. Indeed, MI-773 is capable of wild-type p53 reactivation in cancer cell lines and several preclinical models of cancer, for example, osteosarcoma, leukemia, colon, and prostate cancer (19, 20). Considering the important role of MDM2 in ACC, our group has tested the effect of MI-773 in preclinical models of ACC (21). We observed that therapeutic inhibition of MDM2 with MI-773 restored p53 function, as shown by the activation of its downstream-related protein (i.e., p21). Here, we went a step further and evaluated the effect of MI-773 in combination with cisplatin in preclinical models of ACC. MI-773 and cisplatin drug combination induced robust and durable ACC tumor regression. Furthermore, this therapy significantly decreased the proportion of cancer stem cells (CSC), which has been associated with cisplatin resistance in head and neck tumors (22). Collectively, these results suggest that patients with ACC might benefit from neoadjuvant therapeutic inhibition of the MDM2–p53 interaction combined with conventional chemotherapy with cisplatin.

Materials and Methods

Salivary ACC cells

Primary cell cultures were generated from human tumor specimens and named "University of Michigan Human Adenoid Cystic Carcinoma (UM-HACC)" series, as described previously (21, 23). UM-HACC-2A, UM-HACC-2B, UM-HACC-5, and UM-HACC-6 cells were maintained in salivary gland culture media, that is, high-glucose DMEM (Invitrogen) supplemented with 2 mmol/L L-glutamine (Invitrogen), 1% antibiotic (AAA; Sigma-Aldrich), 10% FBS (Invitrogen), 20 ng/mL EGF (Sigma-Aldrich), 400 ng/mL hydrocortisone (Sigma-Aldrich), 5 μg/mL insulin (Sigma-Aldrich), 50 ng/mL nystatin (Sigma-Aldrich), and 1% amphotericin B (Sigma-Aldrich). Cells were passed using 0.05% trypsin/EDTA (Invitrogen) and used for up to 20 passages. Therefore, these cells are considered here low-passage primary ACC cells (instead of established cell lines). UM-HACC-2A is a low passage cell culture derived from an aggressive primary tumor, and UM-HACC-2B represents ACC cells derived from the lymph node metastasis of the same patient. UM-HACC-5 cells were obtained from a patient that had histologic confirmation of perineural and bone invasion, and UM-HACC-6 cells were derived from a recurrent tumor diagnosed 15 years after initial diagnosis and also presented perineural invasion. All low passage ACC cell cultures used here express wild-type p53 (21).

Studies with patient-derived xenograft model of ACC

Patient-derived xenograft (PDX) models have been increasingly used in translational cancer research (24). Tumor fragments from a PDX model of ACC (UM-PDX-HACC-5; refs. 21, 23) at in vivo passages 5 to 6 were transplanted into the subcutaneous space of the dorsum of SCID mice (C.B.17.SCID; Charles River Laboratories). Tumor volume was calculated using the formula: volume (mm^3) = $L \times W^2/2$ (L, length; W, width). All tumors were surgically retrieved when they reached our UCLACA-approved cut-off volume of 2,000 mm^3. The protocol for animal care was reviewed and approved by appropriate University of Michigan institutional committees. Mice transplanted with UM-PDX-HACC-5 tumors were randomly allocated into four groups (n = 5–6), maintaining the average of tumor volume (500 mm^3/group). Experimental conditions were as follows: vehicle control (saline, intraperitoneally, weekly); 5 mg/kg cisplatin (intraperitoneally, weekly); 200 mg/kg MI-773 (gavage, weekly); or the combination of 5 mg/kg cisplatin + 200 mg/kg MI-773 regimens. Treatment was administered for 30 days, mice were followed for additional 24 days, and then mice were euthanized and tumors retrieved. To compare weekly versus daily regimens of MI-773 combined with fixed doses of cisplatin, 200 mg/kg

MI-773 was divided into equable daily doses (i.e., 28.5 mg/kg MI-773). When tumor reached an average volume of 200 mm^3, animals were randomly distributed into the experimental groups ($n = 7–8$). Treatment was administered for 14 days, and mice were followed for additional 44 days, when experiment was terminated and tumors were collected. To evaluate tumor recurrence, animals were submitted to a neoadjuvant regimen of MI-773. Briefly, mice transplanted with UM-PDX-HACC-5 tumors (average volume of 500 mm^3) were divided into two groups ($n = 8$): vehicle control (polyethylene glycol-200 + D-α-tocopherol polyethylene glycol 1000 succinate; Sigma-Aldrich) or 200 mg/kg MI-773. Initially, animals received either a single dose of MI-773 or vehicle. After 7 days, tumors were surgically removed and incisions were closed with Vetbond (3M). Weekly treatments restarted 7 days after surgery and continued for 30 days. Then, mice were examined twice per week for 300 days for signs of recurrence, as defined as the presence of palpable tumor.

Flow cytometry

Salivary gland CSCs were identified as $ALDH^{bright}CD44^{bright}$ cells, as described previously (25, 26). UM-PDX-HACC-5 tumors were collected, cut in small pieces, and dissociated using the gentleMACS Dissociator Kit (Miltenyi Biotec), incubated in ACK red blood cell lysis buffer (Invitrogen), and filtered through a 40-μm sterile cell strainer. Cells were incubated with 5 μl. activated Aldefluor substrate (BAA) or 5 μl. aldehyde dehydrogenase (ALDH) inhibitor (DEAB), using the Aldefluor Kit (Stem Cell Technologies) for 40 minutes at 37°C. A monoclonal mouse anti-human CD44 antibody (1:60; APC-cat #559942, PE-cat #550989; BD Pharmingen) was incubated for 30 minutes at 4°C, and human cells were separated from murine cells using anti-HLA-ABC (PE-cat #560168; BD Pharmingen). Viable cells were stained using 7-AAD (cat #00-6993-50; eBioscience). For cell-cycle analysis, 5×10^5 UM-HACC-5 or UM-HACC-6 cells were treated with either vehicle control, MI-773, a nal/or cisplatin diluted in salivary gland medium for 24 hours. After harvesting, cells were fixed in 70% cold ethanol and exposed to 0.1% sodium citrate, 25 μg/mL propidium iodide (Sigma-Aldrich), 100 μg/mL RNase A, and 0.1% Triton X-100. Flow cytometry (FACSCalibur; BD Biosciences) was carried out to quantify the percentage of cells in each cell-cycle phase (G_0–G_1, S, and G_2–M), as described previously (23). Data were obtained from triplicates and represent at least three independent experiments. Results were analyzed using FlowJo software (FlowJo, LLC).

Subcellular fractionation

Cytoplasmic and cellular membrane portions were separated from the nucleus, as described previously (27). Briefly, UM-HACC-5 cells were treated with vehicle control, Cisplatin and/or MI-773 for 24 hours. Then, cells were resuspended in cytoplasmic extraction buffer (Panomics) and incubated for 5 minutes on ice. The suspension was centrifuged at 13,000 rpm for 5 minutes at 4°C. Supernatant was collected as cytoplasmic/cell membrane extract. The remaining pellet was resuspended in nuclear extraction buffer (Panomics) with occasional vortexing during 40 minutes. After centrifugation, the supernatant was collected as nuclear extract.

Western blots

Protein lysates from UM-PDX-HACC-5 tumors, UM-HACC-5, and UM-HACC-6 cells were prepared using 1% Nonidet P-40 (NP-40) lysis buffer and loaded onto 9% to 12% SDS-PAGE gels. Membranes were incubated with the following primary antibodies overnight at 4°C: mouse anti-human p53 (1:1,000), β-actin conjugated with horseradish peroxidase (HRP; 1:100,000), rabbit anti-hnRNP (1:1,000) (Santa Cruz Biotechnology); hamster anti-human Bcl-2 (1:500), rabbit anti-human phospho-p53 (S392; 1:1,000), p21 (1:2,000), BAX (1:500), PUMA (1:500), cleaved-caspase 9 (1:1,000) (Cell Signaling Technology); mouse anti-human MDM2 (1:500; Thermo Fisher Scientific); rabbit anti-human Bcl-x_L (1:500; BD Biosciences), or mouse anti-GAPDH (1:1,000,000; Chemicon). Membranes were exposed to affinity-purified secondary antibodies (1:1,000) conjugated with HRP (The Jackson Laboratory), and immunoreactive proteins were visualized by SuperSignal West Pico chemiluminescent substrate (Thermo Scientific).

Cytotoxicity assays

Sulforhodamine B (SRB) assays were performed to evaluate the effect of treatment on ACC cell viability, as described previously (23). Here, 2×10^3 UM-HACC-5 and UM-HACC-6 cells per well were exposed to vehicle, MI-773, and/or cisplatin for 24 to 96 hours. After fixation with 10% cold trichloroacetic acid for 1 hour at 4°C, viable cells were stained by addition of 0.4% SRB dye (Sigma-Aldrich) for 30 minutes at room temperature. The excess unbound dye was removed by 1% acetic acid. SRB-stained cells were resolubilized in 10 mmol/L unbuffered Tris base, and plates were read in a microplate reader at 560 nm (GENios, Tecan). Results were normalized by vehicle control and IC_{50} values were determined. Data were obtained from quadruplicate wells/condition and represent at least three independent experiments.

Fluorometric assay

UM-HACC-5, -6 cells were treated with IC_{50} concentrations of MI-773, cisplatin, or vehicle control for 24 hours. Cell pellets were resuspended in lysis buffer, and cells were incubated with 1 mmol/L IETD-AFC (caspase-8 substrate; Enzo) or 1 mmol/L LEHD-AFC (caspase-9 substrate; Enzo) for up to 2 hours at 37°C. Samples were analyzed in a microplate reader at 400 nm (GENios).

Statistical analyses

Data were analyzed by one-way ANOVA, followed by *post hoc* tests (Tukey) for multiple comparisons or Student *t* test, when indicated. Regression modeling was performed using mixed effect linear regression to account for repeated measures on each tumor. The tumor volume data was log transformed to account for exponential growth. Model fixed effects included time, cisplatin treatment, and MI-773 treatment, and tumor starting size. Random effects included mouse. We assumed an autoregressive correlation structure where more proximate time values have a higher degree of correlation. When comparing different dosing schemes, each dosing category was included as a different factor level in the regression model. Predictions curves were generated directly from the regression model. Kaplan–Meier graphs were analyzed by the Gehan–Breslow–Wilcoxon test. Failure criterion was a 2-fold increase in tumor volume (for tumor growth analysis) or presence of palpable tumor (for recurrence analysis). Significance level (α) was determined at $P < 0.05$. Analysis was performed using the "survival" and "glx" packages in software program, version R 3.1.0.

Results

MI-773 sensitizes ACC PDX tumors to cisplatin

To begin to understand the effect of combining MI-773 with cisplatin in vivo, we performed a pilot study to evaluate drug toxicity. Using published studies as reference, we choose weekly doses of 5 mg/kg cisplatin (22) and 200 mg/kg MI-773 (21) for this experiment. Weight loss did not exceed 20% (compared with pretreatment values), which is our IUCUCA-approved cutoff for systemic toxicities, when we used single-agent cisplatin or MI-773 or combination of both drugs (Supplementary Fig. S1). To evaluate the effect of MI-773 and/or cisplatin on UM-HACC-PDX-5 tumors, we allowed tumors to grow to an average volume of 500 mm^3 and then began treating mice with the same doses mentioned above for 30 days (Fig. 1). We observed that MI-773 as a single agent causes tumor regression, being more effective than single-agent cisplatin (Fig. 1A and C). Cisplatin therapy shows limited therapeutic response, stabilizing the tumor growth, but not causing PDX tumor regression, as reported in humans (6–9). However, combination of MI-773 and cisplatin was more effective than single-agent therapy. There was no tumor rebound upon termination of treatment within the duration of the follow-up in this initial experiment (about 20 days posttreatment; Fig. 1A). Importantly, mice did not show weight loss beyond the 20% cutoff (Fig. 1B). We performed linear mixed effect regression modeling on the tumor volume to account for repeated measures on each tumor and determine the effects of time, cisplatin treatment, MI-773 treatment, and starting tumor size on tumor volume. The rate of tumor growth was significantly less in MI-773 ($P = 0.0002$) and cisplatin ($P = 0.0017$) groups when compared with control (Fig. 1C). Western blot analysis from UM-HACC-PDX-5 tumors shows that therapeutic inhibition of MDM2, combined or not with cisplatin, causes the upregulation of p53 and MDM2 expression (Fig. 1D). MI-773–activated p53 is functional in vivo, as confirmed by the upregulation of its downstream protein p21 and the apoptosis effector protein BAX. In contrast, PUMA appears to be primarily regulated by cisplatin, while the prosurvival protein Bcl-2 did not show considerable changes in expression levels upon treatment. Collectively, these in vivo results

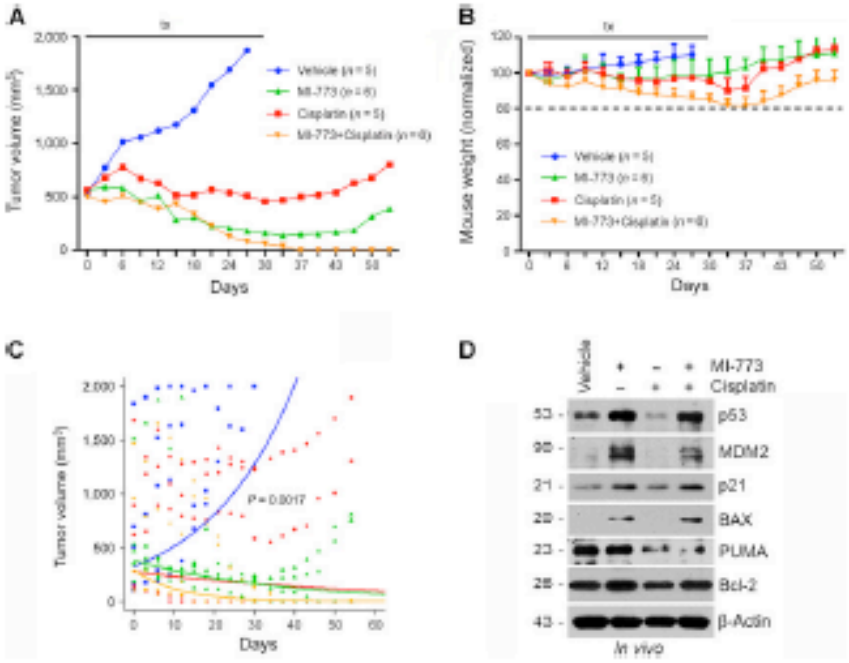

Figure 1.

Effect of MI-773 and/or cisplatin in a preclinical model of ACC. UM-PDX-HACC-5 tumors were transplanted in immunodeficient mice. When tumors reached 500 mm^3, animals were randomly allocated into four different treatment regimens as follows: 5 mg/kg saline (vehicle control), 200 mg/kg MI-773, 5 mg/kg cisplatin, or 200 mg/kg MI-773 combined with 5 mg/kg cisplatin weekly. **A**, graph depicting tumor volume during treatment (tx) and follow-up (28 days) periods. Cisplatin stabilized tumor growth, while MI-773 decreases tumor volume compared with pretreatment values. MI-773 combined with cisplatin ablates tumor in the majority of animals and prevents tumor regrowth after treatment. **B**, graph depicting mouse weight during the experimental period. Data were normalized against pretreatment weight. **C**, graph depicting a linear regression model using repeated measures for each tumor over time. MI-773 and/or cisplatin significantly decrease the tumor growth rate when compared with vehicle control. **D**, Western blot analysis for p53, MDM2, p21, BAX, PUMA, and Bcl-2 in UM-PDX-HACC-5 tumors treated with either MI-773 and/or cisplatin as compared with vehicle control. Tumors were harvested 28 days after the last administration of drugs.

demonstrate that MI-773 mediates ACC tumor regression in a preclinical model of ACC.

Effect of MI-773 and/or cisplatin on ACC cell proliferation and survival

To evaluate the therapeutic potential of each drug in vitro, low passage primary human ACC cells (UM-HACC-5 and UM-HACC-6) were treated with either a dose range of MI-773 (0.01–10 μmol/L) or cisplatin (0.02–20 μmol/L). Alternatively, cells were treated with a fixed dose of cisplatin (2 μmol/L) together with increasing concentrations of MI-773. The percentage of viable cells was determined by SRB assay. Data were normalized against vehicle control. We observed a dose- and time-dependent cytotoxic response in both ACC primary cells evaluated. IC_{50} values for single agent were in the low micromolar range, and for both ACC cells, the IC_{50} for MI-773 was about half concentration as compared with the IC_{50} for cisplatin (Fig. 2A). Combination of both agents further reduced the IC_{50} to 0.73 μmol/L (UM-HACC-5) and 3.79 μmol/L (UM-HACC-6) at 72 hours (Fig. 2A). Representative photomicrographs of cells in culture conditions were taken after 72 hours of treatment using intermediate doses of single or combined drugs regimens (1–2 μmol/L; Supplementary Fig. S2B). To better understand the mechanisms associated with the antitumor effect observed in vivo, UM-PDX-HACC-5 tissue slides were stained for in situ TUNEL to reveal cells undergoing apoptosis (Fig. 2B). The percentage of TUNEL-positive cells is significantly higher ($P < 0.05$) in animals that received either MI-773 or cisplatin (Fig. 2B and C). Combination therapy induced more apoptosis than cisplatin or MI-773 used as a single agent (Fig. 2C). In addition, we evaluated the effect of treatment on cell cycle. UM-HACC-5 or UM-HACC-6 cells were treated for 24 hours using low concentrations of either MI-773 and/or cisplatin (1–2 μmol/L), and the percentage of cells in each cell-cycle phase was determined by flow cytometry (Supplementary Fig. S3). MI-773 causes cell-cycle arrest at the first checkpoint (G_1); a similar trend is seen upon drug combination therapy. As previously reported (28), the majority of cells exposed to cisplatin are retained in the S-phase (Fig. 2D). Taken together, these results indicate that antitumor cell effects seen upon treatment with MI-773 and/or cisplatin involve cell-cycle arrest and induction of apoptosis.

Inhibition of the MDM2–p53 interaction with MI-773 activates p53

To better understand the role of MI-773 on p53 activation in ACC, we first performed Western blot analysis for the basal expression of MDM2 and apoptosis-related proteins (i.e., Bcl-x_L and Bcl-2) in UM-HACC-2A, UM-HACC-2B, UM-HACC-5, and UM-HACC-6 cells (Fig. 3A). Next, we treated ACC cells with single-agent MI-773 or cisplatin at intermediate doses (1–2 μmol/L) and observed that p53, MDM2, p21, BAX, and PUMA (except for UM-HACC-6 cells) expression is increased with MI-773, while Bcl-2 expression was slightly decreased upon treatment with cisplatin (Fig. 3B). Then, we evaluated more closely the expression of p53 in UM-HACC-PDX-5 tumors from experiment reported in Fig. 1. Tumors treated with either vehicle or cisplatin show nuclear localization of p53. Surprisingly, the administration of MI-773 as a single agent or combined with cisplatin causes a partial translocation of p53 to the cytoplasm (Fig. 3C). To confirm this apparent translocation of p53, we exposed UM-HACC-5 cells to low concentrations of MI-773 and/or cisplatin (0.1–0.2 μmol/L). After 24 hours, we performed a subcellular fractionation assay to separate the nucleus compartment from the cytoplasm/membrane components. Confirming the data obtained by IHC, tumors exposed to MI-773 alone or in combination with cisplatin presented p53 in both nucleus and cytoplasm. MI-773 caused a robust increase in MDM2 expression, which was observed in both the nuclear and the cytoplasmic extract (Fig. 3D). Immunofluorescence further confirmed the cytoplasmic presence of p53 upon treatment with MI-773 (Fig. 3E).

To further understand the effect of MI-773 or cisplatin on ACC cells, we performed a series of dose- and time-dependent experiments (Fig. 4). MI-773 induces activation of phospho-p53 (SER 392), p53, MDM2, p21, BAX, and PUMA in a dose-dependent manner, with visible effects already being observed with 0.1 μmol/L in both cell lines (Fig. 4A). The prosurvival protein Bcl-x_L appears to be upregulated by low concentration MI-773 in both ACC cell lines and went down or baseline level at 1.0 μmol/L (Fig. 4A). Cisplatin requires higher doses for the activation of p53, MDM2, p21, and BAX when compared with MI-773 (Fig. 4A and B). The activation of BAX by cisplatin appears to be associated with Bcl-x_L downregulation and does not involve PUMA regulation, which differs from MI-773 treatment.

In a time course evaluation with intermediate dose of MI-773 (1 μmol/L), p53 and p21 were constantly activated over 96 hours, while the expression of MDM2 increased with time particularly in UM-HACC-6 cells (Fig. 4C). Upon cisplatin treatment (2 μmol/L), the peak of p53 activation was at 48 hours in UM-HACC-5 cells; the same trend was observed for MDM2. In UM-HACC-6 cells, p53 activation was constant, but MDM2 expression increased over time (Fig. 4D). To better understand the effect of drugs together, we designed an experiment to evaluate the effect of minimal doses of MI-773 and cisplatin on p53 and MDM2. We observed that MI-773 appears to be the dominant factor driving p53 and MDM2 expression when used in combination with cisplatin in the four low passage ACC cell cultures tested here (Fig. 4E). Collectively, these results demonstrate that MI-773 induces p53, MDM2, and p21 expression via a mechanism that is associated with upregulation of Bax and PUMA. To further understand the mechanisms involved in MI-773–induced apoptosis, we performed fluorometric assays. They revealed that caspase-9 (but not caspase-8) is activated upon treatment of ACC cells with MI-773 and/or cisplatin (Fig. 4G). Of note, the activation of caspase-9 in UM-HACC-5 cells treated with MI-773 + cisplatin (120 minutes) is 5.94-fold higher than vehicle control, and in UM-HACC-6, it is 6.76-fold higher than vehicle (Fig. 4G). These data indicate that this drug combination is equally effective in both ACC cell cultures. Western blots were used to verify the data obtained with the fluorometric assay and confirmed that treatment with MI-773 and/or cisplatin induces expression of cleaved (active) caspase-9 (Fig. 4F).

Dosing and frequency of MI-773 determines efficacy

To further explore the antitumor effect of the combined therapy, we designed an independent experiment evaluating weekly versus daily regimens of MI-773 combined with fixed doses of cisplatin. When UM-HACC-PDX-5 tumors reached the average volume of 200 mm^3, mice were randomly divided into 5 groups ($n = 7–8$), and treatment was administered for 14 days (Fig. 5). A shorter treatment period was chosen here to focus the evaluation on the post-treatment period. Here, we observed that single drugs, MI-773 or cisplatin, stabilize tumor volume during treatment, but ACC tumor growth resumed as soon as treatment was

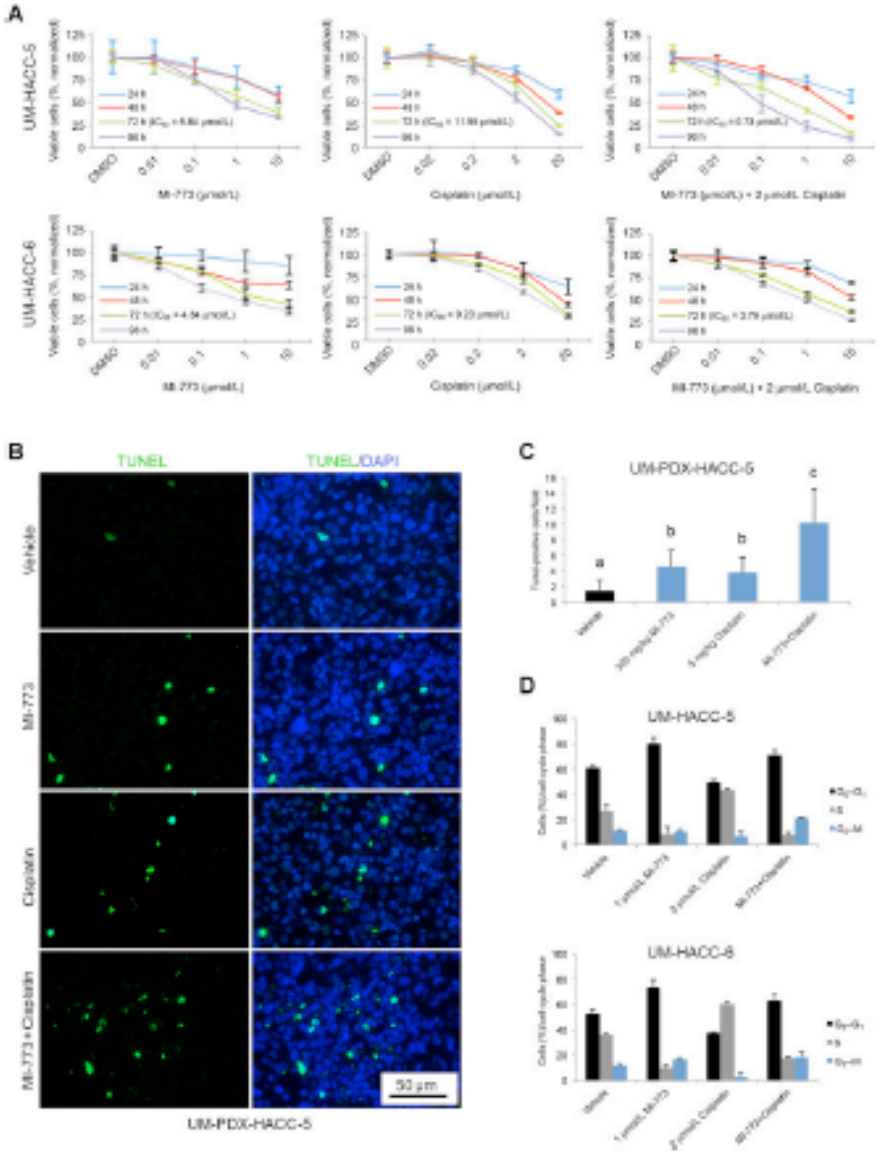

Figure 2.

Effect of MI-773 and/or cisplatin on proliferation and survival of ACC cells. **A**, graphs depicting time- and dose-dependent assays for the effect of MI-773 and/or cisplatin on the viability of UM-HACC-5 and -6 cells, as determined by SRB assay. Data were normalized against vehicle control and represent at least three independent experiments, done in quadruplicate wells per condition. **B**, representative photomicrographs of UM-PDX-HACC-5 tumor histologic sections stained for TUNEL (apoptotic cells, green) and DAPI (nuclei, blue) from mice treated either with vehicle control, MI-773, and/or cisplatin (400×). **C**, graph depicting the percentage of TUNEL-positive cells in 10 random fields per tumor ($n = 4$/group). Different lowercase letters (a, b, and c) indicate statistical difference ($P < 0.05$). **D**, graphs depicting the effect of the drugs on cell cycle. UM-HACC-5 and -6 cells were exposed to MI-773 and/or cisplatin for 24 hours. The percentage of cells in each cell-cycle phase was determined by propidium iodide staining followed by flow cytometry.

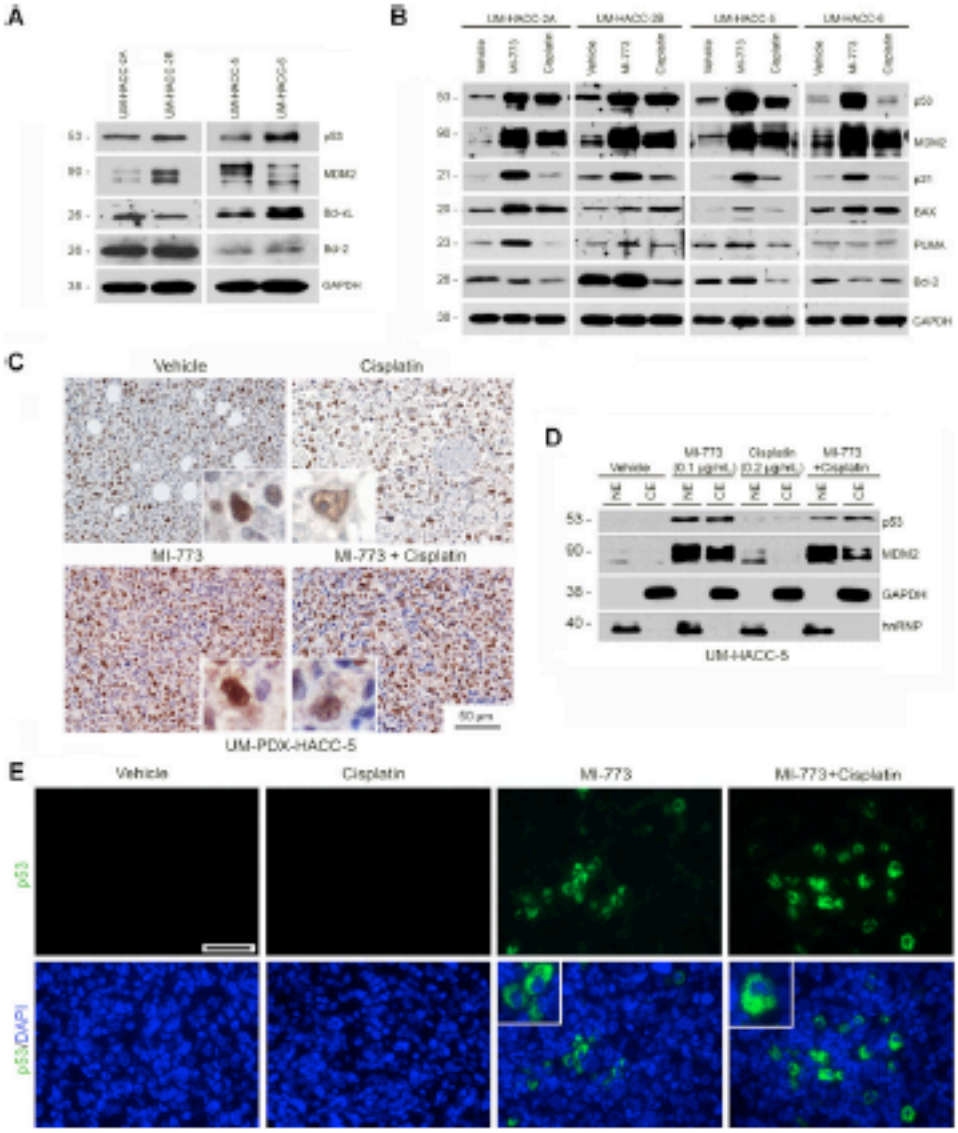

Figure 3.

Treatment with MI-773 causes changes in p53 status. **A,** Western blot analysis showing basal levels of proteins p53, MDM2, Bcl-x_L, and Bcl-2 in UM-HACC-2A, -2B, -5, and -6 cells. **B,** Western blots for p53, MDM2, p21, PUMA, BAX, and Bcl-2 protein expression in UM-HACC cells exposed to predetermined IC_{50} values of MI-773, cisplatin, or vehicle control for 72 hours. **C,** representative photomicrographs of UM-PDX-HACC-5 histologic sections stained for p53 (brown) and counterstained with hematoxylin (200 ×). Nuclear p53 is observed in mice treated with vehicle control or cisplatin, while both nuclear (NE) and cytoplasmic (CE) expression of p53 is evidenced in animals exposed to MI-773 as a single agent or combined with cisplatin (details). **D,** Western blot analysis for p53 and MDM2 expression in UM-HACC-5 cells exposed to MI-773 (0.1 μg/mL) and/or cisplatin (0.2 μg/mL) and submitted to a subcellular fractionation assay to evaluate the nucleus and cytoplasm compartments in separate. **E,** representative photomicrographs obtained by immunofluorescence for p53 (green), which is located in the cytoplasm (detail) of UM-PDX-HACC-5 cells treated with MI-773 as single drug or combined with cisplatin (400 ×). Scale bar, 10 μm.

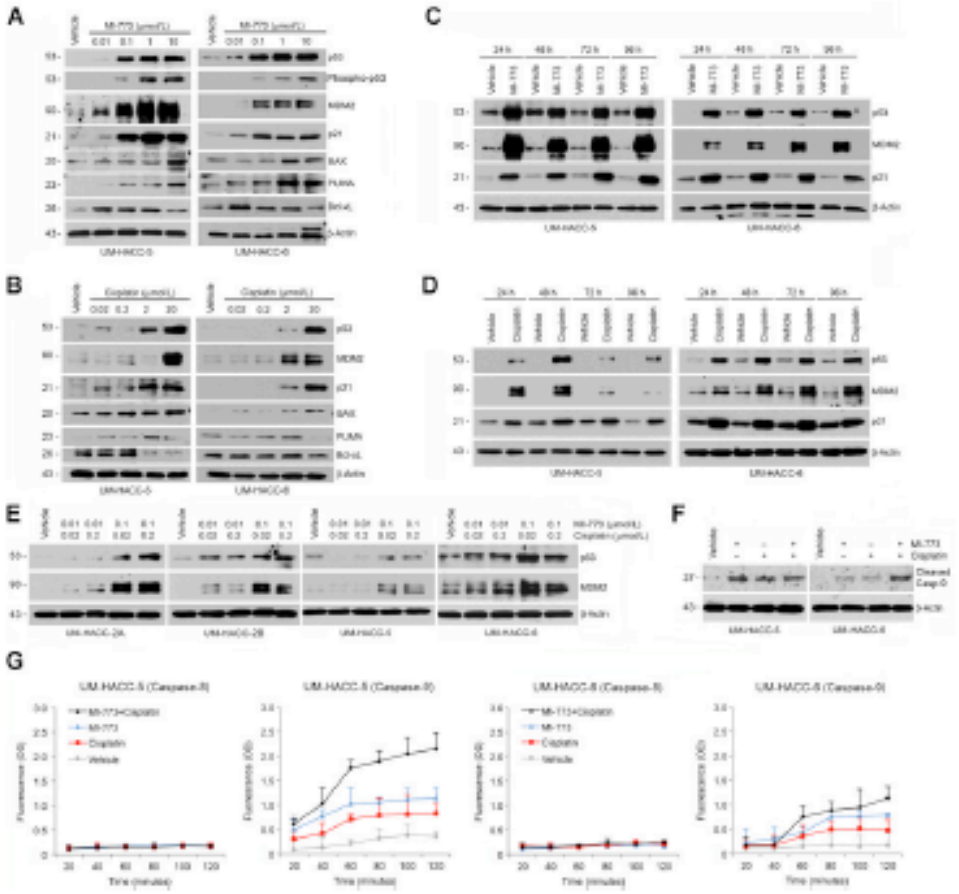

Figure 4.

MI-773 induces apoptosis through PUMA/BAX activation. **A** and **B**, Western blots for phosphorylated and total p53, HDM2, p21, BAX, PUMA, and Bcl-x_L in UM-HACC cells exposed to increasing concentrations of MI-773 (0.01–10 μmol/L) or cisplatin (0.02–20 μmol/L), respectively. **C** and **D**, Western blots for p53, HDM2, and p21 in UM-HACC cells treated with fixed doses of MI-773 (1 μmol/L) or cisplatin (2 μmol/L) for 24 to 96 hours, respectively. **E**, Western blots for p53 and HDM2 in UM-HACC cells upon treatment with lower doses of MI-773 (0.01–0.1 μmol/L) and cisplatin (0.02–0.2 μmol/L) for 24 hours. **F**, Western blots for cleaved caspase-9 in UM-HACC-5 and -6 cell exposed to MI-773and/or cisplatin for 24 hours. **G**, graphs depicting activity of caspase-8 or caspase-9 in UM-HACC-5 and -6 cells after 24 hours of treatment with MI-773 and/or cisplatin, as determined by fluorometric assays. OD, optical density. Caspase activity was measured every 20 minutes for a period of 2 hours.

discontinued (Fig. 5A). When MI-773 and cisplatin were combined, daily and weekly MI-773 regimens caused tumor regression. Remarkably, weekly MI-773 combined with cisplatin had a much more prolonged antitumor effect than daily MI-773 combined with cisplatin, even though the total amount of MI-773 administered in both groups was exactly the same (Fig. 5A). Importantly, none of the treatment regimens resulted in mouse weight loss beyond the 20% cutoff (Fig. 5B). We again performed a linear mixed effect model to evaluate the tumor growth rate over time, now including each dosing strategy as a different factor level. We performed multivariate regression to determine the differences in growth rates between the different treatment approaches. In a model including initial tumor size, overall growth rate, and cisplatin treatment, treatment with MI-773 weekly ($P < 0.0001$), but not daily ($P = 0.6365$), decreased the tumor growth rate (Fig. 5C). In addition, we generated Kaplan–Meier curves using as

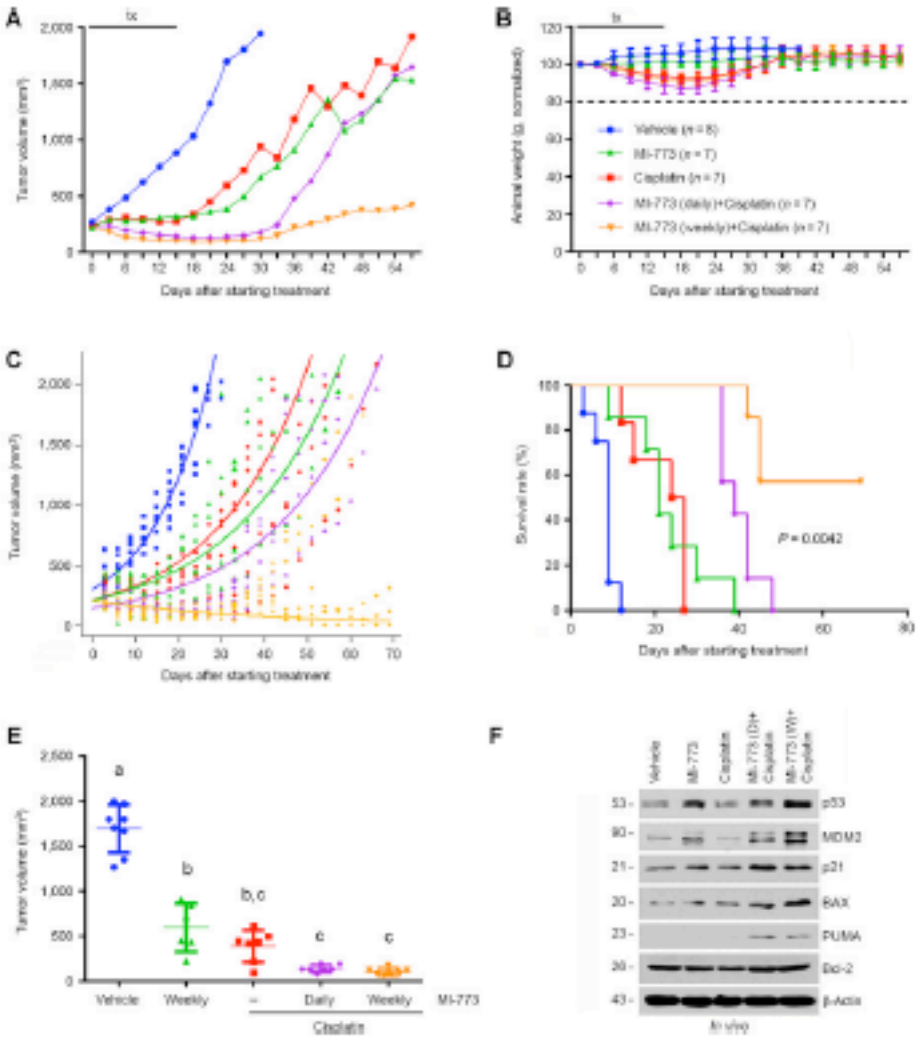

Figure 5.

Effect of MI-773 dosing on long-term efficacy. UM-PDX-HACC-5 tumors were transplanted in immunodeficient mice. When tumors reached 200 mm^3, animals were randomly allocated into five different treatment regimens as follows: 5 mg/kg saline (vehicle control), 200 mg/kg MI-773 (weekly), 5 mg/kg cisplatin, weekly dose of MI-773 (200 mg/kg) combined with 5 mg/kg cisplatin, or daily dose of MI-773 (28.5 mg/kg) combined with 5 mg/kg cisplatin. **A,** graph depicting tumor volume during treatment (tx) and follow-up (43 days) periods. Weekly regimens of MI-773 combined with cisplatin reduced tumors in size and prevented tumor regrowth compared with the other experimental groups or vehicle control. **B,** graph depicting mouse weight during the experimental period. Data were normalized against pretreatment weight. **C,** graph depicting a linear regression model using repeated measures for each tumor over time. Weekly regimens of MI-773 combined with cisplatin significantly decrease the tumor growth rate when compared with daily regimens of MI-773 + cisplatin or single-drug groups ($P < 0.001$). **D,** Kaplan–Meier analysis was done using a 2-fold increase in the tumor volume as a criterion for failure as compared with pretreatment volume. MI-773, cisplatin, or daily MI-773 combined with cisplatin extended time to failure significantly as compared with vehicle control ($P < 0.05$). Graph is depicting the statistical difference between daily and weekly regimens of MI-773 in combination with cisplatin ($P = 0.0042$). **E,** graph depicting the volume of each individual xenograft tumor at the 10th posttreatment day. Different lowercase letters (a, b, and c) indicate statistical difference ($P < 0.05$). **F,** Western blot analysis for p53, MDM2, p21, BAX, PUMA, and Bcl-2 in UM-PDX-HACC-5 tumors treated with either MI-773 or cisplatin as single agents, weekly or daily regimens of MI-773 combined with cisplatin, or vehicle control. Tumors were harvested 43 days after the last administration of drugs.

criterion for "event" a 2-fold increase in tumor volume as compared with pretreatment size. MI-773, cisplatin, and daily doses of MI-773 combined with cisplatin extended time to failure significantly as compared with vehicle control ($P < 0.05$). Notably, weekly MI-773 combined with cisplatin significantly extended time to failure when compared with daily MI-773 combined with cisplatin ($P = 0.0042$; Fig. 5D). Scatter plot graph was generated to depict tumor volume after 10 days of treatment (Fig. 5E). After 57 days, tumors were collected and processed for protein analysis. As previously noticed (Fig. 1D), therapeutic inhibition of MDM2 by MI-773, as a single agent or combined with cisplatin, causes upregulation of p53, MDM2, and p21 (Fig. 5F). Both daily and weekly combined treatments cause upregulation of apoptosis-related proteins BAX and PUMA. Taken together, the results suggest that weekly MI-773 combined with cisplatin is the preferable treatment schedule in preclinical models of ACC.

Therapeutic inhibition of the MDM2–p53 interaction reduces the fraction of CSCs and prevents recurrence of PDX ACC tumors

It is known that ALDH activity and CD44 expression can be used to identify CSCs in salivary gland tumors (23–26). To elucidate the impact of MI-773 and/or cisplatin treatment on ACC CSCs, mice harboring UM-HACC-PDX-5 tumors were divided in 4 groups ($n = 5$) and received MI-773 (200 mg/kg) for one week, combined or not with two single doses of cisplatin (at the first and seventh day; Fig. 6A). Two days after completion of treatment, tumors were retrieved and the proportion of CSCs was analyzed by flow cytometry. Notably, MI-773 alone (or in combination with cisplatin) decreased the fraction of CSCs ($ALDH^{high}CD44^{high}$) when compared with cisplatin alone or vehicle control ($P < 0.05$; Fig. 6B and C). Immunofluorescence for ALDH1 suggested the presence of a larger number of ALDH1-positive cells in the vehicle and cisplatin groups, particularly in close proximity to blood vessels and nerves (Supplementary Fig. S4). These findings suggest the existence of perivascular niches for CSCs in ACC, as it has been described for other tumors (29, 30).

It has been postulated that CSCs play an important role in tumor progression, particularly toward locoregional recurrence and/or metastases (31–33). In an attempt to mimic a clinical trial, we treated mice harboring UM-HACC-PDX-5 tumors ($n = 8$) with a neoadjuvant regimen of MI-773, followed by complete surgical resection of the tumor (Fig. 6D). Confirming data described above, a single dose of 200 mg/kg MI-773 significantly decreases the proportion of CSCs (Fig. 6E). Upon follow-up for 300 days (approximately half of the lifetime of a mouse), we observed that 5 (out of 8) mice from the control group presented tumor recurrence (Fig. 6F). Remarkably, not a single mouse from the MI-773–treated group presented tumor recurrence during this experimental period (Fig. 6F and G).

Discussion

ACCs are resistant to all conventional chemotherapeutic drugs available today. As a consequence, treatment for patients with this cancer is largely limited to surgery and radiation. The development of a safe and effective therapy is therefore urgently needed. It is known that MDM2 is overexpressed in ACCs (17, 18). We have recently demonstrated that therapeutic inhibition of the MDM2–p53 interaction with MI-773 mediates a short-term antitumor effect in preclinical models of ACC (21). Here, for the first time, we show that MI-773 reduces the fraction of ACC cancer stem cells, sensitizes ACC PDXs to cisplatin, and prevents tumor recurrence when used in a neoadjuvant setting.

Mechanisms associated with cancer progression often involve inactivation in p53 tumor suppressor functions, and MDM2 is a common mechanism to inhibit p53 activity (13–16). We demonstrated here that the reactivation of p53 by MI-773 causes a cell-cycle arrest and induces apoptosis of ACC cells. Interestingly, we observed here a partial translocation of p53 from the nucleus to the cytoplasm. Green and Kroemer (34) discussed the cytoplasmic functions of p53 in mitochondrial outer membrane permeabilization–mediated apoptosis. They propose that PUMA (p53-upregulated modulator of apoptosis), a target of nuclear p53, disrupts the Bcl-x_L–p53 interaction in the cytoplasm. Thus, p53 is released and forms a complex with BAX, initiating the caspase-dependent apoptotic pathway. Here, we observed the upregulation of BAX in ACC xenograft tumors treated with MI-773 as a single agent or combined to cisplatin. Cisplatin, in turn, was capable of Bcl-2 downregulation in UM-HACC-5 cells. The complementary mechanisms of action of MI-773 and cisplatin might explain the potentiation of the antitumor effect that was observed here when both drugs are used together in vivo.

It has been shown that the combination of MI-319 (an alternate small-molecule inhibitor of MDM2 from the class as MI-773) with cisplatin suppressed cell growth, colony formation, and induced apoptosis of pancreatic cancer cells (35). Another study showed that combination of cisplatin with Nutlin-3a, a different class of MDM2 inhibitor, enhanced apoptosis and reversed cisplatin resistance in ovarian cancer cells (36). Interestingly, the inhibition of MDM2–p53 interaction was able to radiosensitize tumor cells in a wide range of cancers types (e.g., lung, breast, colorectal, melanoma, and sarcoma; ref. 37). Our work demonstrated the therapeutic benefit of MI-773 and cisplatin combination in ACCs and offered a new hypothesis to explain the antitumor effect of this drug combination, that is, the ablation of CSCs. In addition, we demonstrated here that MI-773 decreases the risk of locoregional recurrence in preclinical models, which is likely associated with its effect on eliminating at least in part the highly tumorigenic CSCs.

The long-term prognosis of patients with ACC is directly affected by late episodes of recurrence and/or metastases (10). In head and neck squamous cell carcinomas, resistance to chemotherapy and recurrence has been associated with CSCs (22, 29, 38). This small population of uniquely tumorigenic cells was also found in salivary gland tumors (25, 26), but their sensitivity to chemotherapy is not understood. Here, we observed that cisplatin did not have a significant effect on the fraction of CSCs in ACC xenograft tumors. In contrast, MI-773 significantly reduced the fraction of CSCs when compared with cisplatin or vehicle control. This finding raises a putative hypothesis to explain the long-term antitumor effect of this drug combination in vivo, that is, MI-773 targets the CSCs (resistant to cisplatin) that have been shown to be mediators of tumor recurrence and/or metastases (33, 38). Indeed, when we exposed mice to a neoadjuvant treatment of MI-773 (i.e., a single dose of MI-773 followed by surgical removal of the tumor, and a subsequent MI-773 therapy for 30 days), we confirmed the reduction of CSCs in the excised tumors. Notably, no recurrence was observed in mice treated with MI-773 even after 300 days of follow-up (about half of the lifetime of mice), while more than half of the mice that received vehicle presented recurrent tumors.

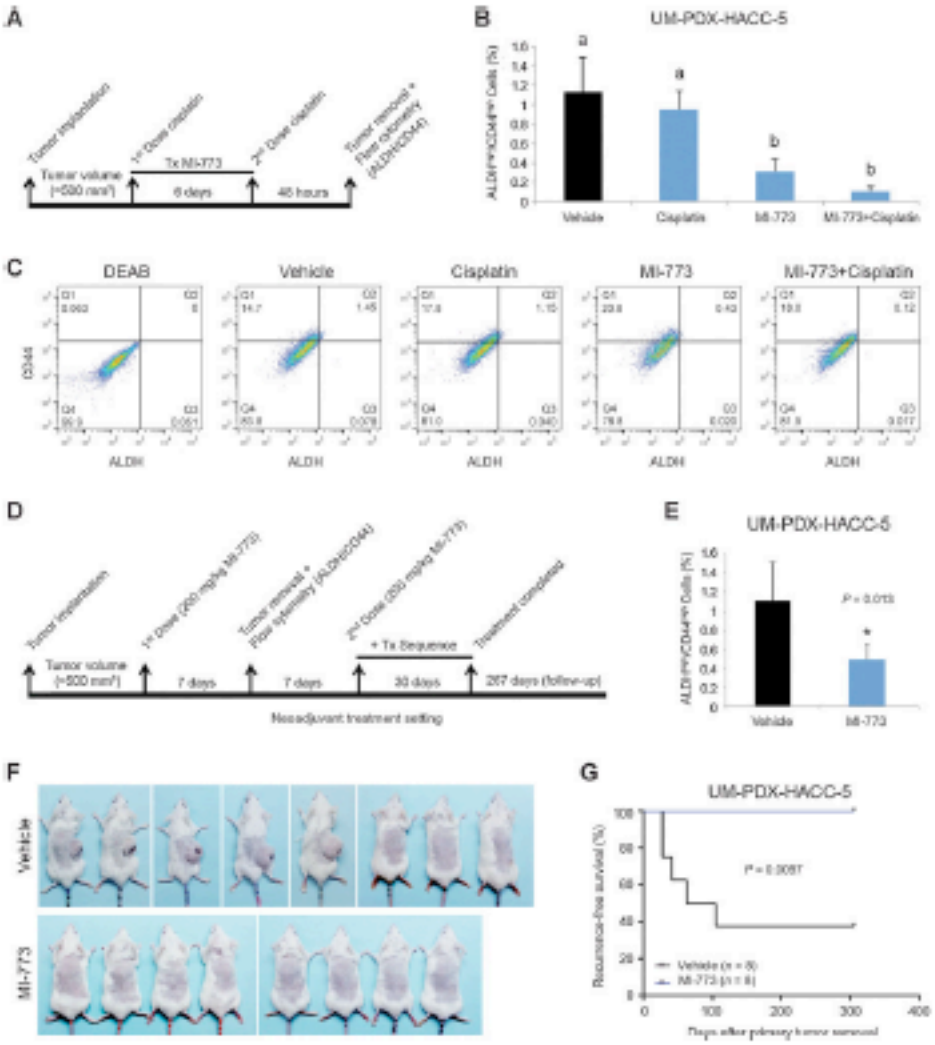

Figure 6.

MI-773 reduces the fraction of CSCs and prevents recurrence in ACC xenograft tumors. **A**, timeline showing the experimental design. **B**, graph depicting the fraction of CSCs ($ALDH^{high}CD44^{+/-}$) identified by flow cytometry in xenograft tumors treated with 5 mg/kg cisplatin and/or 200 mg/kg MI-773. Different lowercase letters (a and b) indicate significant differences among groups ($P < 0.05$). **C**, graphs depicting the flow cytometrygates for the percentage of CSCs (Q2) in UM-PDX-HACC-5 tumors treated with cisplatin and/or MI-773. DEAB is showing the control of the reaction. **D**, timeline showing the neoadjuvant treatment (Tx) design. **E**, graph depicting the fraction of CSCs ($ALDH^{high}CD44^{high}$) identify by flow cytometry in UM-PDX-HACC-5 tumors treated with MI-773 or vehicle control. **F**, macroscopic view of mice harboring recurrent tumors or tumor-free animals at the end of the experiment. **G**, Kaplan–Meier curve depicting recurrence-free survival in mice treated either with 200 mg/kg MI-773 or vehicle control. Recurrence was defined as the presence of a palpable tumor.

In conclusion, this work demonstrated that therapeutic inhibition of the MDM2–p53 interaction with MI-773 is an effective antitumor strategy that mediates ACC tumor regression, reduces the fraction of CSCs, sensitizes xenograft tumors to cisplatin, and prevents tumor recurrence in preclinical models of ACC. These preclinical data provide the conceptual framework for an early

phase I trial testing a combination therapy of MI-773 and cisplatin for treatment of patients with recurrent/metastatic ACC. Once clinical efficacy is established, a step further would be the testing of MI-773 as an adjuvant or neoadjuvant therapy along with surgical resection of the tumor.

Disclosure of Potential Conflicts of Interest

S. Wang reports receiving other commercial research support from and holds ownership interest (including patents) in Ascenta Therapeutics. No potential conflicts of interest were disclosed by the other authors.

Authors' Contributions

Conception and design: F. Nör, G.A. Araújo, J.E. Nör
Development of methodology: F. Nör, K.A. Warner, G.A. Araújo, J.E. Nör
Acquisition of data (provided animals, acquired and managed patients, provided facilities, etc.): K.A. Warner, G.A. Araújo, S.A. Kerk, J.I. Helman
Analysis and interpretation of data (e.g., statistical analysis, biostatistics, computational analysis): F. Nör, G.A. Araújo, A.T. Pearson, M. Sant'Ana Filho, J.E. Nör
Writing, review, and/or revision of the manuscript: F. Nör, K.A. Warner, G.A. Araújo, A.T. Pearson, S.A. Kerk, J.I. Helman, M. Sant'Ana Filho, J.E. Nör
Administrative, technical, or material support (i.e., reporting or organizing data, constructing databases): Z. Zhang, G.A. Araújo
Study supervision: Z. Zhang, M. Sant'Ana Filho, J.E. Nör
Other (provided the MDM2–p53 interaction inhibitor): S. Wang

Acknowledgments

We thank the patients who kindly provided the tumor specimens used to generate the adenoid cystic carcinoma cells and PDX models that enabled this research project. We also thank the surgeons, nurses, and support staff that enabled the process of tumor specimen collection and processing for use in research.

Grant Support

This work was funded by CNPq (to F. Nör), Adenoid Cystic Carcinoma Research Foundation (AACRF), University of Michigan Head and Neck SPORE P50-CA97248 from the NIH/NCI, and grants R01-DE020220 and R01-DE21109 from the NIH/NIDCR (to J.E. Nör).

The costs of publication of this article were defrayed in part by the payment of page charges. This article must therefore be hereby marked advertisement in accordance with 18 U.S.C. Section 1734 solely to indicate this fact.

Received May 13, 2016; revised August 13, 2016; accepted August 15, 2016; published OnlineFirst xx xx, xxxx.

References

1. Coca-Pelaz A, Rodrigo JP, Bradley PJ, Vander Poorten V, Triantafyllou A, Hunt JL, et al. Adenoid cystic carcinoma of the head and neck – An update. Oral Oncol 2015;51:652–61.
2. Kowalski PJ, Padino AF. Perineural invasion in adenoid cystic carcinoma: Is causation/promotion by brain-derived neurotrophic factor. Hum Pathol 2002;33:933–6.
3. Chae YK, Chung SY, Davis AA, Carneiro BA, Chandra S, Kaplan J, et al. Adenoid cystic carcinoma: current therapy and potential therapeutic advances based on genomic profiling. Oncotarget 2015;6:37 117–34.
4. Dillon PM, Chakraborty S, Moskaluk CA, Joshi PJ, Thomas CY. Adenoid cystic carcinoma: a review of recent advances, molecular targets, and clinical trials. Head Neck 2016;38:620–7.
5. Dodd RL, Slevin NJ. Salivary gland adenoid cystic carcinoma: a review of chemotherapy and molecular therapies. Oral Oncol 2006;42:759–69.
6. Ghosal N, Mak K, Shenjere P, Julyan P, Hastings D, Ward T, et al. Phase II study of cisplatin and imatinib in advanced salivary adenoid cystic carcinoma. Br J Oral Maxillofac Surg 2011;49:510–5.
7. Andry G, Hamoir M, Locati LD, Licitra L, Langendijk JA. Management of salivary gland tumors. Expert Rev Anticancer Ther 2012;12:1161–8.
8. Licitra L, Cavina R, Grandi C, Palma SD, Cinquini M, Demichelis R, et al. Cisplatin, doxorubicin and cyclophosphamide in advanced salivary gland carcinoma. A phase II trial of 22 patients. Ann Oncol 1996;7:640–2.
9. Rosa PJ, Teoh EM, Ahern RP, Rhys-Evans PH, Harrington KJ, Nutting CM, et al. Epirubicin, cisplatin and protracted venous infusion 5-fluorouracil chemotherapy for advanced salivary adenoid cystic carcinoma. Clin Oncol (R Coll Radiol) 2009;21:311–6.
10. Lloyd S, Yu JB, Wilson LD, Decker RH. Determinants and patterns of survival in adenoid cystic carcinoma of head and neck, including an analysis of adjuvant radiation therapy. Am J Clin Oncol 2011;34:276–81.
11. Wong SJ, Karrison T, Hayes DN, Kies MS, Cullen KJ, Tan Wysmyon T, et al. Phase II trial of dasatinib for recurrent or metastatic c-KIT expressing adenoid cystic carcinoma and for nonadenoid cystic malignant salivary tumors. Ann Oncol 2016;27:318–23.
12. Gardyl J, Amit M, Kou L, Palmer R, Migliacci J, Kashi N, et al. Nomograms for predicting survival and recurrence in patients with adenoid cystic carcinoma. An international collaborative study. Eur J Cancer 2015;51:2768–76.
13. Hainaut P, Hollstein M. p53 and human cancer: the first ten thousand mutations. Adv Cancer Res 2000;77:81–137.
14. Danjia S, Nicol H, Pierre J. MDM2: life without p53. Trends Genet 2001;17:459–64.
15. Wu X, Bayle JH, Olson D, Levine AJ. The p53-mdm-2 autoregulatory feedback loop. Genes Dev 1993;7:1126–32.
16. Momand J, Wu HH, Dasgupta G. MDM2–master regulator of the p53 tumor suppressor protein. Gene 2000;242:15–29.
17. Araújo VC, Martins MT, Ishe KR, Gomes RS, Araújo NS. Immunohistochemical MDM2 expression in minor salivary gland tumours and its relationship to p53 gene status. Oral Oncol 2000;36:67–9.
18. de Lima Mde D, Marques YM, Alves Sde MJr, Freitas VM, Soares FA, de Araújo VC, et al. MDM2, P53, P21WAF1 and pAKT panel levels in gender and behaviour of adenoid cystic carcinoma. Cancer Epidemiol 2009;33:142–6.
19. Wang S, Sun W, Zhao Y, McEachern D, Meaux I, Barrière C, et al. SAR405838: an optimized inhibitor of MDM2-p53 interaction that induces complete and durable tumor regression. Cancer Res 2014;74:5855–65.
20. Zhao Y, Aguilar A, Bernard D, Wang S. Small-molecule inhibitors of the MDM2-p53 protein-protein interaction (MDM2 Inhibitors) in clinical trials for cancer treatment. J Med Chem 2015;58:1038–52.
21. Warner K, Nör F, Araújo C, Martins M, Zhang Z, McLean SA, et al. Targeting MDM2 for treatment of adenoid cystic carcinoma. Clin Cancer Res 2016;22:3550–9.
22. Nör C, Zhang Z, Warner KA, Bernardi L, Visioli F, Helman JI, et al. Cisplatin induces Bmi-1 and enhances the stem cell fraction in head and neck cancer. Neoplasia 2014;16:137–46.
23. Araújo CA, Warner KA, Nör F, Helman J, Pearson AT, Nör JE. Bmi1-mimetic small molecule inhibits the growth and recurrence of adenoid cystic carcinoma. Oral Oncol 2015;51:859–67.
24. Pearson AT, Finkel EA, Warner KA, Nör F, Tice D, Martins MD, et al. Patient-derived xenograft (PDX) tumors increase growth rate with time. Oncotarget 2016;7:7993–8005.
25. Adams A, Warner K, Nör JE. Salivary gland cancer stem cells. Oral Oncol 2013;49:845–53.
26. Adams A, Warner K, Pearson AT, Zhang Z, Kim HS, Mochizuki D, et al. ALDH/CD44 identifies uniquely tumorigenic cancer stem cells in salivary gland mucoepidermoid carcinomas. Oncotarget 2015;29:26633–50.
27. Zhang Z, Neiva KG, Lingen MW, Ellis LM, Nör JE. VEGF-dependent tumor angiogenesis requires inverse and reciprocal regulation of VEGFR1 and VEGFR2. Cell Death Differ 2010;17:499–512.
28. Wagner JM, Kamitz LM. Cisplatin-induced DNA damage activates replication checkpoint signaling components that differentially affect tumor cell survival. Mol Pharmacol 2009;76:208–214.

29. Krishnamurthy S, Nör JE. Head and neck cancer stem cells. J Dent Res 2012;91:884–890.
30. Ritchie KE, Nör JE. Perivascular stem cell niche in head and neck cancer. Cancer Lett 2013;338:61–6.
31. Reya T, Morrison SJ, Clarke MF, Weissman IL. Stem cells, cancer, and cancer stem cells. Nature 2001;414:105–11.
32. Chinn SB, Darr OA, Owen JH, Bellile E, McHugh JB, Spector ME, et al. Cancer stem cells: mediators of tumorigenesis and metastasis in head and neck squamous cell carcinoma. Head Neck 2015;37:317–26.
33. Islam F, Gopalan V, Smith RA, Lam AK. Translational potential of cancer stem cells: a review of the detection of cancer stem cells and their roles in cancer recurrence and cancer treatment. Exp Cell Res 2015;335:135–47.
34. Green DR, Kroemer G. Cytoplasmic functions of the tumour suppressor p53. Nature 2009;458:1127–30.
35. Azmi AS, Aboukameel A, Banerjee S, Wang Z, Mohammad M, Wu J, et al. MDM2 inhibitor MI-319 in combination with cisplatin is an effective treatment for pancreatic cancer independent of p53 function. Eur J Cancer 2010;46:1122–31.
36. Mir R, Tonsa A, Martinez-Soler F, Vidal A, Condom E, Pérez-Perarnau A, et al. MDM2 antagonists induce apoptosis and synergize with Cisplatin overcoming chemoresistance in TP53 wild-type ovarian cancer cells. Int J Cancer 2013;132:1525–36.
37. Wemer LR, Huang S, Franda DM, Armstrong EA, Ma E, Li C, et al. Small molecule inhibition of MDM2-p53 interaction augments radiation response in human tumors. Mol Cancer Ther 2015;14:1996–2003.
38. Zhang Z, Filho MS, Nör JE. The biology of head and neck cancer stem cells. Oral Oncol 2012;48:1–9.

Supplementary Figure Legends

Supplementary Figure S1. Treatment with MI-773 and/or cisplatin is not toxic to mice. Graph depicting mouse weight during the experimental period. Data were normalized against pre-treatment weight.

Supplementary Figure S2. Representative photomicrographs of UM-HACC-5 and -6 cells exposed to 1 μM MI-773 and/or 2 μM cisplatin, or vehicle control, for 72 hours *in vitro*.

Supplementary Figure S3. Representative graphs depicting the number of UM-HACC-5 (A) and -6 (B) cells in each cell-cycle phase after treatment with 1 μM MI-773 and/or 2 μM cisplatin, or vehicle control, for 24 hours.

Supplementary Figure S4. Representative photomicrographs obtained by immunofluorescence for ALDH (green) in UM-PDX-HACC-5 tumors treated with MI-773 and/or cisplatin. ALDH-positive cells are predominantly observed in vehicle and cisplatin groups (details) and are apparently located in close proximity to blood vessels (*) and nerve structures (N). Scale bar represents 50 μm (400x).

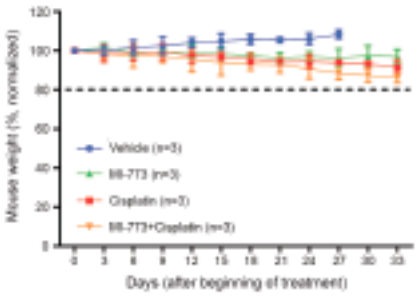

Suppl Figure S1. Nor et al

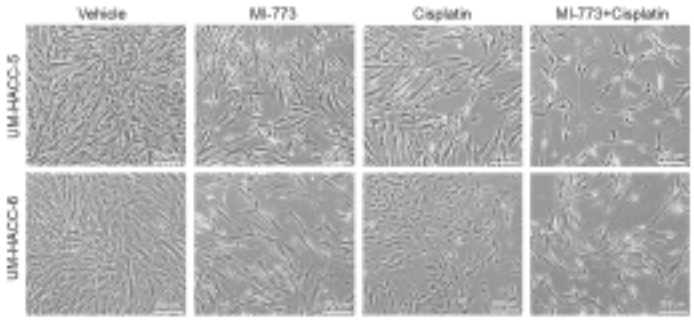

Suppl Figure S2. Nor et al

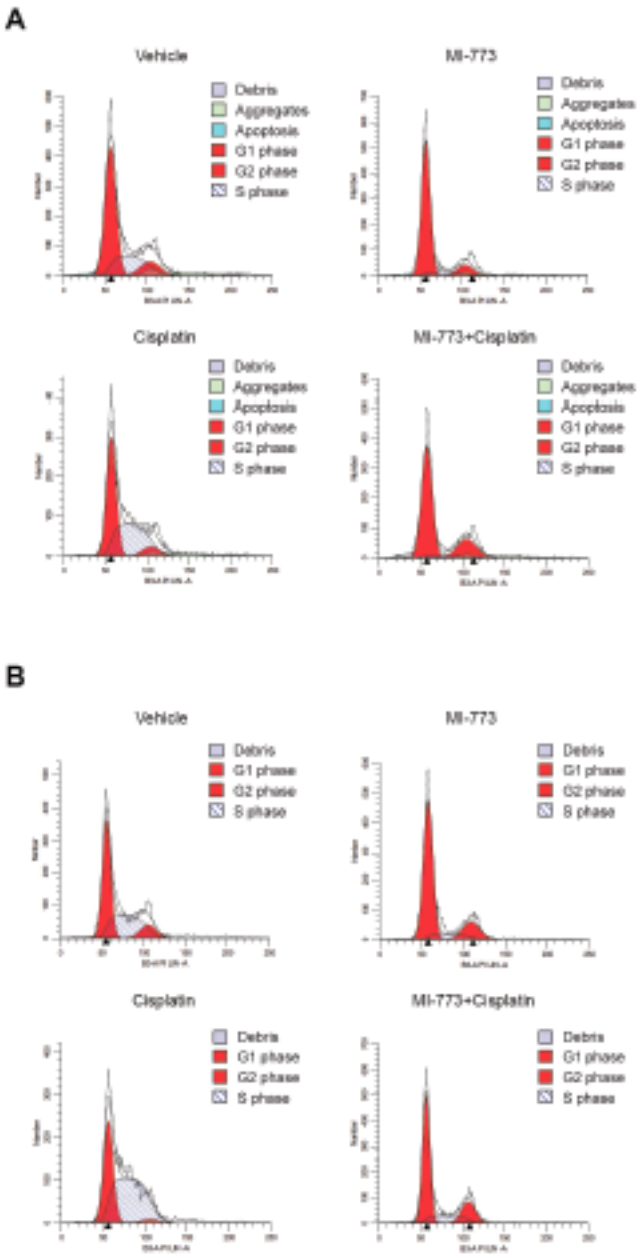

Suppl Figure S3. Nor et al

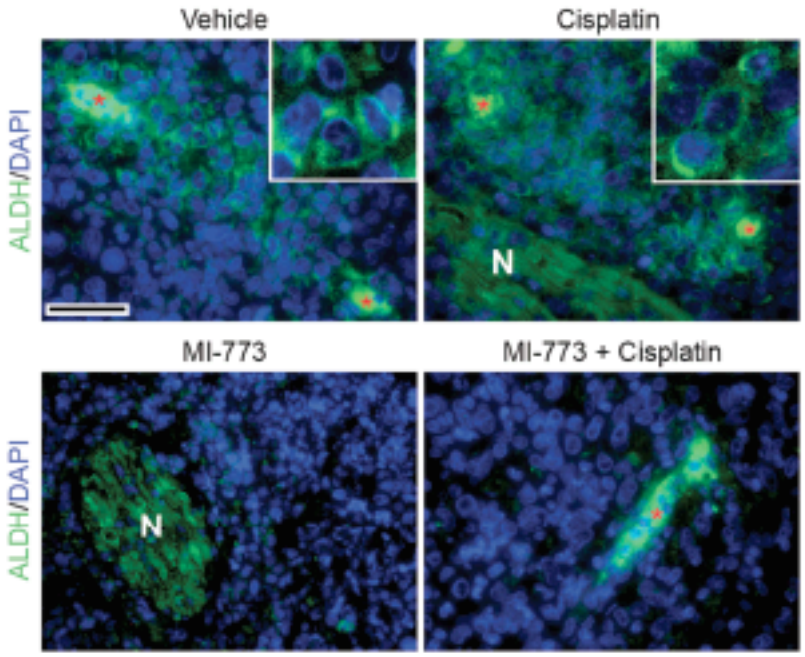

Supll Figure S4. Nor et al

5. CONSIDERAÇÕES FINAIS

Este capítulo final foi pensado e estruturado não com o intuito de simplesmente repetir os resultados apresentados e discutidos nos dois artigos científicos que compõe esta tese. Mas sim, de uma forma simples e objetiva, apresentar as principais contribuições que este trabalho traz no campo do tratamento do carcinoma adenoide cístico e, quem sabe, de outros cânceres. Talvez mais do que isso, gostaríamos de compartilhar algumas dúvidas e limitações que surgiram durante esses 4 anos de estudo acerca deste tema e que, potencialmente, podem embasar o desenvolvimento de novas pesquisas.

A partir da análise da evidência atual acerca das opções terapêuticas já testadas em ensaios clínicos, resumidas no capitulo de revisão da literatura, é notória a falta de uma opção de droga ou regime de quimioterapia para o tratamento de pacientes diagnosticados com carcinoma adenoide cístico. Isso se deve, em grande parte: (i) pela ineficácia dos medicamentos quimioterápicos convencionais (ex. cisplatina); (ii) pela falta de dados confiáveis e relevantes sobre o uso de novas drogas (as chamadas drogas de alvo especifico); (iii) pelo fato do CAC ser uma condição rara, logo existem poucos pacientes com esta lesão que poderiam compor uma amostra adequada de um ensaio clínico.

Dessa maneira, nos parece muito oportuna a discussão sobre os modelos de xenoenxerto derivados de paciente. Como apresentado no inicio desta tese, este modelo traz a grande vantagem de permitir o estudo de um tumor antes único de um paciente. Assim, o desenvolvimento de diversos exemplares deste tumor em animal, e que mantém as características do tumor original, permite o que antes seria inviável: o teste simultâneo de inúmeras drogas e combinações terapêuticas, sem o envolvimento direto do paciente. Os resultados destes estudos podem vir a beneficiar não só o tratamento deste paciente doador do tumor que gerou o modelo *in vivo*, mas também outros tantos que são diagnosticados com a mesma doença.

Ao mesmo tempo em que cresce o interesse e o uso de modelos de xenoenxerto derivado de paciente, é também necessário que haja uma constante avaliação e acompanhamento deste modelo pré-clínico. Isso, pois Pearson et al.

(2016) já mostrou que os modelos XEDP de carcinoma espinocelular de cabeça e pescoço, e de carcinoma adenoide cístico gerados pelo nosso grupo de pesquisa apresentaram mudanças significativas ao longo das passagens entre animais. Verificou-se um aumento na velocidade de crescimento tumoral *in vivo*, além de mudanças em algumas características histopatológicas importantes, como aumento do pleomorfismo celular e alteração do padrão histológico (CAC). A fim de verificar o grau de comprometimento causado por essas mudanças nas propriedades dos tumores, realizamos análise de DNA (STR profiling), que comprovou a semelhança do tumor original com o tumor estabelecido *in vivo*.

O fato do tumor xenoenxertado manter sua identidade, mesmo adquirindo características clinicas e histopatológicas mais agressivas no decorrer das passagens, acaba criando um desafio maior à terapia em estudo. Assim, a droga pode ter sua eficácia testada em diferentes cenários e apresentações do mesmo tumor, ou seja, em passagens iniciais ou tardias. Portanto, abre-se aqui a perspectiva para novos estudos avaliando a ação de agentes terapêuticos em diferentes momentos e passagens *in vivo*. Além disso, outro ponto a ser esclarecido em futuras investigações é o limite de passagens em que o tumor xenoenxertado mantém a semelhança genética com seu doador humano. Se é que este limite existe.

Talvez mais importante do que apresentar as vantagens do modelo XEDP, a presente tese insere na literatura, através dos dois artigos já publicados, forte evidência acerca da eficácia da inibição terapêutica da interação MDM2-p53 como possível tratamento para o carcinoma adenoide cístico. O efeito anti-tumoral significativo da droga MI-773 foi comprovado em experimentos distintos, utilizando tumores de passagens distintas. Os possíveis cenários clínicos foram apresentados ao final do segundo artigo, considerando os resultados positivos da combinação MI-773 + cisplatina. Além disso, o fato de MI-773 ter evitado a recorrência destes tumores, num período de avaliação que compreende o equivalente a metade da vida de um camundongo, o coloca como forte candidato para futuros ensaios clínicos em humanos. É importante lembrar que a recorrência é um dos principais causadores de morte em pacientes com CAC. Nesse sentido, os dados aqui apresentados podem servir de apoio para futuras pesquisas acerca do efeito de MI-773 em outros modelos de CAC proveniente de diferentes pacientes. Dessa forma, é possível

superar a limitação de se ter dados gerados em um único laboratório e tornar ainda mais consistente a evidencia gerada nesta tese. Além disso, esperamos que esta tese também incentive a pesquisa acerca do efeito de MI-773 em outros tipos de câncer. Já se sabe que MI-773 mostrou resultados favoráveis em lipossarcomas (BILL, *et al.*, 2016) e neuroblastomas (LU, *et al.*, 2016) em pesquisas recentes.

O objetivo final de toda pesquisa com novos agentes terapêuticos em câncer, ao nosso entendimento, deve ser a translação dos seus resultados até a prática clínica. E que estes achados, efetivamente, levem a algum benefício aos pacientes. Essa foi a motivação que permeou a concepção, o desenho e a escolha da metodologia empregada nos artigos que compõe esta tese. Esperamos poder acompanhar o sucesso dessa terapia em futuros ensaios clínicos.

6. REFERÊNCIAS

ACASIGUA, G. A. et al. BH3-mimetic small molecule inhibits the growth and recurrence of adenoid cystic carcinoma. **Oral Oncol.**, v. 51, no. 9, p. 839-847, Sep. 2015.

ADELSTEIN, D. J. et al. Biology and management of salivary gland cancers. **Semin Radiat Oncol.**, v. 22, no. 3, p. 245-253, Jul. 2012.

AGULNIK, M. et al. Phase II study of lapatinib in recurrent or metastatic epidermal growth factor receptor and/or erbB2 expressing adenoid cystic carcinoma and non adenoid cystic carcinoma malignant tumors of the salivary glands. **J Clin Oncol.**, v. 25, no. 25, p. 3978-3984, Sep. 2007.

AIROLDI, M. et al. Cisplatin, epirubicin and 5-fluorouracil combination chemotherapy for recurrent carcinoma of the salivary gland. **Tumori.**, v. 75, no. 3, p. 252-256, Jun. 1989.

AIROLDI, M. et al. Paclitaxel and carboplatin for recurrent salivary gland malignancies. **Anticancer Res.**, v. 20, no. 5C, p. 3781-3783, Oct. 2000.

AIROLDI, M. et al. Phase II randomized trial comparing vinorelbine versus vinorelbine plus cisplatin in patients with recurrent salivary gland malignancies. **Cancer.**, v. 91, no. 3, p. 541-547, Feb. 2001.

ALARCON-VARGAS, D.; RONAI, Z. p53-Mdm2--the affair that never ends. **Carcinogenesis.**, v. 23, no. 4, p. 541-547, Apr. 2002.

BAI, L. et al. BM-1197: a novel and specific Bcl-2/Bcl-xL inhibitor inducing complete and long-lasting tumor regression in vivo. **PLoS One.** , v. 9, no. 6, e99404, Jun. 2014.

BARNES, L. et al. **Health Organization classification of tumours. Pathology and genetics of tumours of the head and neck**. Lyon: IARC Press, 2005.

BELANI, C. P.; EISENBERGER, M. A.; GRAY, W. C. Preliminary experience with chemotherapy in advanced salivary gland neoplasms. **Med Pediatr Oncol.**, v. 16, no. 3, p. 197-202. 1988.

BELL, D. et al. Cell type-dependent biomarker expression in adenoid cystic carcinoma: biologic and therapeutic implications. **Cancer.**, v. 116, no. 24, p. 5749-5756, Dec. 2010.

BILL, K. L. et al. SAR405838: A Novel and Potent Inhibitor of the MDM2:p53 Axis for the Treatment of Dedifferentiated Liposarcoma. **Clin Cancer Res.**, v. 22, no. 5, p. 1150-1160, Mar. 2016.

BRILL, L. B. et al. Analysis of MYB expression and MYB-NFIB gene fusions in adenoid cystic carcinoma and other salivary neoplasms. **Mod Pathol.**, v. 24, no. 9, p. 1169-1176, Sep. 2011.

CAWSON, R.; ODELL, E. **Neoplastic and non-neoplastic diseases of salivary glands: salivary glands neoplasms**. 6th ed.; Hong Kong Churchill Livingstone an imprint of Elsevier Science, 2003. p.247–256.

CHAE, Y. K. et al. Adenoid cystic carcinoma: current therapy and potential therapeutic advances based on genomic profiling. **Oncotarget.**, v. 6, no. 35, p. 37117-37134, Nov. 2015.

COCA-PELAZ, A. et al. Adenoid cystic carcinoma of the head and neck--An update. **Oral Oncol.**, v. 51, no. 7, p. 652-661, Jul. 2015.

CORDON-CARDO, C. et al. Molecular abnormalities of mdm2 and p53 genes in adult soft tissue sarcomas. **Cancer Res.**, v. 54, no. 3, p. 794-799, Feb. 1994.

CREAGAN, E. T. et al. Cisplatin-based chemotherapy for neoplasms arising from salivary glands and contiguous structures in the head and neck. **Cancer.**, v. 62, no. 11, p. 2313-2319, Dec. 1988.

DAUJAT, S.; NEEL, H.; PIETTE, J. MDM2: life without p53. **Trends Genet.**, v. 17, no. 8, p. 459-464, Aug. 2001.

DE HAAN, L. D. et al. Cisplatin-based chemotherapy in advanced adenoid cystic carcinoma of the head and neck. **Head Neck.**, v. 14, no. 4, p. 273-277, Aug. 1992.

DE LIMA MDE, D. et al. MDM2, P53, P21WAF1 and pAKT protein levels in genesis and behaviour of adenoid cystic carcinoma. **Cancer Epidemiol.**, v. 33, no. 2, p. 142-146, Aug. 2009.

DEROSE, Y. S. et al. Tumor grafts derived from women with breast cancer authentically reflect tumor pathology, growth, metastasis and disease outcomes. **Nat Med.**, v. 17, no. 11, p. 1514-1520, Oct. 2011.

DI PALMA, S. et al. Primary sinonasal adenoid cystic carcinoma presenting with skin metastases--genomic profile and expression of the MYB-NFIB fusion biomarker. **Histopathology.**, v. 64, no. 3, p. 453-455, Feb. 2014.

DILLON, P. M. et al. Adenoid cystic carcinoma: A review of recent advances, molecular targets, and clinical trials. **Head Neck.**, v. 38, no. 4, p. 620-627, Apr. 2016.

DODD, R. L.; SLEVIN, N. J. Salivary gland adenoid cystic carcinoma: a review of chemotherapy and molecular therapies. **Oral Oncol.**, v. 42, no. 8, p. 756-769, Sep. 2006.

DREYFUSS, A. I. et al. Cyclophosphamide, doxorubicin, and cisplatin combination chemotherapy for advanced carcinomas of salivary gland origin. **Cancer.**, v. 60, no. 12, p. 2869-2872, Dec. 1987.

FICHTNER, I. et al. Establishment of patient-derived non-small cell lung cancer xenografts as models for the identification of predictive biomarkers. **Clin Cancer Res.**, v. 14, no. 20, p. 6456-6468, Oct. 2008.

GEDLICKA, C. et al. Mitoxantrone and cisplatin in recurrent and/or metastatic salivary gland malignancies. **Anticancer Drugs.**, v. 13, no. 5, p. 491-495, Jun. 2002.

GHOSAL, N. et al. Phase II study of cisplatin and imatinib in advanced salivary adenoid cystic carcinoma. **Br J Oral Maxillofac Surg.**, v. 49, no. 7, p. 510-515, Oct. 2011.

GILBERT, J. et al. Phase II trial of taxol in salivary gland malignancies (E1394): a trial of the Eastern Cooperative Oncology Group. **Head Neck.**, v. 28, no. 3, p. 197-204, Mar. 2006.

GLISSON, B. et al. Phase II trial of gefitinib in patients with incurable salivary gland câncer. **Proc Am Soc Clin Oncol.**, v. 23, abstract 5532. 2005.

HAUPT, Y. et al. Mdm2 promotes the rapid degradation of p53. **Nature.**, v. 387, no. 6630, p. 296-299, May. 1997.

HIDALGO, M. et al. Patient-derived xenograft models: an emerging platform for translational cancer research. **Cancer Discov.**, v. 4, no. 9, p. 998-1013, Sep. 2014.

HILL, M. E. et al. Cisplatin and 5-fluorouracil for symptom control in advanced salivary adenoid cystic carcinoma. **Oral Oncol.**, v. 33, no. 4, p. 275-278, Jul. 1997.

HOLST, V. A. et al. KIT protein expression and analysis of c-kit gene mutation in adenoid cystic carcinoma. **Mod Pathol.**, v. 12, no. 10, p. 956-960, Oct. 1999.

HOTTE, S. J. et al. Imatinib mesylate in patients with adenoid cystic cancers of the salivary glands expressing c-kit: a Princess Margaret Hospital phase II consortium study. **J Clin Oncol.**, v. 23, no. 3, p. 585-590, Jan. 2005.

HOTTE, S. J. et al. Imatinib mesylate in patients with adenoid cystic cancers of the salivary glands expressing c-kit: a Princess Margaret Hospital phase II consortium study. **J Clin Oncol.**, v. 23, no. 3, p. 585-590, Jan. 2005.

IZUMCHENKO, E. et al. Patient-derived xenografts as tools in pharmaceutical development. **Clin Pharmacol Ther.**, v. 99, no. 6, p. 612-621, Jun. 2016.

JAIN, A. et al. Characterization and localization of c-kit and epidermal growth factor receptor in different patterns of adenoid cystic carcinoma. **J Cancer Res Ther.**, v. 12, no. 2, p. 834-839, Apr. 2016.

JENG, Y. M.; LIN, C. Y.; HSU, H. C. Expression of the c-kit protein is associated with certain subtypes of salivary gland carcinoma. **Cancer Lett.**, v. 154, no. 1, p. 107-111, Jun. 2000.

JOHNSON, J. I. et al. Relationships between drug activity in NCI preclinical in vitro and in vivo models and early clinical trials. **Br J Cancer.**, v. 84, no. 10, p. 1424-1431, May. 2001.

JONES, S. N. et al. Overexpression of Mdm2 in mice reveals a p53-independent role for Mdm2 in tumorigenesis. **Proc Natl Acad Sci U S A.**, v. 95, no. 26, p. 15608-15612, Dec. 1998.

JONES, S. N. et al. Rescue of embryonic lethality in Mdm2-deficient mice by absence of p53. **Nature.**, v. 378, no. 6553, p. 206-208, Nov. 1995.

KEYSAR, S. B. et al. A patient tumor transplant model of squamous cell cancer identifies PI3K inhibitors as candidate therapeutics in defined molecular bins. **Mol Oncol.**, v. 7, no. 4, p. 776-790, Aug. 2013.

KOWALSKI, P. J.; PAULINO, A. F. Perineural invasion in adenoid cystic carcinoma: Its causation/promotion by brain-derived neurotrophic factor. **Hum Pathol.**, v. 33, no. 9, p. 933-936, Sep. 2002.

KUBBUTAT, M. H.; JONES, S. N.; VOUSDEN, K. H. Regulation of p53 stability by Mdm2. **Nature.**, v. 387, no. 6630, p. 299-303, May. 1997.

LAURIE, S. A. et al. A phase 2 study of platinum and gemcitabine in patients with advanced salivary gland cancer: a trial of the NCIC Clinical Trials Group. **Cancer.**, v. 116, no. 2, p. 362-368, Jan. 2010.

LAURIE, S. A. et al. Systemic therapy in the management of metastatic or locally recurrent adenoid cystic carcinoma of the salivary glands: a systematic review. **Lancet Oncol.**, v. 12, no. 8, p.815-824, Aug. 2011.

LAURIE, S. A.; LICITRA, L. Systemic therapy in the palliative management of advanced salivary gland cancers. **J Clin Oncol.**, v. 24, no. 17, p. 2673-2678, Jun. 2006.

LICITRA, L. et al. Cisplatin in advanced salivary gland carcinoma. A phase II study of 25 patients. **Cancer.**, v. 68, no. 9, p. 1874-1877, Nov. 1991.

LICITRA, L. et al. Cisplatin, doxorubicin and cyclophosphamide in advanced salivary gland carcinoma. A phase II trial of 22 patients. **Ann Oncol.**, v. 7, no. 6, p. 640-642, Aug. 1996.

LICITRA, L. et al. Cetuximab (C225) in recurrent and/or metastatic salivar gland carcinomas (RMSGCs): a monoinstitutional phase II study. **Proc Am Soc Clin Oncol.**, v. 24, abstract 5547. 2006.

LIN, C. H. et al. Unexpected rapid progression of metastatic adenoid cystic carcinoma during treatment with imatinib mesylate. **Head Neck.**, v. 27, no. 12, p. 1022-1027, Dec. 2005.

LLOYD, S. et al. Determinants and patterns of survival in adenoid cystic carcinoma of the head and neck, including an analysis of adjuvant radiation therapy. **Am J Clin Oncol.**, v. 34, no. 1, p. 76-81, Feb. 2011.

LOYOLA, A. M. et al. Minor salivary gland tumours. A retrospective study of 164 cases in a Brazilian population. **Oral Oncol Eur J Cancer**., v. 31B, no. 3, p. 197-201, May. 1995.

LU, J. et al. Novel MDM2 inhibitor SAR405838 (MI-773) induces p53-mediated apoptosis in neuroblastoma. **Oncotarget.**, Epub, Oct. 2016.

MANTESSO, A. et al. Mdm2 mRNA expression in salivary gland tumour cell lines. **J Oral Pathol Med.**, v. 33, no. 2, p. 96-101, Feb. 2004.

MATTOX, D. E.; VON HOFF, D. D.; BALCERZAK, S. P. Southwest Oncology Group study of mitoxantrone for treatment of patients with advanced adenoid cystic carcinoma of the head and neck. **Invest New Drugs.**, v. 8, no. 1, p. 105-107, Feb. 1990.

MENDENHALL, W. M. et al. Radiotherapy alone or combined with surgery for adenoid cystic carcinoma of the head and neck. **Head Neck.**, v. 26, no. 2, p. 154-162, Feb. 2004.

MICHAEL, D.; OREN, M. The p53 and Mdm2 families in cancer. **Curr Opin Genet Dev.**, v. 12, no. 1, p. 53-59, Feb. 2002.

MILANO, A. et al. Recent advances in the treatment of salivary gland cancers: emphasis on molecular targeted therapy. **Oral Oncol.**, v. 43, no. 8, p. 729-734, Sep. 2007.

MITANI, Y. et al. Comprehensive analysis of the MYB-NFIB gene fusion in salivary adenoid cystic carcinoma: Incidence, variability, and clinicopathologic significance. **Clin Cancer Res.**, v. 16, no. 19, p. 4722-4731, Oct. 2010.

MOMAND, J. et al. The MDM2 gene amplification database. **Nucleic Acids Res.**, v. 26, no. 15, p. 3453-3459, Aug. 1998.

MONTES DE OCA LUNA, R.; WAGNER, D. S.; LOZANO, G. Rescue of early embryonic lethality in mdm2-deficient mice by deletion of p53. **Nature.**, v. 378, no. 6553, p. 203-206, Nov. 1995.

MOSKALUK, C. A. et al. Development and characterization of xenograft model systems for adenoid cystic carcinoma. **Lab Invest.**, v. 91, no. 10, p. 1480-1490, Oct. 2011.

NÖR, F. et al. Therapeutic inhibition of the MDM2-p53 interaction prevents recurrence of adenoid cystic carcinomas. **Clin Cancer Res.**, in press. 2016.

OCHEL, H. J. et al. Effects of imatinib mesylate on adenoid cystic carcinomas. **Anticancer Res.**, v. 25, no. 5, p. 3659-3664, Sep. 2005.

OLINER, J. D. et al. Oncoprotein MDM2 conceals the activation domain of tumour suppressor p53. **Nature.**, v. 362, no. 6423, p. 857-860, Apr. 1993.

PAPASPYROU, G. et al. Chemotherapy and targeted therapy in adenoid cystic carcinoma of the head and neck: a review. **Head Neck.**, v. 33, no. 6, p. 905-911, Jun. 2011.

PEARSON, A. T. et al. Patient-derived xenograft (PDX) tumors increase growth rate with time. **Oncotarget.**, v. 7, no. 7, p. 7993-8005, Feb. 2016.

PENG, S. et al. Tumor grafts derived from patients with head and neck squamous carcinoma authentically maintain the molecular and histologic characteristics of human cancers. **J Transl Med.**, v. 11, p. 198, Aug. 2013.

PFEFFER, M. R. et al. A phase II study of Imatinib for advanced adenoid cystic carcinoma of head and neck salivary glands. **Oral Oncol.**, v. 43, no. 1, p. 33-36, Jan. 2007.

RIZK, S. et al. Activity of chemotherapy in the palliative treatment of salivary gland tumors: review of the literature. **Eur Arch Otorhinolaryngol.**, v. 264, no. 6, p. 587-594, Jun. 2007.

ROSS, P. J. et al. Epirubicin, cisplatin and protracted venous infusion 5-Fluorouracil chemotherapy for advanced salivary adenoid cystic carcinoma. **Clin Oncol (R Coll Radiol).**, v. 21, no. 4, p. 311-314, May. 2009.

RUBIO-VIQUEIRA, B. et al. An in vivo platform for translational drug development in pancreatic cancer. **Clin Cancer Res.**, v. 12, no. 15, p. 4652-4661, Aug. 2006.

SCHRAMM, V. L. JR.; SRODES, C.; MYERS, E. N. Cisplatin therapy for adenoid cystic carcinoma. **Arch Otolaryngol.**, v. 107, no. 12, p. 739-741, Dec. 1981.

SEETHALA, R. R. An update on grading of salivary gland carcinomas. **Head Neck Pathol.,** v. 3, no. 1, p. 69-77, Mar. 2009.

SHANGARY, S.; WANG, S. Targeting the MDM2-p53 interaction for cancer therapy. **Clin Cancer Res.**, v. 14, no. 17, p. 5318-5324, Sep. 2008.

SIMPSON, R. H. et al. Recent advances in the diagnostic pathology of salivary carcinomas. **Virchows Arch**., v. 465, no. 4, p. 371-384, Oct. 2014.

STENMAN, G. Fusion oncogenes in salivary gland tumors: molecular and clinical consequences. **Head Neck Pathol.**, v. 7, no. suppl 1, p. S12-19, Jul. 2013.

SURAKANTI, S. G.; AGULNIK, M. Salivary gland malignancies: the role for chemotherapy and molecular targeted agents. **Semin Oncol.**, v. 35, no. 3, p. 309-319, Jun. 2008.

TERHAARD, C. H. et al. Salivary gland carcinoma: independent prognostic factors for locoregional control, distant metastases, and overall survival: results of the Dutch head and neck oncology cooperative group. **Head Neck.**, v. 26, no. 8, p. 681-692, Aug. 2004.

TSUKUDA, M. et al. Chemotherapy for recurrent adeno- and adenoidcystic carcinomas in the head and neck. **J Cancer Res Clin Oncol.**, v. 119, no. 12, p. 756-758. 1993.

VAN DER WAL, J. E. et al. Distant metastases of adenoid cystic carcinoma of the salivary glands and the value of diagnostic examinations during follow-up. **Head Neck.**, v. 24, no. 8, p. 779-783, Aug. 2002.

VAN HERPEN, C. M. et al. Phase II study on gemcitabine in recurrent and/or metastatic adenoid cystic carcinoma of the head and neck (EORTC 24982). **Eur J Cancer.**, v. 44, no. 17, p. 2542-2545, Nov. 2008.

VASCONCELOS, A. C. et al. Clinicopathological analysis of salivary gland tumors over a 15-year period. **Braz Oral Res**., v. 30, e2. 2016.

VATTEMI, E. et al. Systemic therapies for recurrent and/or metastatic salivary gland cancers. **Expert Rev Anticancer Ther.**, v. 8, no. 3, p. 393-402, Mar. 2008.

VERMORKEN, J. B. et al. Epirubicin in patients with advanced or recurrent adenoid cystic carcinoma of the head and neck: a phase II study of the EORTC Head and Neck Cancer Cooperative Group. **Ann Oncol.**, v. 4, no. 9, p. 785-788, Nov. 1993.

VERWEIJ, J. et al. Phase II study on mitoxantrone in adenoid cystic carcinomas of the head and neck. EORTC Head and Neck Cancer Cooperative Group. **Ann Oncol.**, v. 7, no. 8, p. 867-869, Oct. 1996.

WANG, S. et al. SAR405838: an optimized inhibitor of MDM2-p53 interaction that induces complete and durable tumor regression. **Cancer Res.**, v. 74, no. 20, p. 5855-5865, Oct. 2014.

WARNER, K. A. et al. Targeting MDM2 for Treatment of Adenoid Cystic Carcinoma. **Clin Cancer Res.**, v. 22, no. 14, p. 3550-3559, Jul. 2016.

WU, X. et al. The p53-mdm-2 autoregulatory feedback loop. **Genes Dev.**, v. 7, no. 7A, p. 1129-1932, Jul. 1993.

ZHANG, X. et al. A renewable tissue resource of phenotypically stable, biologically and ethnically diverse, patient-derived human breast cancer xenograft models. **Cancer Res.**, v. 73, no. 15, p. 4885-4897, Aug. 2013.

ZHAO, Y. et al. Small-molecule inhibitors of the MDM2-p53 protein-protein interaction (MDM2 Inhibitors) in clinical trials for cancer treatment. **J Med Chem.**, v. 58, no. 3, p. 1038-1052, Feb. 2015.

https://www.nccn.org/professionals/physician_gls/pdf/head-and-neck.pdf - acessado em outubro de 2016.

https://www.accrf.org/research/resources-for-researchers/databases/ - acessado em outubro de 2016.

https://clinicaltrials.gov/ct2/results?term=SAR405838&Search=Search - acessado em outubro de 2016.